Caloric Restriction Causes a Distinct Remodeling of the Lipidome in Quiescent Cells of Budding Yeast

Emmanuel Orfanos

A Thesis
in
The Department
of
Biology

Presented in Partial Fulfillment of the Requirements
for the Degree of Master of Sciences at
Concordia University
Montreal, Quebec, Canada

March 2021

CONCORDIA UNIVERSITY

School of Graduate Studies

This is to certify that the Thesis prepared

By: Emmanuel Orfanos

Entitled: Caloric Restriction Causes a Distinct Remodeling of the Lipidome in Quiescent Cells of Budding Yeast

and submitted in partial fulfillment of the requirements for the degree of

Master of Sciences (Biology)

complies with the regulations of the University and meets the accepted standards with respect to originality and quality.

Signed by the final examining committee:

_____ Chair

Dr. Alisa Piekny

_____ External Examiner

Dr. Aashiq Kachroo

_____ Examiner

Dr. Chiara Gamberi

_____ Examiner

Dr. Alisa Piekny

_____ Supervisor

Dr. Vladimir Titorenko

Approved by _____

Dr. Robert Weladji, Chair of Department or Graduate Program Director

_____

Dr. Pascale Sicotte, Dean of Faculty of Arts and Science

Date _____

ABSTRACT

Caloric Restriction Causes a Distinct Remodeling of the Lipidome in Quiescent Cells of Budding Yeast

Emmanuel Orfanos

After budding yeast cells cultured in a nutrient-rich liquid medium with glucose ferment glucose to ethanol and then consume it as a carbon source, they enter the stationary phase of culturing and the process of their chronological aging begins. At that point, yeast cells in the culture arrest their cell cycle and enter a state of quiescence, also known as the G_0 state. Shortly following such cell cycle arrest, the yeast culture begins to accumulate quiescent and non-quiescent cells. The Titorenko laboratory has recently used gradient centrifugation to purify the high- and low-density sub-populations quiescent and non-quiescent cells. They demonstrated that caloric restriction, a robust aging-delaying (geroprotective) dietary intervention, decreases the concentrations of the neutral storage lipids triacylglycerols and increases the concentration of the mitochondrial membrane lipid cardiolipin in quiescent and non-quiescent cells. The studies described in my Thesis had the following two objectives. First, I sought to investigate how caloric restriction influences the concentrations of all lipid classes (not only triacylglycerols and cardiolipin concentrations) within the high- and low-density sub-populations of quiescent and non-quiescent yeast cells on different stages of the chronological aging process. My second objective was to compare the effects of caloric restriction, the *tor1Δ* mutation (a genetic geroprotective intervention) and lithocholic acid (a pharmacological geroprotective intervention) on the lipidomes of the high- and low-density sub-populations of quiescent and non-quiescent yeast cells on different stages of chronological aging. To attain these objectives, I used liquid chromatography coupled with tandem mass spectrometry quantitative lipidomics to assess the aging-associated changes in high- and low-density cells' lipidomes. I provided the first evidence that caloric restriction statistically significantly alters the concentrations of 18 different lipid classes through most of the chronological lifespan of high- and low-density cells. Caloric restriction decreased triacylglycerol concentration, increased free fatty acid concentration, raised ceramide concentration, and elevated phospholipid concentrations in high- and low-density cells through most of the chronological lifespan. My data also provided the first evidence that caloric restriction

creates lipidomic patterns of chronologically aging high- and low-density cells that differ from the lipidomic patterns of these cells established by the *tor1Δ* mutation and lithocholic acid.

Acknowledgments

I would like to thank my supervisor Dr. Titorenko for his continuous guidance and support throughout my graduate studies in his laboratory. I would also like to thank my committee members Dr. Chiara Gamberi and Dr. Alisa Piekny for their valuable suggestions that contributed to my research and learning experience, as well as current and past members of the Titorenko lab for their support. More specifically, I would like to thank one of the PhD candidates in the Titorenko lab, Karamat Mohammad, for teaching me the laboratory and computer techniques required to independently complete the experimental and analytical components of my Thesis. Finally, I would like to extend my thanks to every other lab member and volunteer who were not mentioned above. The combinatorial effects of each individual's support and guidance have provided me with a pleasant and informative experience during my graduate studies.

Table of Contents

List of Figures and Tables

List of Abbreviations

Ac-CoA, acetyl-CoA

CER, ceramide

CL, cardiolipins

CLS, chronological lifespan

CR, caloric restriction

DAG, diacylglycerols

ER, the endoplasmic reticulum

FFA, free fatty acid

HD, high density

LD, low density

LPA, lysophosphatidic acid

LPC, lysophosphatidylcholine

LPE, lysophosphatidylethanolamine

LPS, lysophosphatidylserine

LPI, lysophosphatidylinositol

non-CR, non-caloric restriction

non-Q, non-quiescent

PA, phosphatidic acid

PC, phosphatidylcholine

PE, phosphatidylethanolamine

PS, phosphatidylserine

PI, phosphatidylinositol

Q, quiescent

RCD, regulated cell death

ROS, reactive oxygen species

ST, stationary

TAG, triacylglycerols

WT, wild-type strain

$\Delta\Psi_m$, the electrochemical potential across the inner mitochondrial membrane

Chapter 1: Introduction

1.1 An overview of a cellular quiescence program in budding yeast, its link to chronological aging and its regulation by a low-calorie diet

Culturing budding yeast *Saccharomyces cerevisiae* aerobically in a medium supplemented with 2% glucose as a single carbon source provides yeast with enough calories to proliferate and survive (Fraenkel, 2011). The term "non-caloric restriction (non-CR)" was coined to describe these conditions of culturing (Goldberg et al., 2009). At some point of culturing under non-CR conditions, *S. cerevisiae* cells consume all exogenous glucose and slow down their growth (Goldberg et al., 2009). These cells enter a diauxic shift period, during which they produce ethanol and catabolize it aerobically (Fraenkel, 2011). After consuming ethanol, yeast culture's growth is further decelerated (Goldberg et al., 2009; Fraenkel, 2011). The culture enters a post-diauxic shift marked by active mitochondrial respiration (Goldberg et al., 2009; Fraenkel, 2011). At that point, the cell-division cycle of some yeast in the culture is arrested in the late G_1 phase (Allen et al., 2006). This cell-division cycle arrest occurs at the nutrient-dependent checkpoint called "START A" (Allen et al., 2006). The cell cycle arrest at the "START A" checkpoint coincides with the appearance of two cell sub-populations in the yeast culture under non-CR conditions. These sub-populations are quiescent (Q) and non-quiescent (NQ) cells (Allen et al., 2006; Werner-Washburne et al., 2012). The physical, morphological, reproductive, biochemical and physiological properties of the Q and NQ cell sub-populations are different (Allen et al., 2006; Werner-Washburne et al., 2012). These properties are developed under the control of a nutrient-sensing signaling network that includes several signaling pathways and protein kinases (De Virgilio, 2012).

After the post-diauxic shift on the non-CR culture is completed, it enters the stationary (ST) phase of culturing (Fraenkel, 2011; Arlia-Ciommo et al., 2014). At that point, all yeast cells in the culture enter a G_0 state of quiescence and begin age chronologically (Fraenkel, 2011; Werner-Washburne et al., 2012; Arlia-Ciommo et al., 2014). The length of time during which a yeast cell maintains a G_0 state of quiescence is traditionally used to measure the pace of chronological aging in *S. cerevisiae* (Figure 1.1) (Longo et al., 2012; Arlia-Ciommo et al., 2014). The maintenance of quiescence is monitored with the help of a clonogenic plating assay. In this assay, a yeast cell from an ST-phase liquid culture that consumed nutrients is plated on the surface of a solid medium rich in nutrients. If the plated cell can form a colony on this solid medium's

surface, this cell is considered viable (Longo et al., 2012; Arlia-Ciommo et al., 2014). The yeast chronological aging assay measures a time-dependent loss in the viability of quiescent cells present within the ST-phase cell culture (Figure 1.1) (Longo et al., 2012; Arlia-Ciommo et al., 2014). It is commonly accepted that the chronological mode of aging in yeast mirrors the aging of post-mitotic quiescent cells like neurons or myocytes in multicellular eukaryotes (Longo et al., 2012; Arlia-Ciommo et al., 2014).

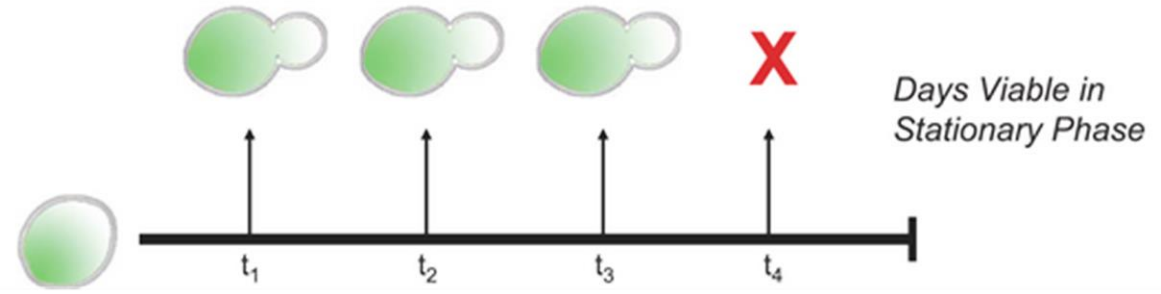

Figure 1.1: The chronological mode of aging in the budding yeast *Saccharomyces cerevisiae*. The chronological aging of budding yeast is assessed by measuring a time-dependent loss in the viability of quiescent cells populating a liquid culture that reaches the ST phase of culturing. From Kaeberlein et al., 2007.

Further below, I provide a comparative description of the properties exhibited by the Q and NQ yeast cells grown under non-CR conditions. It needs to be emphasized that a multi-step cellular quiescence program operates in these yeast cells and defines their properties (Aragon et al., 2008; Davidson et al., 2011; Werner-Washburne et al., 2012; Miles et al., 2013). The program begins when yeast cells enter the diauxic period of growth under non-CR conditions and continues during the ST phase of culturing (Aragon et al., 2008; Davidson et al., 2011; Werner-Washburne et al., 2012; Miles et al., 2013). It seems that this cellular quiescence program is an essential contributor to the chronological aging of budding yeast not limited in calorie supply (Aragon et al., 2008; Davidson et al., 2011; Werner-Washburne et al., 2012; Miles et al., 2013). The major properties of the cellular quiescence program operating in yeast under non-CR conditions have been described (De Virgilio, 2012; Werner-Washburne et al., 2012; Sagot et al., 2019). These properties include the following. The cellular quiescence program is initiated in response to nutrient deprivation and the onset of chronological aging. The program integrates a series of cellular events;

these events follow each other in a particular order and are under the tight control of a signaling network of yeast quiescence. Specific genetic manipulations that alter the information flow down the program's consecutive steps can accelerate or decelerate the program. Finally, akin to other programmed biological events, the cellular quiescence program is beneficial for the survival and stress resistance of a yeast cell's population.

CR is a low-calorie diet without malnutrition that slows aging, extends longevity and delays the onset of aging-associated pathologies in budding yeast and many other eukaryotic organisms (Sinclair, 2005; Madeo et al., 2019). Nutrient-rich complete media or nutrient-limited synthetic minimal media supplemented with 0.2% or 0.5% glucose are traditionally used to assess how CR influences budding yeast's chronological aging (Longo et al., 2012; Arlia-Ciommo et al., 2014). It has been shown that the use of a nutrient-rich complete medium supplemented with 0.2% or 0.5% glucose provides all nutrients needed for the growth and survival of budding yeast (Feldmann, 2012). Moreover, it appears that the use of this medium is beneficial for studying the effects of CR on the chronological mode of yeast aging (Goldberg et al., 2009).

The Titorenko laboratory purified Q and NQ cells' sub-populations from budding yeast cultures in a nutrient-rich medium under CR or non-CR conditions (Leonov et al., 2017). They compared the properties of Q and NQ cell sub-populations recovered at different stages of yeast chronological aging (Leonov et al., 2017). In the subsequent Introduction sections, I discuss how CR alters Q cells' properties to decelerate the aging-associated conversion of Q cells into NQ cells. Besides, I critically evaluate a body of evidence indicating that CR's ability to change Q cells' properties is an essential contributor to CR's ability to slow chronological aging in budding yeast.

1.2 The Q and NQ cells' sub-populations in yeast cultured under non-CR conditions differ in many of their characteristic traits

The budding yeast cells under non-CR conditions that arrest their cell cycle and enter a G_0 state give rise to Q cells' sub-population (Werner-Washburne et al., 2012). This is unlike the budding yeast cells that under the same culturing conditions do not undergo cell cycle arrest; these cells form three different sub-populations of NQ cells (Werner-Washburne et al., 2012). As described below and shown in Figure 1.2, many characteristic traits of the Q and NQ cell sub-populations are different.

The sub-population of Q cells under non-CR conditions includes unbudded cells of a uniform diameter; these cells have a thick cell wall, refract light if examined by phase-contrast microscopy and exhibit a high buoyant density (Figure 1.2) (Allen et al., 2006; Aragon et al., 2008; Davidson et al., 2011; Werner-Washburne et al., 2012; Miles et al., 2013). Q cells under non-CR conditions are highly metabolically active (Figure 1.2). They stockpile significant amounts of glycogen and trehalose (Figure 1.2). The mitochondria in these Q cells are respiratory functional and exhibit a high membrane potential (Figure 1.2). The concentration of reactive oxygen species (ROS) and extent of oxidative macromolecular damage are low in Q cells under non-CR conditions (Figure 1.2). These Q cells exhibit both characteristic traits of quiescence; they maintain the clonogenicity on the surface of solid media and synchronously divide if transferred from a nutrient-depleted to a nutrient-rich liquid medium (Figure 1.2). Q cells under non-CR conditions are stress-resistant and exhibit a low DNA mutation rate (Figure 1.2). The aging-associated onsets of the apoptotic and necrotic forms of cell death are delayed in these cells (Figure 1.2).

Recent studies have shown that several heat-shock proteins move from the cytosol to the nucleus in Q cells under non-CR conditions (Figure 1.2) (Sagot et al., 2019). Yet, other heat-shock proteins and various enzymes accumulate in the numerous cytosolic foci or filaments found in these Q cells (Figure 1.2) (Sagot et al., 2019). Nuclear morphology, chromosome positioning in the nucleus and nuclear gene transcription undergo significant changes in the Q cells cultured under non-CR conditions (Figure 1.2) (Sagot et al., 2019). Because these cells amass cytosolic P-bodies and stress granules, displace dysfunctional proteasome subunits from the nucleus to the insoluble protein deposits, and relocate functional proteasome subunits from the nucleus to the proteasome storage granules, they excel in maintaining cellular proteostasis (Figure 1.2) (Sagot et al., 2019). Actin cytoskeleton and microtubules, including stable microtubules in the nucleus, undergo significant remodeling in Q cells under non-CR conditions (Figure 1.2) (Sagot et al., 2019). Fragmentation of the dynamic mitochondrial network in these cells results in numerous small and globular mitochondria at the cell periphery (Figure 1.2) (Sagot et al., 2019).

A body of evidence indicates that some of the above traits of Q cells under non-CR conditions play essential roles in these cells' abilities to exit a quiescent state, return to the cell cycle and restart proliferation (Allen et al., 2006; Aragon et al., 2008; Davidson et al., 2011; Werner-Washburne et al., 2012; Miles et al., 2013; Leonov et al., 2017; Sagot et al., 2019). It seems that some of these traits are also essential for longevity assurance in chronologically aging

budding yeast (Allen et al., 2006; Aragon et al., 2008; Davidson et al., 2011; Werner-Washburne et al., 2012; Miles et al., 2013; Leonov et al., 2017; Sagot et al., 2019). It is presently unknown how Q cells under non-CR conditions control the establishment of the numerous characteristic traits described above and shown in Figure 1.2. The mechanistic links between each of these traits and quiescence exit, cell cycle re-entry, proliferation reinstatement and longevity assurance remain to be determined.

Three NQ cell sub-populations can be found in a budding yeast culture under non-CR conditions (Allen et al., 2006; Aragon et al., 2008; Davidson et al., 2011; Werner-Washburne et al., 2012; Miles et al., 2013). The characteristic traits of these sub-populations are described below and shown in Figure 1.2.

NQ cell sub-population 1 includes mainly the mother cells of the first and higher generations with one or more bud scars on their surface (Figure 1.2) (Allen et al., 2006; Aragon et al., 2008; Davidson et al., 2011; Werner-Washburne et al., 2012; Miles et al., 2013). These bud scars appear on the mother cell's surface after a new daughter cell (bud) separates from it (Cabib et al., 2013). NQ cells in this sub-population exhibit a high rate of metabolism and are clonogenic (Figure 1.2) (Allen et al., 2006; Aragon et al., 2008; Davidson et al., 2011; Werner-Washburne et al., 2012; Miles et al., 2013). The characteristic features of NQ cells in this sub-population are their low buoyant density, reduced mitochondrial respiration, elevated ROS, and high frequencies of mutations in the nuclear and mitochondrial DNA (Figure 1.2) (Allen et al., 2006; Aragon et al., 2008; Davidson et al., 2011; Werner-Washburne et al., 2012; Miles et al., 2013).

NQ cell sub-population 2 also contains various generations of mother cells that are metabolically active (Figure 1.2) (Allen et al., 2006; Aragon et al., 2008; Davidson et al., 2011; Werner-Washburne et al., 2012; Miles et al., 2013). A characteristic feature of NQ cells in this sub-population is that they are not clonogenic (Figure 1.2) (Allen et al., 2006; Aragon et al., 2008; Davidson et al., 2011; Werner-Washburne et al., 2012; Miles et al., 2013). It is commonly accepted, therefore, that these NQ cells are descendants of NQ cells from the sub-population 1 (Figure 1.2) (Allen et al., 2006; Aragon et al., 2008; Davidson et al., 2011; Werner-Washburne et al., 2012; Miles et al., 2013).

NQ cell sub-population 3 consists of cells that are not clonogenic (Figure 1.2) (Allen et al., 2006; Aragon et al., 2008; Davidson et al., 2011; Werner-Washburne et al., 2012; Miles et al., 2013). Because these cells exhibit markers of apoptosis and necrosis, it is believed that their

predecessors are NQ cells from the sub-population 2 (Figure 1.2) (Allen et al., 2006; Aragon et al., 2008; Davidson et al., 2011; Werner-Washburne et al., 2012; Miles et al., 2013).

The distinct traits exhibited by NQ cells of the sub-populations 1, 2 and 3 indicate the order of their stepwise conversion during chronological aging (Figure 1.2). It is tempting to speculate that NQ cells of sub-population 1 are descendants of Q cells (Figure 1.2, red arrow). It is presently unclear how yeast's chronological aging promotes Q cells' conversion into NQ cells of the sub-population 1.

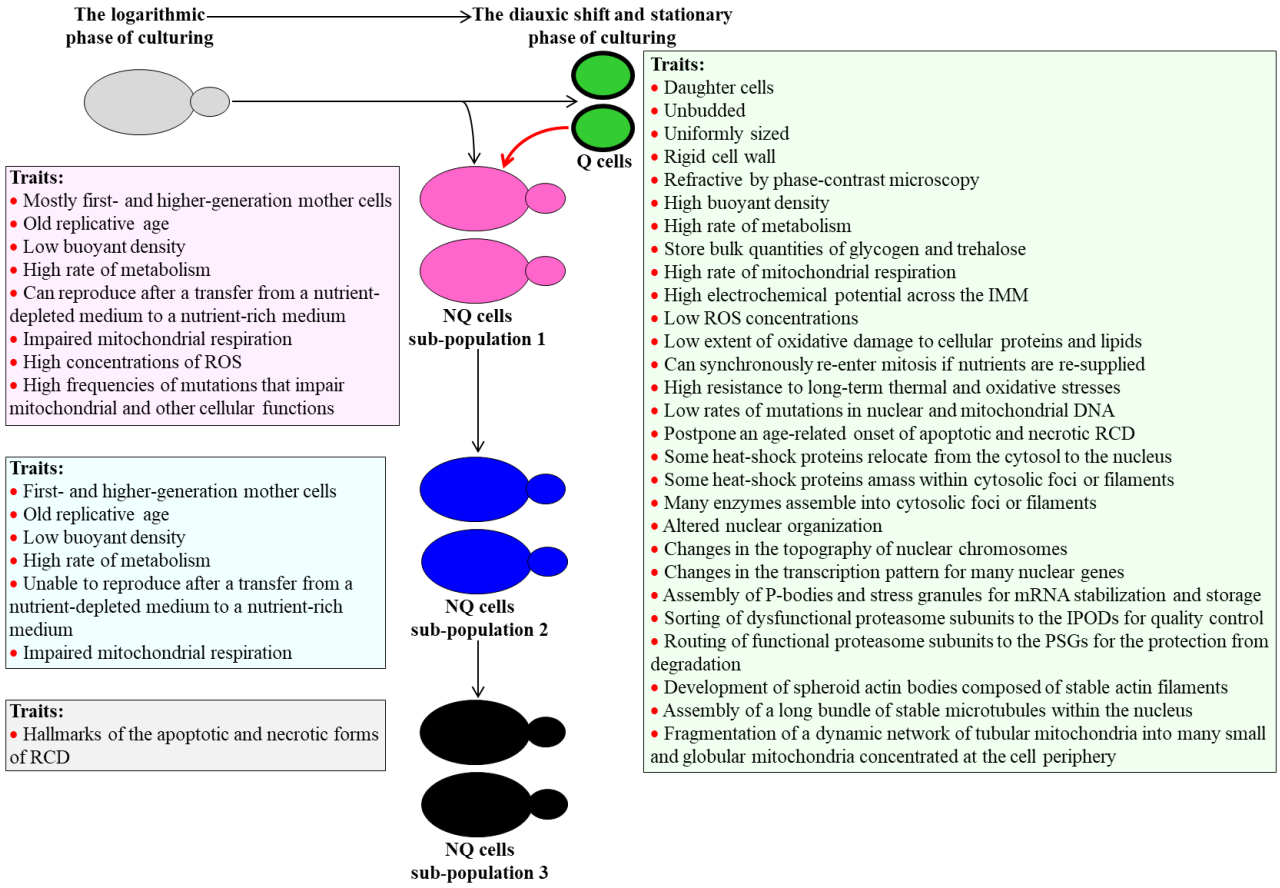

Figure 1.2: When budding yeast culture under non-CR conditions enters a post-diauxic shift, Q and NQ cells' sub-populations appeared in this culture. A stepwise conversion of NQ cells in the indicated order leads to the appearance of three sub-populations of these cells during chronological aging of this culture. The distinct traits exhibited by Q cells and the three sub-populations of NQ cells are different. NQ cells of sub-population 1 are descendants of Q cells. More details are provided in the text. Abbreviations: IMM, the inner mitochondrial membrane;

IPODs, insoluble protein deposits; PSGs, proteasome storage granules; RCD, regulated cell death; ROS, reactive oxygen species.

1.3 CR affects the characteristic traits of Q and NQ cells and the dynamics of their appearance during chronological aging

The purification Q and NQ cells and their comparative analyses have been reported for budding yeast cultures that aged chronologically under CR conditions (Leonov et al., 2017). Below, I discuss (and show in Figure 1.3) how the low-calorie diet influences the characteristic traits of Q and NQ cells and affects the age-related dynamics of their appearance during chronological aging.

Following glucose consumption by the yeast culture under non-CR conditions, cells enter the G_0 state and give rise to the high-density Q cell sub-population due to the cell cycle arrest in late G_1 (Allen et al., 2006; Aragon et al., 2008; Davidson et al., 2011; Werner-Washburne et al., 2012; Miles et al., 2013). On the contrary, when the yeast culture under CR conditions consumes glucose, it enters the G_0 state and develops the high-density Q cell sub-population because the cell cycle arrest occurs in early G_1 (Figure 1.3A) (Leonov et al., 2017).

The percentage of low-density Q cells in the yeast culture under non-CR conditions reaches a maximum after the culture enters the ST growth phase (Leonov et al., 2017). This is in contrast to the yeast culture under CR conditions, which begins to accumulate the maximal percentage of low-density Q cells when it enters the post-diauxic growth phase (Figure 1.3B) (Leonov et al., 2017).

CR affects both criteria of the chronological age-related quiescence decline by the sub-populations of Q and NQ cells. Indeed, CR extends the time during which both these cell sub-populations retain their clonogenicity (Figure 1.3C) (Leonov et al., 2017). Besides, CR slows a chronological aging-associated decline in Q and NQ cells' ability to synchronously divide if transferred from a nutrient-depleted to a nutrient-rich liquid medium (Figure 1.3D) (Leonov et al., 2017).

CR increases glycogen and trehalose concentrations in both Q and NQ cells (Figure 1.3E) (Leonov et al., 2017). The high molecular mass branched polysaccharide glycogen and the nonreducing disaccharide trehalose are used to store glucose in budding yeast cells (François and

Parrou, 2001). Trehalose also maintains proteostasis in budding yeast cells and protects these cells from a chronic stress-inflicted death (Kyryakov et al., 2012).

CR causes a substantial decline in the concentrations of the neutral lipids triacylglycerols (TAG) within both Q and NQ cells (Figure 1.3F) (Leonov et al., 2017). After the synthesis of TAG in the endoplasmic reticulum (ER), they are deposited in lipid droplets (LD) (Mitrofanova et al., 2018). TAG stored in LD provide free (non-esterified) fatty acids that can be oxidized to produce energy or used to synthesize various phospholipids (Mitrofanova et al., 2018).

CR elicits a considerable rise in the concentrations of cardiolipins (CL) within both Q and NQ cells (Figure 1.3G) (Leonov et al., 2017). CL are synthesized and reside in the inner mitochondrial membrane (IMM) (Mitrofanova et al., 2018). These diphosphatidylglycerol lipids are essential contributors to mitochondrial morphology and function (Mitrofanova et al., 2018).

CR stimulates mitochondrial respiration and increases the electrochemical potential across the inner mitochondrial membrane ($\Delta\Psi_m$) (Figure 1.3H) in both Q and NQ cells (Leonov et al., 2017). Both mitochondrial respiration and $\Delta\Psi_m$ are known to play essential roles in regulating longevity of chronologically aging yeast (Leonov and Titorenko., 2013; Beach et al., 2015).

CR decreases cellular ROS concentrations in chronologically "young" cells that did not enter the ST growth phase and increases these concentrations in chronologically "old" cells that enter the ST phase (Figure 1.3I) (Leonov et al., 2017). These effects of CR on cellular ROS concentrations are observed in both Q and NQ cells (Leonov et al., 2017). ROS are by-products of mitochondrial respiration (Giorgio et al., 2007) that play essential roles in longevity assurance of budding yeast (Giorgio et al., 2007; Goldberg et al., 2009; Leonov and Titorenko., 2013; Arlia-Ciommo et al., 2014; Beach et al., 2015; Dakik et al., 2019).

CR reduces the extent of oxidative damage to cellular macromolecules (including proteins, lipids and DNA) during chronological aging of both Q and NQ cells (Figure 1.3J) (Leonov et al., 2017). This type of macromolecular damage is an essential contributor to budding yeast's chronological aging (Gladyshev et al., 2013; Leonov and Titorenko., 2013; Beach et al., 2015; Dakik et al., 2019; Ogrodnik et al., 2019).

CR makes both Q and NQ cells more resistant to chronic thermal and oxidative stresses (Figure 1.3K) (Leonov et al., 2017). A rise in yeast cells' resistance to these stresses contributes to the delay of budding yeast's chronological aging (Goldberg et al., 2009; Arlia-Ciommo et al., 2014; Leonov and Titorenko., 2013; Beach et al., 2015; Dakik et al., 2019).

CR delays the chronological age-related onset of the apoptotic and necrotic forms of regulated cell death (RCD) in both Q and NQ cells (Figure 1.3L) (Leonov et al., 2017). CR also makes both Q and NQ cells more resistant to the apoptotic and necrotic forms of RCD inflicted by exogenous chemical interventions (Figure 1.3M) (Leonov et al., 2017). Both these RCD forms are known to terminate the life of chronologically "old" budding yeast cells (Herker et al., 2004; Arlia-Ciommo et al., 2014; Richard et al., 2014; Sheibani et al., 2014).

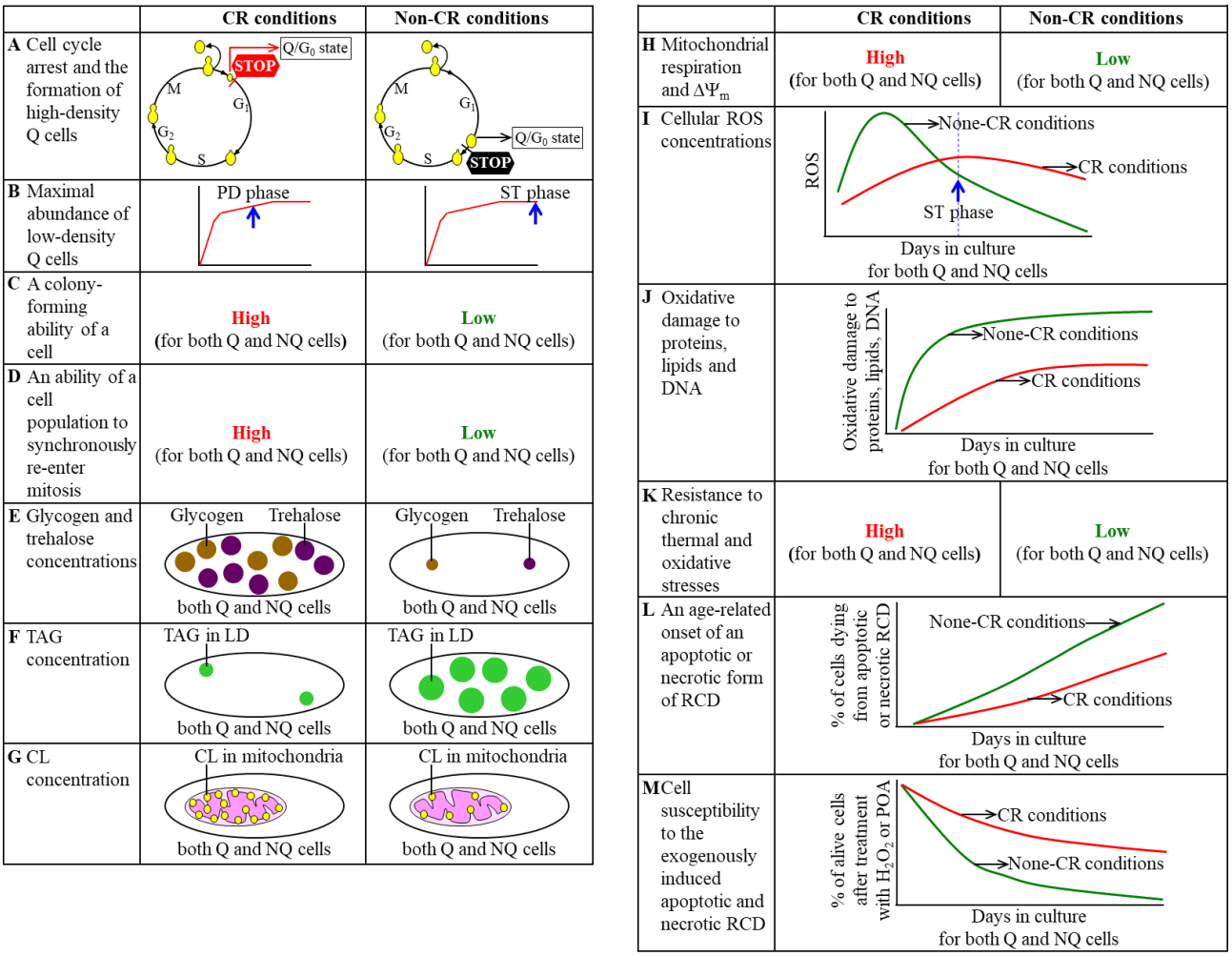

Figure 1.3: CR affects the characteristic traits of Q and NQ cells and the dynamics of their appearance during chronological aging. Different panels of the figure outline these traits of Q and NQ cells. More details are provided in the text. Abbreviations: CL, cardiolipins; LD, lipid droplets; POA, palmitoleic acid; RCD, regulated cell death; ROS, reactive oxygen species; TAG, triacylglycerols; $\Delta\Psi_m$, the electrochemical potential across the inner mitochondrial membrane.

1.4 A hypothetical mechanism through which CR delays yeast chronological aging by affecting the characteristic traits of Q cells and their age-related dynamics

Together with other Titorenko laboratory members, I evaluated how CR influences the characteristic traits of high- and low-density Q cells and their age-related conversion into high- and low-density NQ cells. Based on this evaluation, a hypothesis was proposed on the mechanism by which CR can decelerate the chronological aging of budding yeast because it influences the characteristic traits of Q cells and their aging-associated dynamics.

I discuss this hypothesis below. Figure 1.4 is a graphical representation of the proposed hypothesis. The central tenet of the hypothesis is that the CR-dependent delay of yeast chronological aging is due to the low-calorie diet's ability to affect several essential processes within Q cells.

CR arrests the cell cycle in early G_1 and creates small Q^{HD} cells (Figure 1.4, process 1) (Leonov et al., 2017). The hypothesis posits that these small Q^{HD} cells exhibit the improved pro-longevity traits named in Figure 1.4, including the greater reproductive competence, higher resistance to oxidative and thermal stresses etc.

CR accelerates Q^{HD} cells' transformation into Q^{LD} cells during budding yeast's chronological aging (Figure 1.4, process 2) (Leonov et al., 2017). The hypothesis suggests that the accelerated Q^{HD}-into-Q^{LD} transformation might contribute to the development of improved pro-longevity traits named in Figure 1.4.

CR decelerates a conversion of long-lived Q^{LD} cells into short-lived NQ^{LD} cells (Figure 1.4, process 3) (Leonov et al., 2017). The hypothesis postulates that the decelerated Q^{LD}-into-NQ^{LD} conversion might be an essential contributor to improving pro-longevity traits named in Figure 1.4.

CR slows the transformation of long-lived Q^{HD} cells into short-lived NQ^{HD} cells (Figure 1.4, process 4) (Leonov et al., 2017). The hypothesis posits that, by decelerating the Q^{LD}-into-NQ^{LD} transformation, CR might contribute to the development of improved pro-longevity traits named in Figure 1.4.

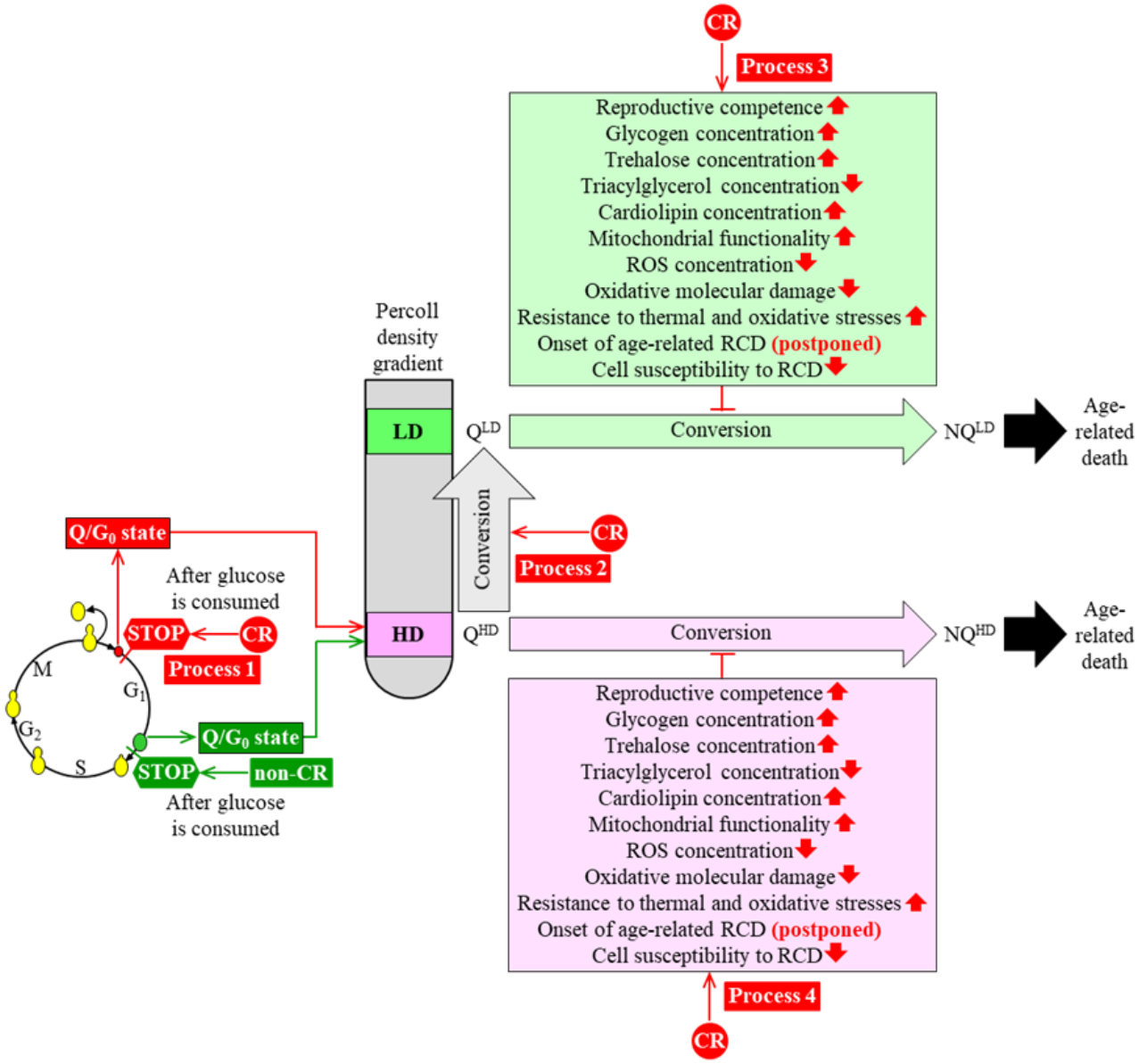

Figure 1.4: A hypothetical mechanism through which CR delays yeast chronological aging by affecting the characteristic traits of Q cells and their age-related dynamics. The proposed mechanism's central tenet is that the CR-dependent delay of yeast chronological aging is due to the low-calorie diet's ability to affect four essential processes within Q cells. More details are provided in the text. Abbreviations: HD, high-density cells; LD, low-density cells; Q^{HD}, quiescent cell of high density; Q^{LD}, quiescent cell of low density; NQ^{HD}, non-quiescent cell of high density; NQ^{LD}, non-quiescent cell of low density; RCD, regulated cell death; ROS, reactive oxygen species. ↑ Increased by CR; ↓ Decreased by CR; ⊣ Slows the conversion of Q^{LD} cells into NQ^{LD} cells or the Q^{HD}-into-NQ^{HD} cell conversion.

1.5 An intricate network of pathways coordinates lipid metabolism and interorganellar transport in budding yeast

As discussed in section 1.3, the CR diet elicits a considerable decline in TAG concentration and a significant rise in CL concentration within HD and LD cells of the Q and NQ types (Leonov et al., 2017). The intracellular concentrations of TAG and CL depend on the intensity of metabolite flow throughout an elaborate network of pathways for the metabolism and interorganellar transport of other lipid classes. This network has been intensively reviewed (Carman et al., 2011; Henry et al., 2012; Kohlwein et al., 2013; Klug and Daum, 2014; Mitrofanova et al., 2018; Tamura et al., 2019). It is schematically depicted in Figure 1.5 and briefly described below.

Glucose, the only carbon source exogenously added to yeast cultures, is initially converted to pyruvate in the cytosol via the ten-step glycolytic pathway (Figure 1.5). Pyruvate is then used to synthesize acetyl-CoA (Ac-CoA) via three consecutive reactions catalyzed by the following enzymes: 1) the cytosolic pyruvate decarboxylase isozymes Pdc1, 5, and 6, 2) the aldehyde dehydrogenases Ald2 and 6, and 3) the Ac-CoA synthetase isoforms Acs1 and 2 (Figure 1.5). Peroxisomal reactions also contribute to the cytosolic pool of Ac-CoA through free fatty acid (FFA) β-oxidation via Fox1-, 2-, and 3-dependent chemical reactions (Figure 1.5). Following its synthesis, Ac-CoA acts as a substrate for FFA formation in the cytosolic via the Ac-CoA carboxylase Acc1 and fatty acid synthase complex Fas1/Fas2 (Figure 1.5). FFA can also be produced in lipid droplets (LD) via the hydrolysis of TAG by the Tgl1, 3, 4, and 5 lipases as well as the lipolytic degradation of diacylglycerols (DAG) and monoacylglycerols (MAG), both of which are TAG-derived. Such processes are carried out by the lipases Tgl3 and Yju3, respectively, in LDs (Figure 1.5).

Following the formation of FFA via the above-mentioned processes, long-chain acyl-CoA synthetases Faa1, Faa4, and Fat1 located in the endoplasmic reticulum (ER) will catalyze reactions which convert these FFAs into fatty acyl-CoA esters (FA-CoA) (Figure 1.5). The latter is then used for the *de novo* synthesis of TAG, CL, and glycerophospholipids such as PA, PS, PE, PC, and PI via enzymes confined to the ER and the mitochondria (Figure 1.5).

This process begins in the ER, where glycerol-3-phosphate (G3P)/dihydroxyacetone phosphate acetyltransferases Sct1 and Gpt2 catalyze the formation of lysophosphatidic acid (LPA) or acyl-dihydroxyacetone phosphate (ADHAP) from FA-CoA and G3P or DHAP, respectively (Figure 1.5). ADHAP is also converted to LPA via an Ayr1-driven reaction (Figure 1.5). LPA

formed from FA-CoA or ADHAP can then be converted to phosphatidic acid (PA) via the LPA acyl-transferases Slc1, Slc4, Loa1, and Ale1 (Figure 1.5). Firstly, a Cds1-driven reaction can convert PA into cytidine diphosphate (CDP)-DAG, a common precursor for other phospholipids (Figure 1.5). As such, a Pis1-dependent synthesis of phosphatidylinositol (PI) from this precursor can occur in the ER (Figure 1.5). Alternatively, a Cho1-dependent reaction can convert CDP-DAG to phosphatidylserine (PS) (Figure 1.5). The latter can be shuttled to the outer mitochondrial membrane (OMM) through the mitochondria-ER contact sites, and subsequently through the intermembrane space (IMS) to the inner mitochondrial membrane (IMM) via Ups2-driven transport (Figure 1.5). Within the IMM, phosphatidylethanolamine (PE) is synthesized by Psd1 from PS and is then shuttled back to the ER (Figure 1.5). A Cho2- and Opi3-dependent synthesis of phosphatidylcholine (PC) occurs in the ER from the shuttled PE (Figure 1.5). Secondly, PA can also be converted to DAG in a reaction catalyzed by the PA phosphatases Pah1, App1, Dpp1, and Lpp1 in the ER (Figure 1.5). Subsequently, DAG can be acylated to TAG via an FA-CoA-dependent reaction driven by Dga1, Are1, and Are2, and in a PE- and PC-dependent catalyzed by Lro1 (Figure 1.5). Following the *de novo* synthesis of TAG in the ER, these molecules can be deposited in LDs and broken down into FFAs as mentioned above (Figure 1.5). Thirdly, PA can be transported from the ER to the IMM in a similar fashion as PS, this time with the help of Ups1 (Figure 1.5). Within the IMM, PA can be converted into CDP-DAG using Tam41 (Figure 1.5). Then, CDP-DAG can either be converted into phosphatidylglycerol (PG) using the Pgs1 and Gep4 enzymes, respectively or into CL and then MLCL via Crd1 and Cld1 respectively (Figure 1.5). PC can also be converted to CL in the IMM via the Taz1 enzyme (Figure 1.5). Finally, the accumulation of CL in the IMM creates a negative feedback loop on the Ups1-dependent transport of PA into the IMM from the ER, ultimately inhibiting the accumulation of PA in the mitochondria (Figure 1.5).

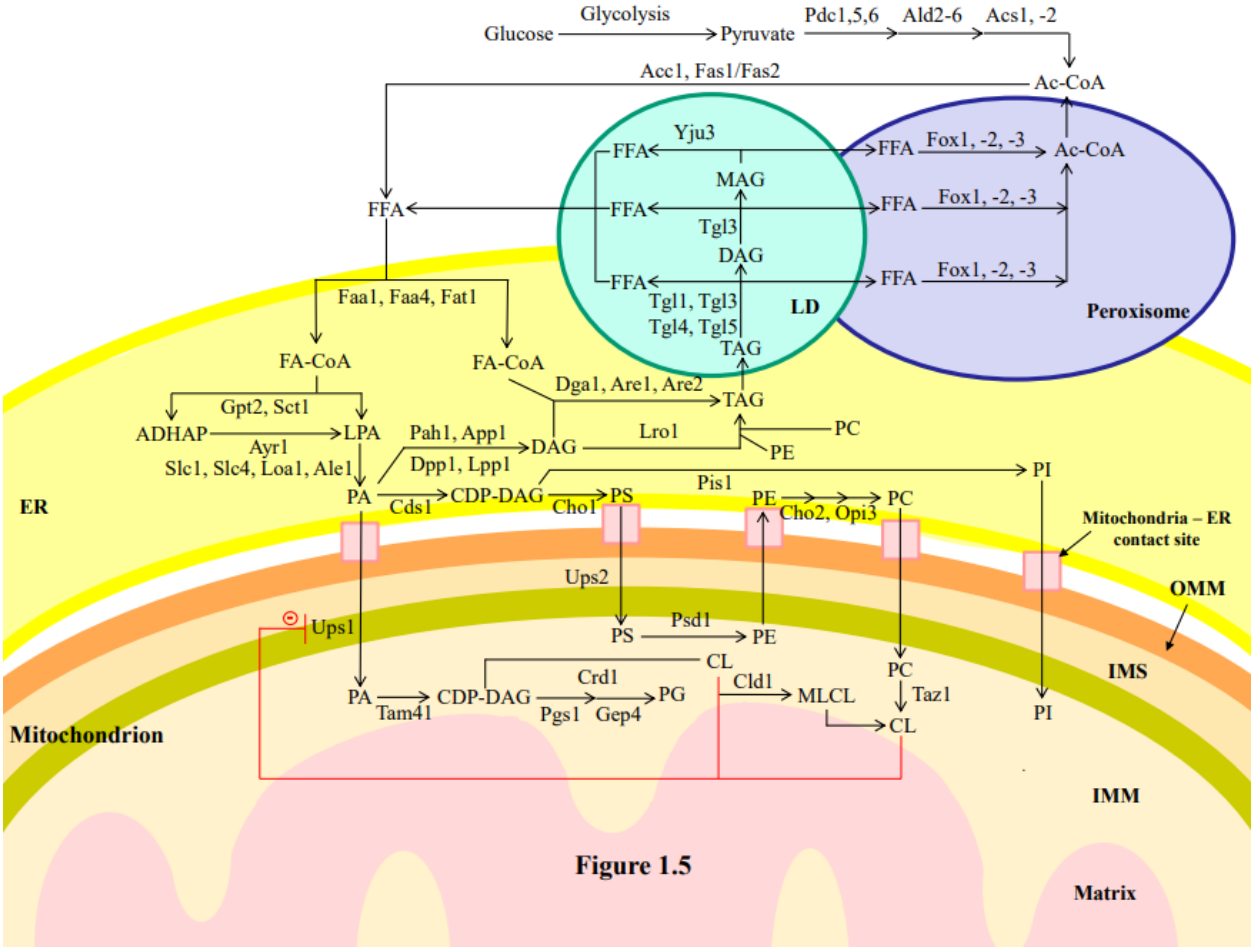

Figure 1.5

Figure 1.5: Metabolic and interorganellar transport processes catalyzed by enzymes residing in the cytosol, ER, mitochondria, LD, and peroxisomes alter the concentrations of various lipid classes in yeast cells. A T-bar in red depicts the CL-dependent negative feedback on the transport of PA from the ER to the IMM. See text for further details. Other abbreviations not specified in the text include: Ale1, acyltransferase for lysophosphatidylethanolamine 1; App1, actin patch protein 1; Are1/2, acyl-coenzyme A: cholesterol acyl transferase-related enzymes 1 and 2; Ayr1, acyl-dihydroxyacetone-phosphate reductase 1; Cds1, CDP-diacylglycerol synthase 1; Cho1/2, choline requiring 1 and 2; Cld1, cardiolipin-specific deacylase 1; Crd1, cardiolipin synthase 1; Dga1, diacylglycerol acyltransferase 1; Dpp1, diacylglycerol pyrophosphate phosphatase 1; Faa1 and Faa4, fatty acid activation proteins 1 and 4; Fas1 and Fas2, fatty acid synthetases 1 and 2; Fat1, fatty acid transporter 1; Fox1, Fox2 and Fox3, fatty acid oxidation proteins 1, 2 and 3; Gep4, genetic interactor of prohibitins protein 4; Gpt2, glycerol-3-phosphate acyltransferase; Loa1, lysophosphatidic acid: oleoyl-CoA acyltransferase 1; Lpp1, lipid phosphate

phosphatase 1; Lro1, lecithin cholesterol acyl transferase related open reading frame 1; MLCL, monolysocardiolipin; Opi3, overproducer of inositol 3; Pah1, phosphatidic acid phosphohydrolase 1; Pgs1, phosphatidylglycerolphosphate synthase 1; Pis1, phosphatidylinositol synthase 1; Psd1, phosphatidylserine decarboxylase 1; Sct1, suppressor of choline-transport mutants 1; Slc1 and Slc4, sphingolipid compensation proteins 1 and 4; Tam41, translocator assembly and maintenance protein 41; Taz1, tafazzin protein 1; Tgl1, Tgl3, Tgl4, Tgl5, triglyceride lipases 1, 3, 4 and 5; Ups1 and Ups2, unprocessed proteins 1 and 2; Yju3, monoglyceride lipase.

1.6 The objectives of studies described in this thesis

The studies described here had the following two objectives.

First, I sought to investigate how CR influences the concentrations of all lipid classes (not only TAG and CL concentrations) within HD and LD cell sub-populations of the wild-type (WT) strain on different stages of the chronological aging process. As I indicated earlier, an HD cell sub-population contains both Q and NQ cells; the percentage of NQ cells in the HD sub-population slowly increases during chronological aging (Leonov et al., 2017). An LD cell sub-population also contains both Q and NQ cells; however, the percentage of NQ cells in the LD sub-population increases quicker during chronological aging than in the HD sub-population (Leonov et al., 2017). To attain my first objective, I used centrifugation in a Percoll density gradient to purify these cell sub-populations from WT yeast cultured under CR or non-CR conditions and recovered on different days of culturing. I then employed liquid chromatography coupled with tandem mass spectrometry (LC-MS/MS) to identify and quantitate various lipid classes present in these cell sub-populations.

It needs to be emphasized that my study is the first attempt to assess the dynamics of changes in the entire lipidome of Q and NQ cells at different stages of the chronological aging process. Therefore, it was unclear if these age-related changes in the lipidomes of Q and NQ cells are permanent through the chronological aging process or there are some critical periods of the aging process at which the specific changes occur.

My second objective was to compare the effects of CR, the *tor1Δ* mutation and lithocholic acid (LCA) on the lipidomes of the HD and LD cell sub-populations on different stages of chronological aging. All these geroprotectors significantly increase the chronological lifespan (CLS) of yeast (Figure 1.6).

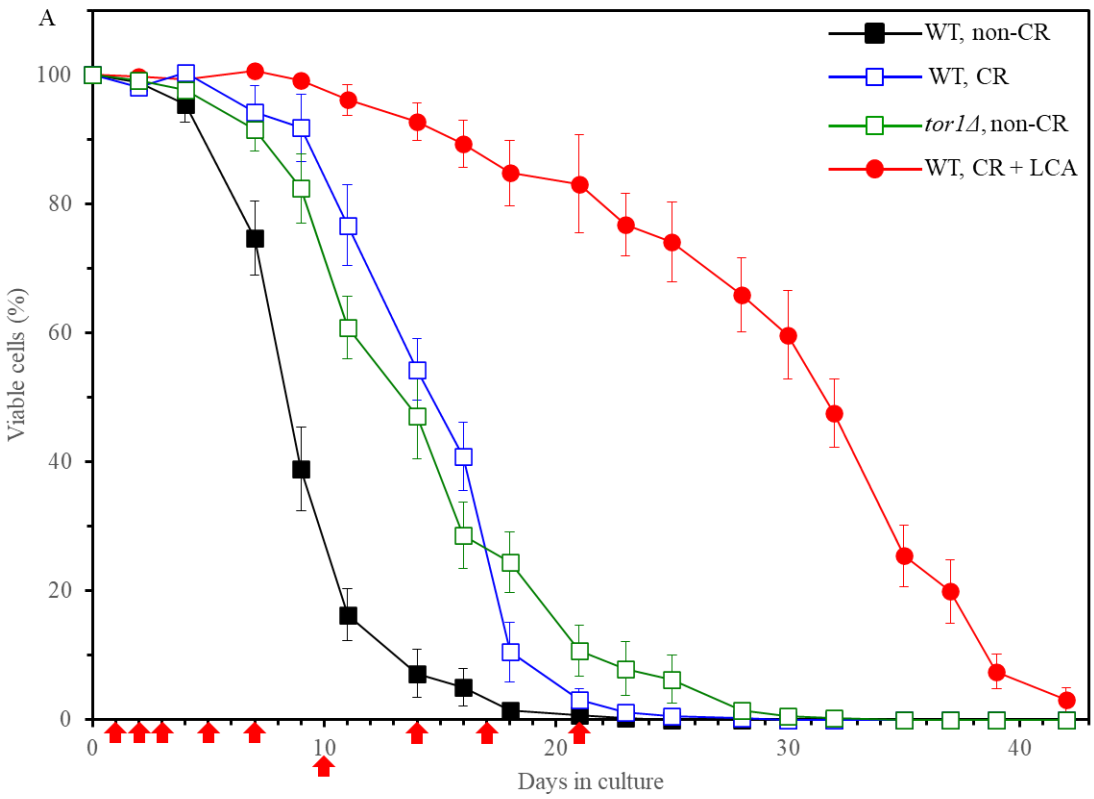

Figure 1.6: The longevity of chronologically aging can be prolonged by CR, the *tor1Δ* mutation and LCA. The effect of CR on yeast longevity was assessed in WT cells cultured in the nutrient-rich YP medium supplemented with 0.2% (w/v) glucose; WT cells cultured in the same medium supplemented with 2% (w/v) glucose were used as a control non-CR culture in these experiments. The effect of the *tor1Δ* mutation (in the BY4742 genetic background) on yeast longevity was assessed in the mutant yeast cells cultured in the YP medium supplemented with 2% (w/v) glucose; WT cells cultured in the same medium supplemented with 2% (w/v) glucose were used as a control culture in these experiments. The effect of LCA on yeast longevity was assessed in WT cells cultured in the YP medium supplemented with 0.2% (w/v) glucose and 50 μM; WT cells cultured in the same medium supplemented with 0.2% (w/v) glucose and lacking LCA were used as a control culture in these experiments. Survival curves are shown. Data are presented as means ± SEM (n = 3). CLS extension was significant for all three longevity-extending interventions tested ($p < 0.05$; the logrank test was used to calculate the p values for comparing each pair of survival curves). Arrows mark the time points at which cell aliquots were taken for the lipidomic analysis by LC-MS/MS.

There were three reasons for choosing CR, the *tor1Δ* mutation and LCA for these studies. The first reason was that these three geroprotectors differ from each other in the way of applying them to slow aging. Indeed, CR is a dietary geroprotective intervention, the *tor1Δ* mutation is a genetic geroprotective intervention and LCA is a pharmacological geroprotective intervention. The second reason was that these three geroprotectors delay aging by targeting different cellular processes. In fact, CR is a geroprotective dietary regimen that slows budding yeast's chronological aging by affecting carbohydrate and lipid metabolism, protein import into various organelles, different aspects of mitochondrial functionality, protein synthesis in the cytosol and mitochondria, cellular proteostasis, autophagic degradation of aged, dysfunctional and damaged macromolecules and organelles, cell resistance to various chronic (long-lasting) stresses, and cell susceptibility to the apoptotic and necrotic forms of RCD (Longo et al., 2012; Arlia-Ciommo et al., 2014). The *tor1Δ* mutation inactivates the TORC1 protein complex; TORC1 is known to delay budding yeast's chronological aging by influencing protein synthesis in the cytosol and mitochondria, autophagic degradation of aged, dysfunctional and damaged macromolecules and organelles, and cell resistance to different chronic stresses (Longo et al., 2012; Arlia-Ciommo et al., 2014). LCA is a pharmacological geroprotective agent that accumulates in the inner and outer mitochondrial membranes and alters the number, size and functional state of mitochondria (Beach et al., 2015; Leonov et al., 2017). The third reason for choosing CR, the *tor1Δ* mutation and LCA for these studies, was that LCA delays yeast chronological aging and extends longevity significantly more efficiently than the two other geroprotective interventions (Figure 1.6). Thus, it was plausible that LCA affects the lipidomes of the HD and LD cell sub-populations differently than the two other geroprotectors.

In studies described here, yeast cells were cultured in the nutrient-rich YP (1% yeast extract and 2% peptone) medium supplemented with glucose as a sole carbon source. The effect of CR on the cellular lipidome was examined in WT cells cultured in the YP medium supplemented with 0.2% (w/v) glucose; WT cells cultured in the same medium supplemented with 2% (w/v) glucose were used as a control non-CR culture in these experiments. The effect of the *tor1Δ* mutation (in the BY4742 genetic background) on the cellular lipidome was examined in the mutant yeast cells cultured in the YP medium supplemented with 2% (w/v) glucose, the most efficient glucose concentration for observing the longevity-extending effect of *tor1Δ* (Goldberg et al., 2009); WT cells cultured in the same medium supplemented with 2% (w/v) glucose were used as a control

culture in these experiments. The effect of LCA on the cellular lipidome was examined in WT cells cultured in the YP medium supplemented with 0.2% (w/v) glucose and 50 μM, the most efficient glucose and LCA concentrations for observing the longevity-extending effect (Goldberg et al., 2010); WT cells cultured in the same medium supplemented with 0.2% (w/v) glucose and lacking LCA were used as a control culture in these experiments.

Chapter 2: Materials and Methods

2.1 Yeast strains, media and growth conditions

The wild-type (WT) strain *Saccharomyces cerevisiae* BY4742 (*MATα his3Δ1 leu2Δ0 lys2Δ0 ura3Δ0*) from Thermo Scientific/Open Biosystems was grown in YP medium (1% yeast extract, 2% peptone, both from Fisher Scientific) initially containing the following: 1) 2% (w/v) glucose (Fisher Scientific) as a carbon source, 2) 0.2% (w/v) glucose as a carbon source or 3) 0.2% (w/v) glucose as a carbon source and 50 μM lithocholic acid (LCA). The *tor1Δ* single-gene-deletion mutant strain in the BY4742 genetic background from Thermo Scientific/Open Biosystems was grown in YP medium initially containing 2% (w/v) glucose as a carbon source. Cells were cultured at 30ºC with rotational shaking at 200 rpm in Erlenmeyer flasks at a "flask volume/medium volume" ratio of 5:1. Cell aliquots for the separation of high-density and low-density quiescent cells by centrifugation in Percoll density gradient were collected on days 1, 2, 3, 5, 7, 10, 14, 17 and 21 of culturing.

2.2 Separation of high-density and low-density quiescent cells by centrifugation in Percoll density gradient

2 ml of 1.5 M NaCl (#S7653; Sigma) was placed into a 50-ml conical polypropylene centrifuge tube (#055398; Fisher Scientific), and 16 ml of the Percoll solution (#P1644; Sigma) was added to this tube. The NaCl and Percoll solutions were then mixed by pipetting. To form four Percoll density gradients, 4 ml of the NaCl/Percoll mixture was put into each of the four polyallomer tubes for an MLS-50 rotor for an Optima MAX ultracentrifuge (all from Beckman Coulter, Inc.). The tubes were centrifuged at 25,000 × g (16,000 rpm) for 15 min at 4ºC in an Optima MAX ultracentrifuge. A sample of yeast cells was taken from a culture at a particular time-point (see section 2.1). A fraction of the sample was diluted to determine the total number of cells per ml of culture using a hemacytometer (#0267110; Fisher Scientific). For each Percoll density gradient, 1×10^9 yeast cells were placed into a 15-ml conical polypropylene centrifuge tube (#0553912; Fisher Scientific) and then pelleted by centrifugation at 5,000 rpm for 7 min at room temperature in an IEC Centra CL2 clinical centrifuge (Thermo Electron Corporation). Pelleted cells were resuspended in 500 μl of 50 mM Tris/HCl buffer (pH 7.5), overlaid onto the preformed Percoll gradient and centrifuged at 2,300 × g (5,000 rpm) for 30 min at 25ºC in an Optima MAX

ultracentrifuge. The upper and lower fractions of cells were collected with a pipette, Percoll was removed by washing cells twice with 50 mM Tris/HCl buffer (pH 7.5) and cells were resuspended in 50 mM Tris/HCl buffer (pH 7.5) for lipid extraction.

2.3 Identification and quantitation of cellular lipids using liquid chromatography coupled with tandem mass spectrometry (LC-MS/MS)

After measuring the cell titer with the help of a hemocytometer, a volume of the cell suspension in 50 mM Tris/HCl buffer (pH 7.5) that contains the total number of 5.0×10^7 cells was transferred into a pre-cooled at 4ºC 1.5-ml microcentrifuge Eppendorf tube. The cells were harvested by centrifugation at 16,000 × g for 1 min at 4°C, and the supernatant was discarded. 1.5 ml of ice-cold nano-pure water was added to the pellet, the cells were washed by centrifugation at 16,000 × g for 1 min at 4°C, and the supernatant was discarded. 1.5 ml of ice-cold ammonium bicarbonate (ABC) solution was added to the pellet, the cells were washed by centrifugation at 16,000 × g for 1 min at 4°C, and the supernatant was discarded. The cell pellet was stored at -80°C before lipid extraction. After being held at -80 °C, the cell pellet on ice was thawed on ice and then resuspended in 200 µl of ice-cold nano-pure water. The cell suspension was transferred to a 15-ml high-strength glass screw-top centrifuge tube with a polytetrafluoroethylene lined cap. The following was added to this tube: 1) 25 µl of the mixture of internal lipid standards prepared in chloroform/methanol (2:1) mixture, 2) 100 µl of 425–600 µM acid-washed glass beads, and 3) 600 µl of chloroform/methanol (17:1) mixture. The tube was vortexed at high speed for 5 min at room temperature (RT) to disrupt the cells. The tube was then vortexed at low speed for 1 h at RT to facilitate lipids extraction. The sample was incubated for 30 min on ice to promote protein precipitation and the separation of the aqueous and organic phases from each other. The tube was centrifuged in a clinical centrifuge at 3,000 × g for 5 min at RT to facilitate the separation of the upper aqueous phase and the lower organic phase, which contained all lipid classes. A borosilicate glass pipette was used to transfer the lower organic phase (~400 µl) to another 15-ml high-strength glass screw-top centrifuge tube with a polytetrafluoroethylene lined cap. The lower organic phase was kept under the flow of nitrogen gas. 300 µl of chloroform-methanol (2:1) mixture was added to the remaining upper aqueous phase to allow the extraction of sphingolipids, lysophosphatidic acid (LPA), lysophosphatidylglycerol (LPG), lysophosphatidylinositol (LPI), lysophosphatidylserine (LPS), phosphatidic acid (PA), phosphatidylglycerol (PG),

phosphatidylinositol (PI) and phosphatidylserine (PS). The tube was vortexed vigorously for 5 min at RT and then centrifuged in a clinical centrifuge at 3,000 × g for 5 min at RT. A borosilicate glass pipette was used to transfer the lower organic phase (~ 200 µl) formed after centrifugation to the organic phase collected at the previous step. The solvent in the combined organic phases was evaporated under the flow of nitrogen gas. The tube containing the lipid film was closed under the flow of nitrogen gas and then stored at -80 °C.

500 µl of acetonitrile (ACN)/2-propanol/nano-pure water (65:35:5) mixture was added to a tube containing the lipid film stored at -80°C, and the tube was vortexed 3 times for 10 s at RT. The tube's content was subjected to ultrasonic sonication for 15 min, and the tube was vortexed again 3 times for 10 s at RT. 100 µl of a sample was taken from the tube and added to a glass vial with an insert used for a wellplate. An LC system was used to separate different lipid species on a reverse-phase C18 column CSH coupled to a pre-column system (Waters). During lipid separation, the column was maintained at 55°C and a flow rate of 0.3 ml/min, and the sample was kept in the wellplate at RT. The mobile phases that consisted of mixture A (ACN/water [60:40 (v/v)]) and mixture B (isopropanol/ACN [90:10 (v/v)]) were used for the chromatographic separation of lipids. For a positive mode of detecting parent ions created using the electrospray ionization (ESI) ion source, the ESI (+) mode, the mobile phases A and B contained ammonium formate at the final concentration of 10 mM. For a negative mode of parent ions detection, the ESI (-) mode, the mobile phases A and B contained ammonium acetate at the final concentration of 10 mM. A sample volume of 10 µl was used for the injection into both the ESI (+) and ESI (-) mode. Different lipid species were separated by LC using the following LC gradient: 0–1 min 10% (phase B); 1–4 min 60% (phase B); 4–10 min 68% (phase B); 10–21 min 97% (phase B); 21–24 min 97% (phase B); 24–33 min 10% (phase B). Extraction blanks were run as the first sample, between every four samples, and as the last sample. The background was subtracted to normalize data.

A mass spectrometer equipped with a HESI (heated electrospray ionization) ion source was used to analyze lipids separated by LC. The settings used for such analysis are provided in Table 2.1. The Fourier transform analyzer was used to detect parent ions (MS1) at a resolution of 60,000 and within the mass range of 150–2,000 Da. The settings shown in Table 2.2 were used to detect secondary ions (MS2).

The Lipid Search software (V4.1; Fisher Scientific) was used to identify and quantify different lipids from raw LC-MS/MS files. This software uses the largest lipid database, containing

more than 1.5 million lipid ion precursors (MS1) and their predicted fragment ions (MS2). The software also uses MS1 peaks for lipid quantitation and MS2 for lipid identification. LC-MS raw files containing full-scan MS1 data and data-dependent MS2 data were searched for free (unesterified) fatty acids (FFA), cardiolipin (CL), PA, phytoceramide (PHC), phytosphingosine (PHS), phosphatidylcholine (PC), phosphatidylethanolamine (PE), PG, PI, PS, LPA, lysophosphatidylcholine (LPC), LPG, lysophosphatidylethanolamine (LPE), LPI, LPS, and triacylglycerol (TAG) lipid classes. The m/z tolerance values of 5 ppm and 10 ppm were used for MS1 and MS2 ions. Other search parameters are provided in Table 2.3. To identify and quantitate different lipid classes and species with the help of freely available open-source alternatives for the Lipid Search software, the Lipid Data Analyzer (http://genome.tugraz.at/lda2/lda_download.shtml), MZmine 2 (http://mzmine.github.io/) or XCMS (https://bioconductor.org/packages/release/bioc/html/xcms.html) software can be used to process raw data from LC-MS/MS.

Table 2.1: The settings used for mass spectrometric analysis of lipids that were separated by LC. Abbreviation: HESI, heated electrospray ionization.

FTMS - p resolution	60000
Mass range (dalton)	150-2000
Ion source type	HESI
Capillary temperature (°C)	300
Source heater temperature (°C)	300
Sheath gas flow	10
Aux gas flow	5
Positive polarity voltage (kV)	3
Negative polarity voltage (kV)	3
Source current (µA)	100

Table 2.2: The settings for detecting MS2 ions with the help of the Fourier transform analyzer.

Instrument polarity	Positive	Negative
Activation type	High-energy-induced-collision-dissociation	Collision-induced-dissociation
Minimal signal required	5000	5000
Isolation width	2	2
Normalized collision energy	55	35
Default charge state	2	2
Activation time	0.1	10
FTMS - C resolution	7500	
5 most intense peaks were selected for ms/ms		

Table 2.3: The parameters used to identify and quantify lipids from the LC-MS raw files containing full-scan MS1 data and data-dependent MS2 data.

Identification	
Database	Orbitrap
Peak detection	Recall isotope (ON)
Search option	Product search Orbitrap
Search type	Product
Experiment type	LC-MS
Precursor tolerance	10 ppm
Product tolerance	High-energy-induced-collision-dissociation [ESI (+) mode]: 20 ppm
	Collision-induced-dissociation [ESI (-) mode]: 0.5 Daltons
Quantitation	
Execute quantitation	ON
m/z tolerance	-5.0; +5.0
Tolerance type	ppm

Filter	
Top rank filter	ON
Main node filter	Main isomer peak
m-score threshold	5
c-score threshold	2
FFA priority	ON
ID quality filter	A: Lipid class & all fatty acids are completely identified
	B: Lipid class & some fatty acids are identified
	C: Lipid class or FA are identified
	D: Lipid identified by other fragment ions (H2O, etc.)
Lipid Class	
High-energy-induced-collision-dissociation [ESI (+) mode]	PC, TAG
Collision-induced-dissociation [ESI (-) mode]	CER, CL, FFA, PE, PG, PI, PS
Ions	
High-energy-induced-collision-dissociation [ESI (+) mode]	+ H; + NH4; + Na
Collision-induced-dissociation [ESI (-) mode]	- H; - 2H; - HCOO

Chapter 3: Results

3.1 Only CR, but not the *tor1Δ* mutation or LCA, significantly decreases TAG concentration in HD and LD cells through most of the chronological lifespan

The previous study has shown that CR reduces TAG concentration in both HD and LD cell sub-populations through most chronological lifespans (Leonov et al., 2017). A mass spectrometric quantitative assessment of the yeast lipidome in these experiments was performed using the direct-injection method (Leonov et al., 2017). Since then, Concordia's Centre for Biological Applications of Mass Spectrometry has changed the standard operating procedures by prohibiting using direct-injection methods for lipidomics and metabolomics. Therefore, the Titorenko laboratory has developed a novel liquid chromatography coupled with a tandem mass spectrometry (LC-MS/MS) method of quantitative lipidomics (Mohammad et al., 2020). I used the LC-MS/MS method of quantitative lipidomics in my studies.

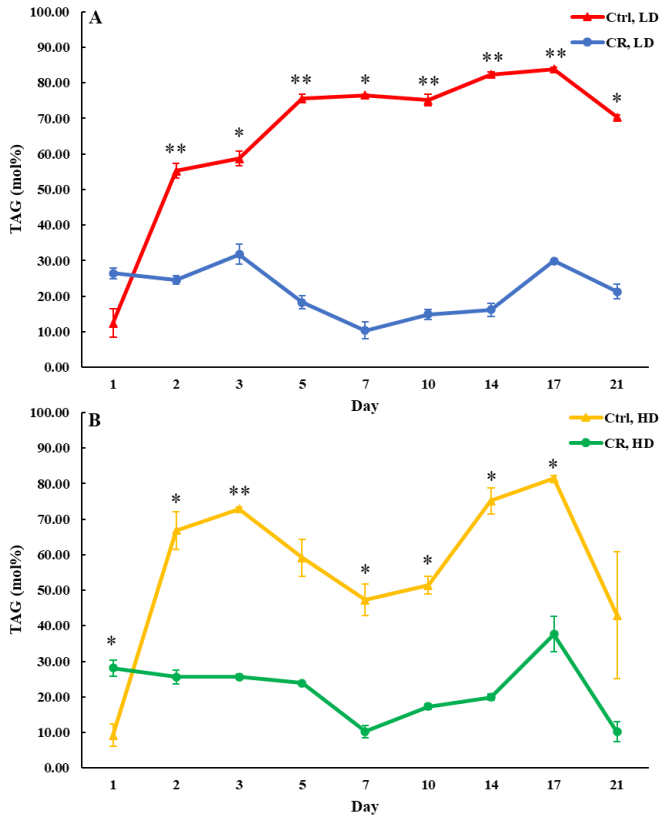

Figure 3.1. CR decreases TAG concentration in HD and LD cells through most of the chronological lifespan. Samples of WT yeast cultured in YP medium initially containing 0.2% glucose (CR conditions) or 2% glucose (control non-CR conditions) were recovered on different days of culturing and subjected to centrifugation in Percoll density gradient to purify HD and LD cell sub-populations. TAG concentrations were measured by LC-MS/MS. Data are presented as means ± SD (n = 2; *P < 0.05; **P < 0.01).

As I mentioned in the Introduction section, an HD cell sub-population is a mixture of Q and NQ cells; the percentage of NQ cells in this cell sub-population slowly rises during chronological lifespan (Leonov et al., 2017). An LD cell sub-population is also a mixture of Q and NQ cells; however, the percentage of NQ cells in this cell sub-population increases faster during chronological aging than in the HD cell sub-population (Leonov et al., 2017).

I confirmed that CR lowers TAG concentration in both HD and LD cells through most of the chronological lifespan (Figures 3.1A and 3.1B), except for day 1 of culturing. Yet, neither the *tor1Δ* mutation nor LCA elicited long-lasting changes in TAG concentrations within HD or LD cells (Figures 3.2A, 3.2B, 3.3A and 3.3B, respectively). Of note, the *tor1Δ* mutation increased TAG concentration in HD cells between days 5 and 10 of cell culturing (Figure 3.2B), whereas LCA decreased TAG concentration in HD cells between days 10 and 17 of cell culturing (Figure 3.3B).

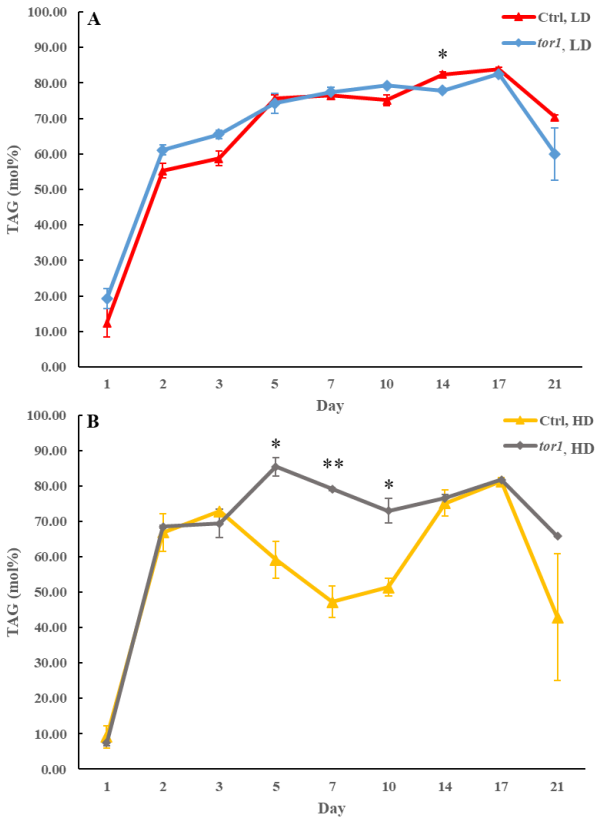

Figure 3.2. The *tor1Δ* mutation increases TAG concentration in HD cells between days 5 and 10 of cell culturing. Samples of WT (control) and *tor1Δ* yeast cultured in YP medium initially containing 2% glucose (non-CR conditions) were recovered on different days of culturing and subjected to centrifugation in Percoll density gradient to purify HD and LD cell sub-populations. TAG concentrations were measured by LC-MS/MS. Data are presented as means ± SD (n = 2; *P < 0.05; **P < 0.01).

Based on these observations, I concluded that, while CR creates a continuing trend of decreasing TAG concentration in both HD and LD cells through the most chronological lifespan,

neither the *tor1Δ* mutation nor LCA exhibits a similar long-lasting effect on TAG concentration. The future research will address the importance of a temporary rise of TAG in HD cells carrying the *tor1Δ* mutation (Figure 3.2B). The significance of a temporary decline in TAG concentration within HD cells of WT treated with LCA also remains unclear (Figure 3.3B).

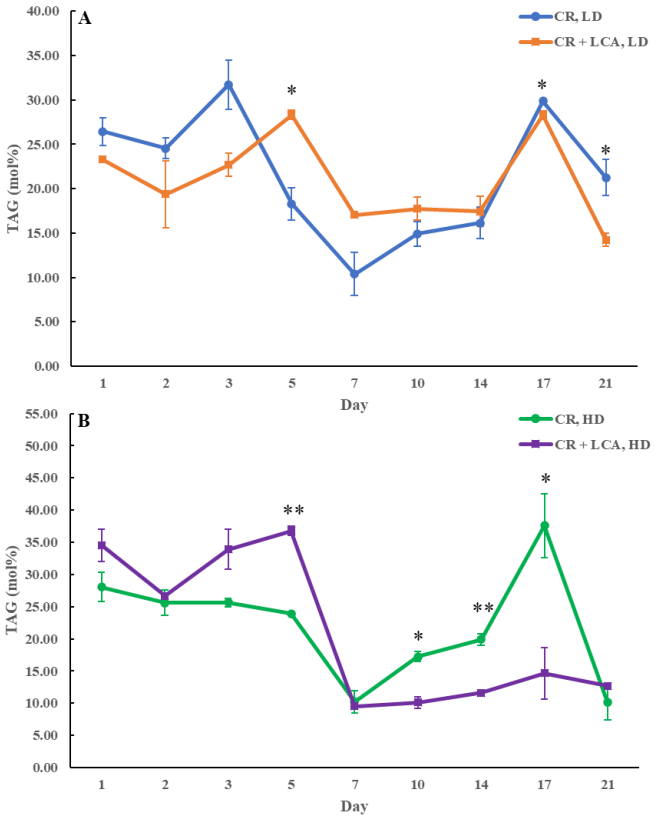

Figure 3.3. LCA decreases TAG concentration in HD cells between days 10 and 17 of cell culturing. Samples of WT yeast cultured in YP medium initially containing 0.2% glucose (CR conditions) with 50 μM LCA or without it (control) were recovered on different days of culturing and subjected to centrifugation in Percoll density gradient to purify HD and LD cell sub-populations. TAG concentrations were measured by LC-MS/MS. Data are presented as means ± SD (n = 2; *P < 0.05; **P < 0.01).

3.2 Only CR, but not the *tor1Δ* mutation or LCA, significantly increases FFA concentration in HD and LD cells through most of the chronological lifespan

One way of decreasing TAG concentration in HD and LD cells under CR conditions is by stimulating TAG lipolysis within lipid droplets (LD) (Figure 1.5). The stimulation of TAG lipolysis alone results in a rise of free fatty acids (FFA) (Figure 1.5). Suppose such stimulation of TAG lipolysis and FFA formation within LD does not coincide with a change in FFA oxidation rate within peroxisomes. In that case, TAG lipolysis stimulation is expected to increase the intracellular concentration of FFA (Figure 1.5). I observed a significant rise in FFA concentration within HD and LD cells under CR conditions after day 2 of the chronological lifespan (Figure 3.4). Thus, CR intensifies TAG lipolysis in LD without changing the rate of FFA oxidation in

peroxisomes (Figure 1.5). The *tor1Δ* mutation decreased FFA concentration in HD cells between days 5 and 10 of cell culturing (Figure 3.5B). Moreover, although LCA increased FFA concentration in LD cells and altered FFA concentration in HD cells through most of the chronological lifespan, LCA treatment effects on FFA concentration within HD and LD cells were not as dramatic as the ones for CR (Figures 3.6A and 3.6B).

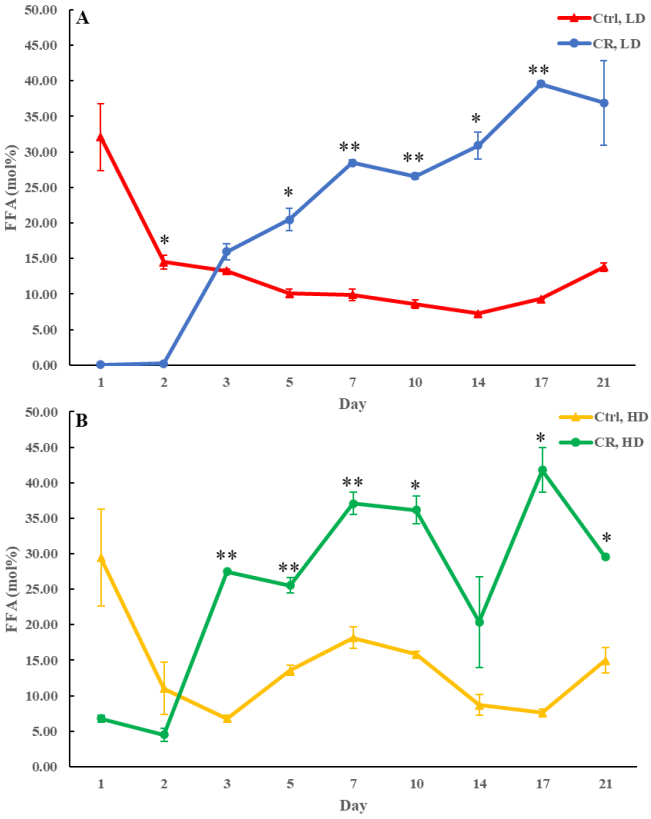

Figure 3.4. CR significantly increases FFA concentration in HD and LD cells after day 2 of the chronological lifespan. Samples of WT yeast cultured in YP medium initially containing 0.2% glucose (CR conditions) or 2% glucose (control non-CR conditions) were recovered on different days of culturing and subjected to centrifugation in Percoll density gradient to purify HD and LD cell sub-populations. FFA concentrations were measured by LC-MS/MS. Data are presented as means ± SD (n = 2; *P < 0.05; **P < 0.01).

Based on these observations, I concluded that, while CR creates a long-lasting trend of significantly rising FFA concentration in both HD and LD cells through the most chronological lifespan, neither the *tor1Δ* mutation nor LCA shows a similar continuing effect on FFA concentration.

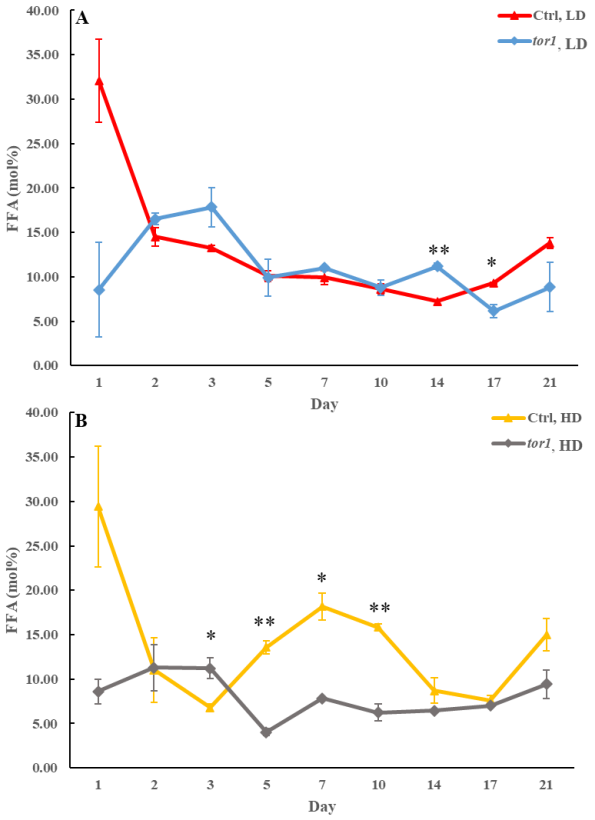

Figure 3.5. The *tor1Δ* mutation decreases FFA concentration in HD cells between days 5 and 10 of cell culturing. Samples of WT (control) and *tor1Δ* yeast cultured in YP medium initially containing 2% glucose (non-CR conditions) were recovered on different days of culturing and subjected to centrifugation in Percoll density gradient to purify HD and LD cell sub-populations. FFA concentrations were measured by LC-MS/MS. Data are presented as means ± SD (n = 2; *P < 0.05; **P < 0.01).

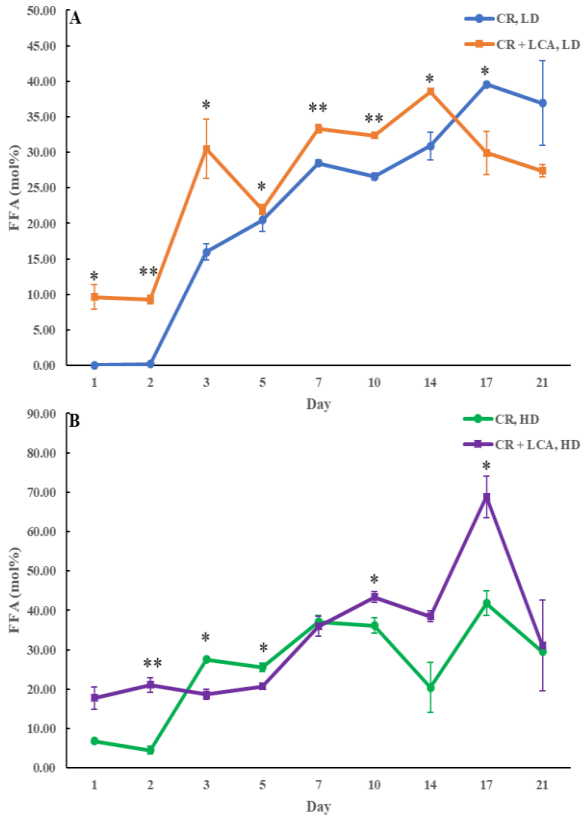

Figure 3.6. LCA increases FFA concentration in LD cells and alters FFA concentration in HD cells through most of the chronological lifespan. Samples of WT yeast cultured in YP medium initially containing 0.2% glucose (CR conditions) with 50 μM LCA or without it (control) were recovered on different days of culturing and subjected to centrifugation in Percoll density gradient to purify HD and LD cell sub-populations. FFA concentrations were measured by LC-MS/MS. Data are presented as means ± SD (n = 2; *P < 0.05; **P < 0.01).

3.3 Neither CR, the *tor1Δ* mutation nor LCA has a long-lasting effect on DAG concentration in HD and LD cells through the chronological lifespan

The other way of decreasing TAG concentration in HD and LD cells under CR conditions is by lowering TAG synthesis from DAG within the endoplasmic reticulum (ER) (Figure 1.5). CR did not cause any statistically significant change in DAG concentration (neither in HD cells nor in LD cells) through the chronological lifespan (Figure 3.7). Therefore, I concluded that deterioration of TAG synthesis from DAG does not elicit the observed long-term decline in TAG concentration within these cells under CR conditions. Of note, neither the *tor1Δ* mutation nor LCA caused a significant continuing effect on DAG concentration in HD and LD cells (Figures 3.8 and 3.9, respectively).

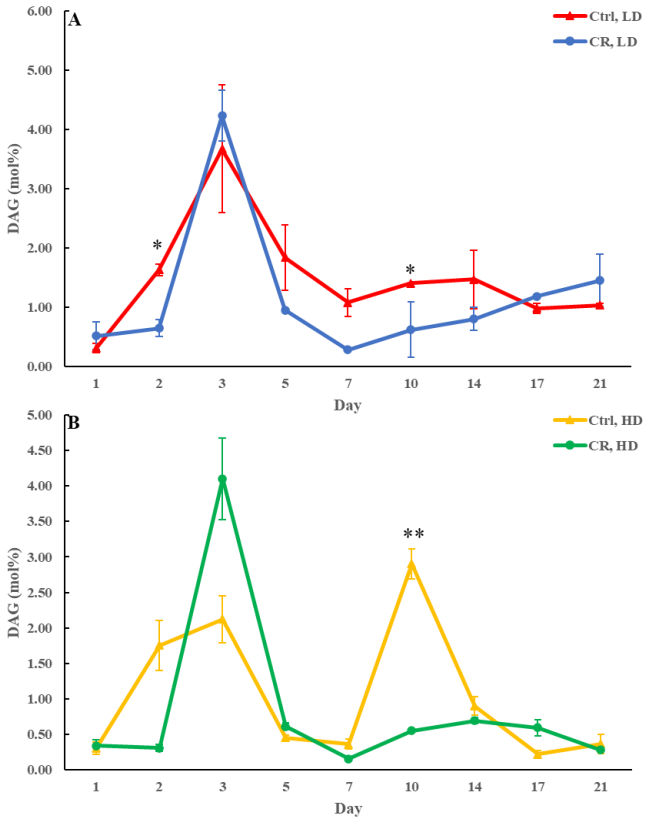

Figure 3.7. CR does not have a long-lasting effect on DAG concentration in HD and LD cells through the chronological lifespan. Samples of WT yeast cultured in YP medium initially containing 0.2% glucose (CR conditions) or 2% glucose (control non-CR conditions) were recovered on different days of culturing and subjected to centrifugation in Percoll density gradient to purify HD and LD cell sub-populations. DAG concentrations were measured by LC-MS/MS. Data are presented as means ± SD (n = 2; *P < 0.05; **P < 0.01).

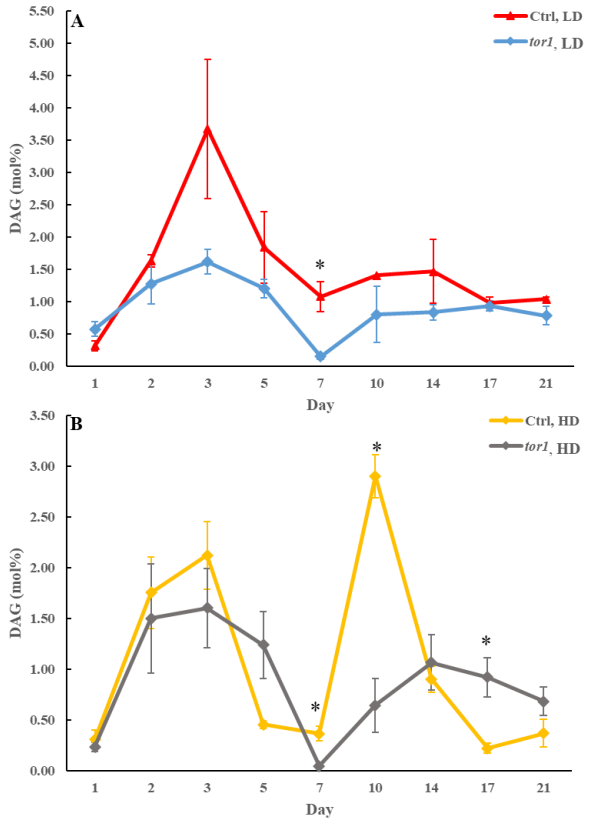

Figure 3.8. The *tor1Δ* mutation does not have a long-lasting effect on DAG concentration in HD and LD cells through the chronological lifespan. Samples of WT (control) and *tor1Δ* yeast cultured in YP medium initially containing 2% glucose (non-CR conditions) were recovered on different days of culturing and subjected to centrifugation in Percoll density gradient to purify HD and LD cell sub-populations. DAG concentrations were measured by LC-MS/MS. Data are presented as means ± SD (n = 2; *P < 0.05; **P < 0.01).

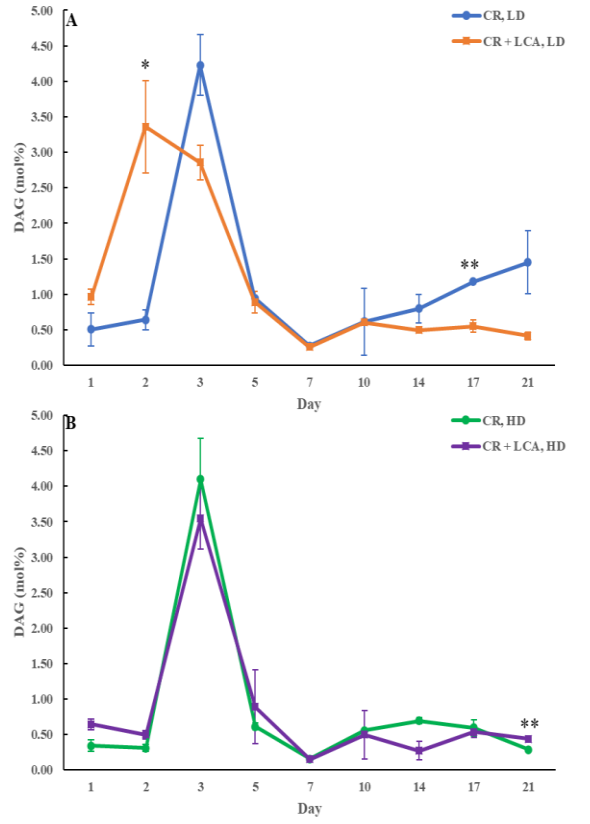

Figure 3.9. LCA does not have a long-lasting effect on DAG concentration in HD and LD cells through the chronological lifespan. Samples of WT yeast cultured in YP medium initially containing 0.2% glucose (CR conditions) with 50 μM LCA or without it (control) were recovered on different days of culturing and subjected to centrifugation in Percoll density gradient to purify HD and LD cell sub-populations. DAG concentrations were measured by LC-MS/MS. Data are presented as means ± SD (n = 2; *P < 0.05; **P < 0.01).

3.4 Only CR, but not the *tor1Δ* mutation or LCA, significantly increases ceramide (CER) concentration in LD cells through the entire chronological lifespan

To assess the flow of the excessive amounts of FFA accumulating in HD and LD cells under CR conditions, I analyzed how CR influences CER concentrations in these cells. CER is formed in the ER from fatty acyl-CoA esters of palmitic acid and serine (Dickson, 2008; Dickson, 2010). I found that CR significantly increases CER concentration in LD cells through the entire chronological lifespan (Figure 3.10A). CR also raised CER concentration in HD cells through the entire chronological lifespan, but this rise was not statistically significant (Figure 3.10B). In contrast, the *tor1Δ* mutation decreased CER concentration in HD cells through the most chronological lifespan (Figure 3.11B). LCA exhibited a similar effect on CER concentration in LD cells (Figure 3.12A).

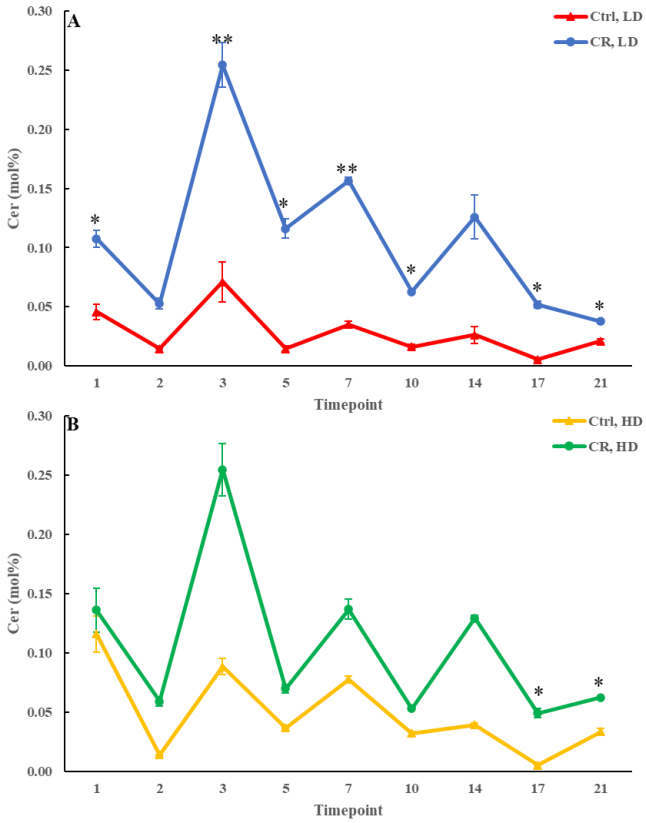

Figure 3.10. CR significantly increases CER concentration in LD cells through the entire chronological lifespan. Samples of WT yeast cultured in YP medium initially containing 0.2% glucose (CR conditions) or 2% glucose (control non-CR conditions) were recovered on different days of culturing and subjected to centrifugation in Percoll density gradient to purify HD and LD cell sub-populations. CER concentrations were measured by LC-MS/MS. Data are presented as means ± SD (n = 2; *P < 0.05; **P < 0.01).

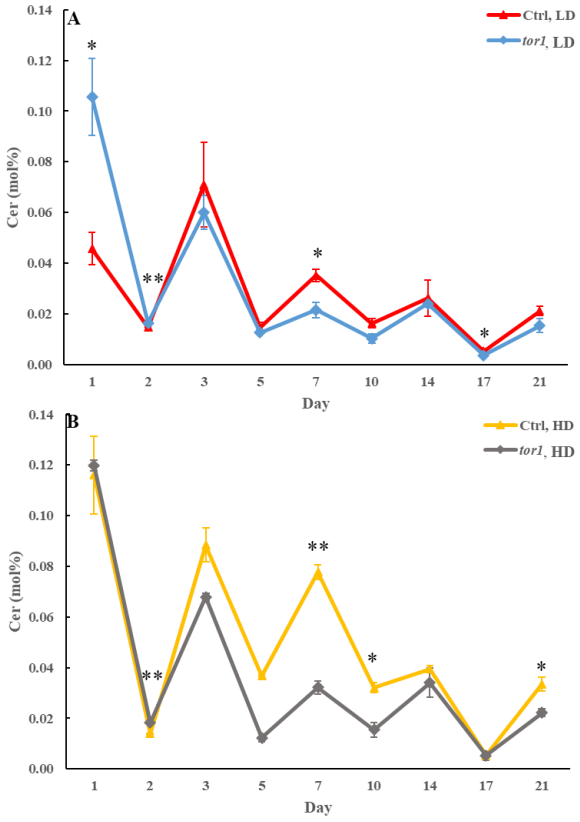

Figure 3.11. The *tor1Δ* mutation decreases CER concentration in HD cells through most of the chronological lifespan. Samples of WT (control) and *tor1Δ* yeast cultured in YP medium initially containing 2% glucose (non-CR conditions) were recovered on different days of culturing and subjected to centrifugation in Percoll density gradient to purify HD and LD cell sub-populations. CER concentrations were measured by LC-MS/MS. Data are presented as means ± SD (n = 2; *P < 0.05; **P < 0.01).

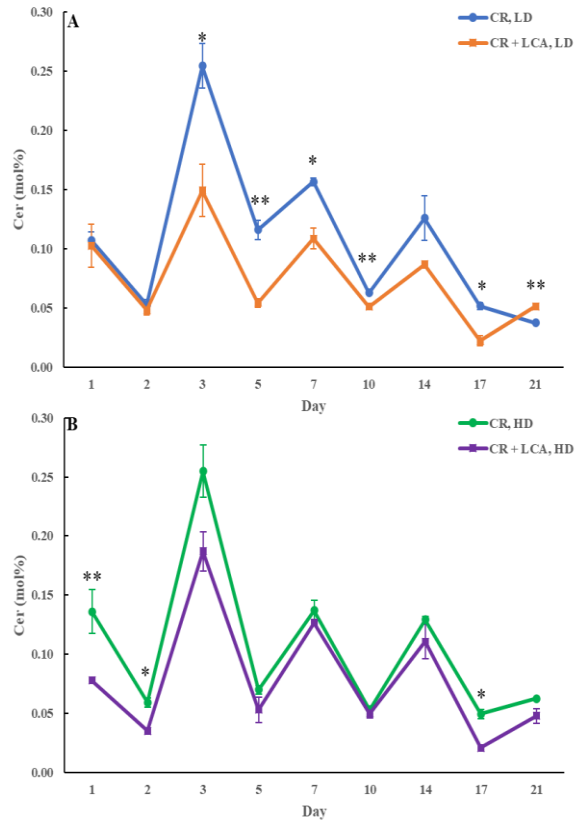

Figure 3.12. LCA decreases CER concentration in LD cells through most of the chronological lifespan. Samples of WT yeast cultured in YP medium initially containing 0.2% glucose (CR conditions) with 50 μM LCA or without it (control) were recovered on different days of culturing and subjected to centrifugation in Percoll density gradient to purify HD and LD cell sub-populations. CER concentrations were measured by LC-MS/MS. Data are presented as means ± SD (n = 2; *P < 0.05; **P < 0.01).

3.5 Neither CR, the *tor1Δ* mutation nor LCA has a long-lasting effect on the concentrations of complex sphingolipids (SPH) in HD and LD cells through the chronological lifespan

SPH are the lipids generated in the ER from CER (Dickson, 2008; Dickson, 2010). I found that, although CR significantly increases CER concentration in LD cells, this low-calorie diet does not considerably affect SPH concentrations in HD and LD cells through the chronological lifespan (Figure 3.13). Noteworthy, neither the *tor1Δ* mutation nor LCA caused a significant long-lasting effect on SPH concentrations in HD and LD cells (Figures 3.14 and 3.15, respectively).

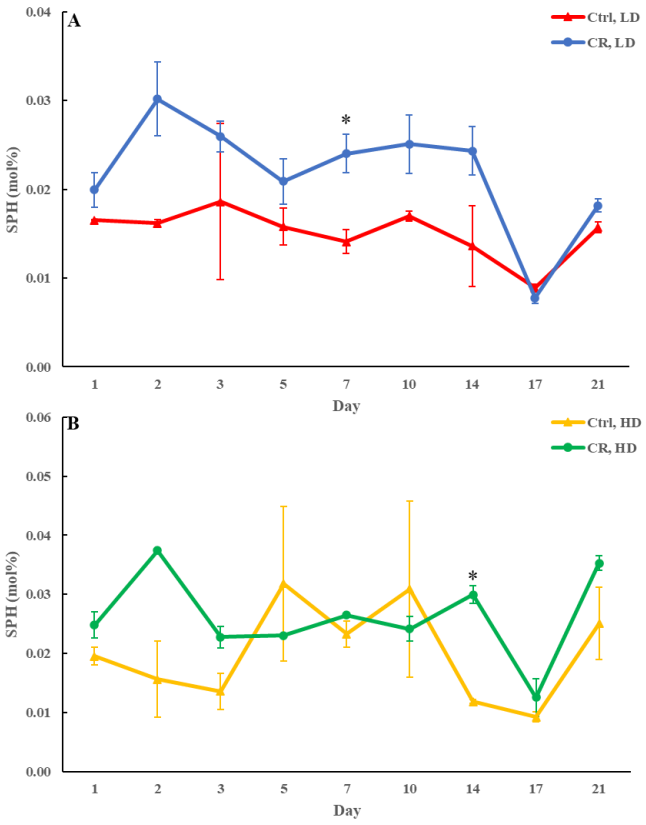

Figure 3.13. CR does not significantly alter SPH concentrations in HD and LD cells through the chronological lifespan. Samples of WT yeast cultured in YP medium initially containing 0.2% glucose (CR conditions) or 2% glucose (control non-CR conditions) were recovered on different days of culturing and subjected to centrifugation in Percoll density gradient to purify HD and LD cell sub-populations. SPH concentrations were measured by LC-MS/MS. Data are presented as means ± SD (n = 2; *P < 0.05).

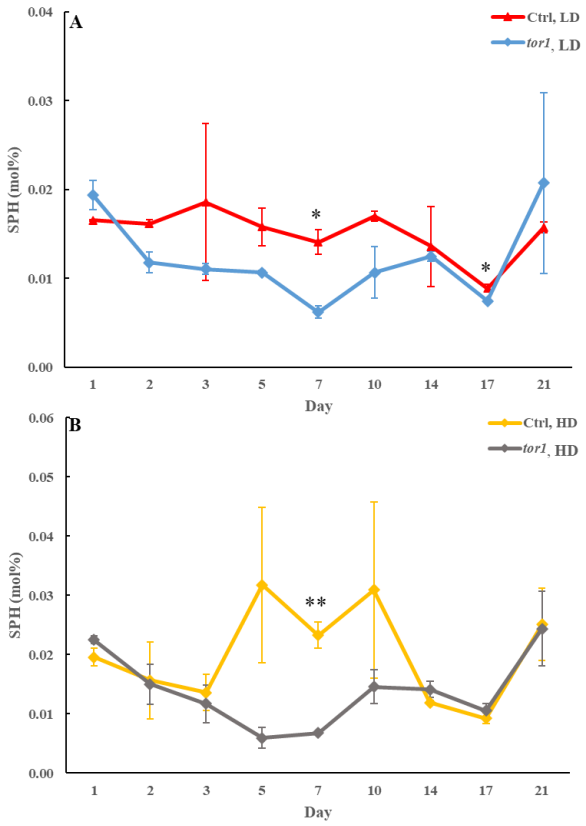

Figure 3.14. The *tor1Δ* mutation does not cause a significant long-lasting effect on SPH concentrations in HD and LD cells. Samples of WT (control) and *tor1Δ* yeast cultured in YP medium initially containing 2% glucose (non-CR conditions) were recovered on different days of culturing and subjected to centrifugation in Percoll density gradient to purify HD and LD cell sub-populations. SPH concentrations were measured by LC-MS/MS. Data are presented as means ± SD (n = 2; *P < 0.05; **P < 0.01).

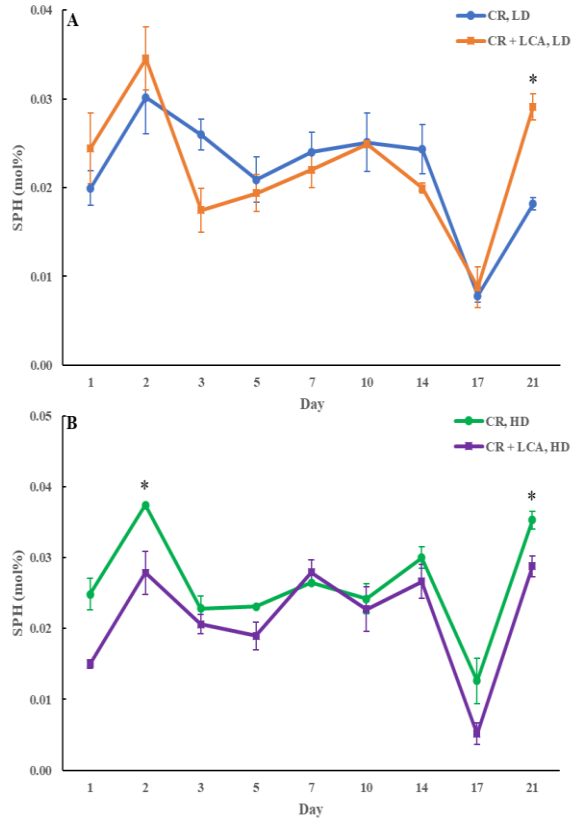

Figure 3.15. LCA does not elicit a significant continuing effect on SPH concentrations in HD and LD cells. Samples of WT yeast cultured in YP medium initially containing 0.2% glucose (CR conditions) with 50 μM LCA or without it (control) were recovered on different days of culturing and subjected to centrifugation in Percoll density gradient to purify HD and LD cell sub-populations. SPH concentrations were measured by LC-MS/MS. Data are presented as means ± SD (n = 2; *P < 0.05).

3.6 Only CR, but not the *tor1Δ* mutation or LCA, significantly increases the concentrations of all ER- and mitochondria-synthesized phospholipids in HD and LD cells through most of the chronological lifespan

I assessed the concentrations of phospholipids in differently aged HD and LD cells. These phospholipids included the so-called major forms of phospholipids (Carman and Han, 2011; Henry et al., 2012; Klug and Daum, 2014) LPA, PA, PI, PS and PC synthesized in the ER (Figure 1.5) as well as PE, PG and CL formed in mitochondria (Figure 1.5). These phospholipids included the so-called minor forms of phospholipids (Carman and Han, 2011; Henry et al., 2012; Klug and Daum, 2014) lysophosphatidylinositol (LPI), lysophosphatidylserine (LPS), lysophosphatidylethanolamine (LPE), lysophosphatidylcholine (LPC), and lysophosphatidylglycerol (LPG). These minor forms of phospholipids are synthesized in the enzymatic reactions catalyzed by the broad-specificity lysophospholipid acyltransferase Ale1 in the ER, LPC acyltransferase Taz1 in mitochondria, and LPI acyltransferase Psi1 in LD and mitochondria (Carman and Han, 2011; Henry et al., 2012; Klug and Daum, 2014). I found that CR increases the concentrations of all these phospholipids in HD and LD cells through most of the chronological lifespan. Please see below the data for the effects of CR on LPA (Figure 3.16), PA (Figure 3.17), PI (Figure 3.18), PS (Figure 3.19), PE (Figure 3.20), PC (Figure 3.21), LPI (Figure 3.22), LPS (Figure 3.23), LPE (Figure 3.24), LPC (Figure 3.25), PG (Figure 3.26), CL (Figure 3.27) and LPG (Figure 3.28). Of note, a relative rise in the concentrations of many of these phospholipids within short-lived LD sub-populations of Q and NQ cells exceeded that in long-lived HD sub-populations of Q and NQ cells.

Unlike CR, neither the *tor1Δ* mutation nor LCA elicited significant and long-lasting changes in all these phospholipids' concentrations within HD and LD cells. Please see the appendix (chapter 6) for the data on how *tor1Δ* and LCA affected LPA (Figures 6.1 and 6.2), PA (Figures 6.3 and 6.4), PI (Figures 6.5 and 6.6), PS (Figures 6.7 and 6.8), PE (Figures 6.9 and 6.10), PC (Figures 6.11 and 6.12), LPI (Figures 6.13 and 6.14), LPS (Figures 6.15 and 6.16), LPE (Figures 6.17 and 6.18), LPC (Figures 6.19 and 6.20), PG (Figures 6.21 and 6.22), CL (Figures 6.23 and 6.24) and LPG (Figures 6.25 and 6.26) concentrations in differently aged HD and LD cells.

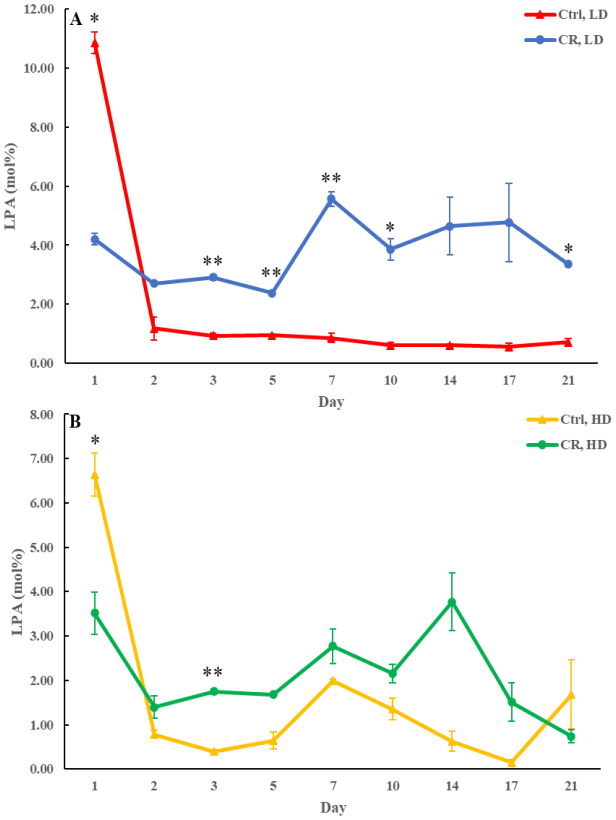

Figure 3.16. CR increases LPA concentration in HD and especially in LD cells after day 1 of the chronological lifespan. Samples of WT yeast cultured in YP medium initially containing 0.2% glucose (CR conditions) or 2% glucose (control non-CR conditions) were recovered on different days of culturing and subjected to centrifugation in Percoll density gradient to purify HD and LD cell sub-populations. LPA concentrations were measured by LC-MS/MS. Data are presented as means ± SD (n = 2; *P < 0.05; **P < 0.01).

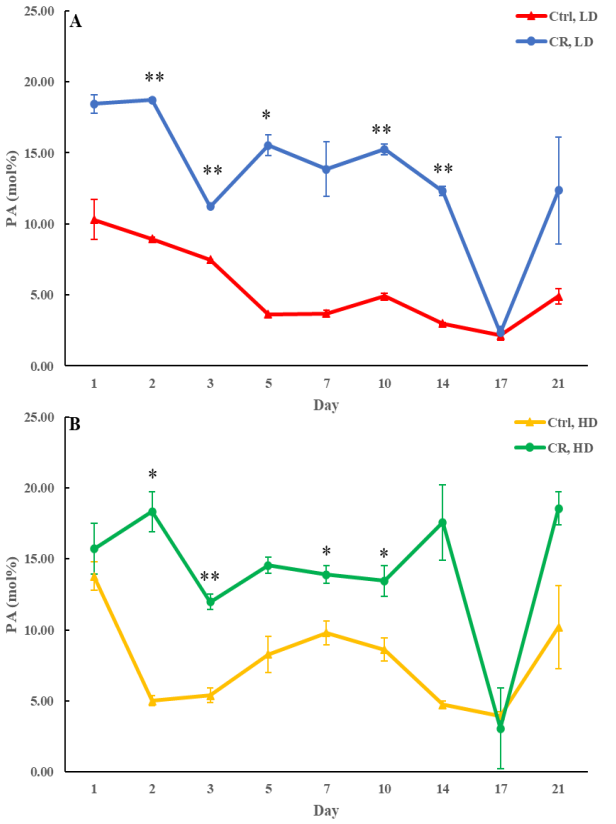

Figure 3.17. CR significantly rises PA concentration in both HD and LD cells through the chronological lifespan. Samples of WT yeast cultured in YP medium initially containing 0.2% glucose (CR conditions) or 2% glucose (control non-CR conditions) were recovered on different days of culturing and subjected to centrifugation in Percoll density gradient to purify HD and LD cell sub-populations. PA concentrations were measured by LC-MS/MS. Data are presented as means ± SD (n = 2; *P < 0.05; **P < 0.01).

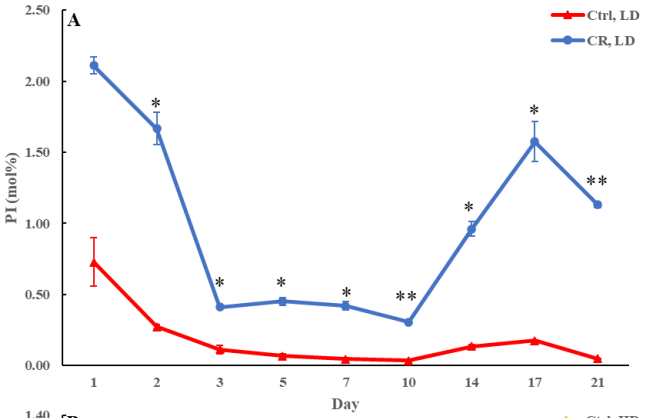

Figure 3.18. CR significantly increases PI concentration in HD and especially in LD cells through the entire chronological lifespan. Samples of WT yeast cultured in YP medium initially containing 0.2% glucose (CR conditions) or 2% glucose (control non-CR conditions) were recovered on different days of culturing and subjected to centrifugation in Percoll density gradient to purify HD and LD cell sub-populations. PI concentrations were measured by LC-MS/MS. Data are presented as means ± SD (n = 2; *P < 0.05; **P < 0.01).

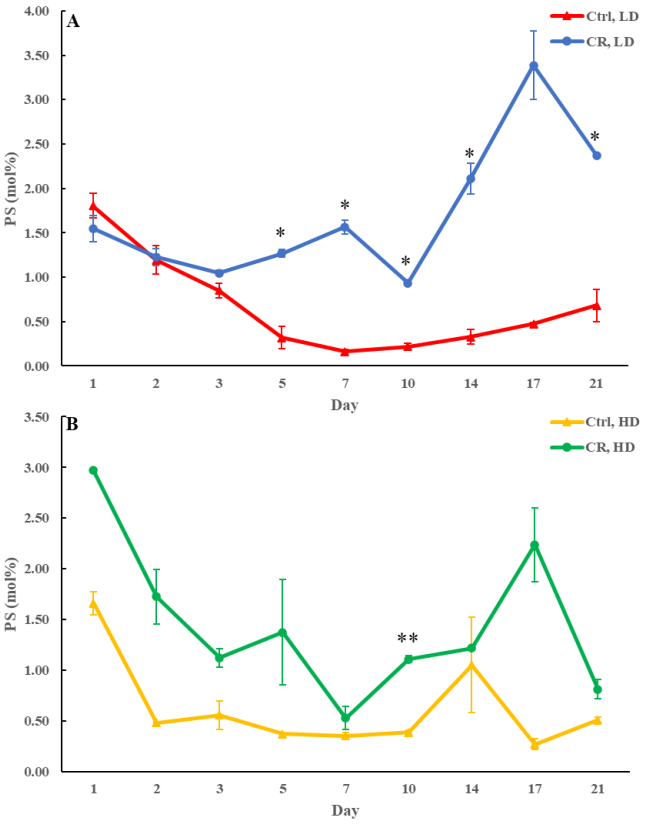

Figure 3.19. CR rises PS concentration in HD and especially in LD cells throughout the chronological lifespan. Samples of WT yeast cultured in YP medium initially containing 0.2% glucose (CR conditions) or 2% glucose (control non-CR conditions) were recovered on different days of culturing and subjected to centrifugation in Percoll density gradient to purify HD and LD cell sub-populations. PS concentrations were measured by LC-MS/MS. Data are presented as means ± SD (n = 2; *P < 0.05; **P < 0.01).

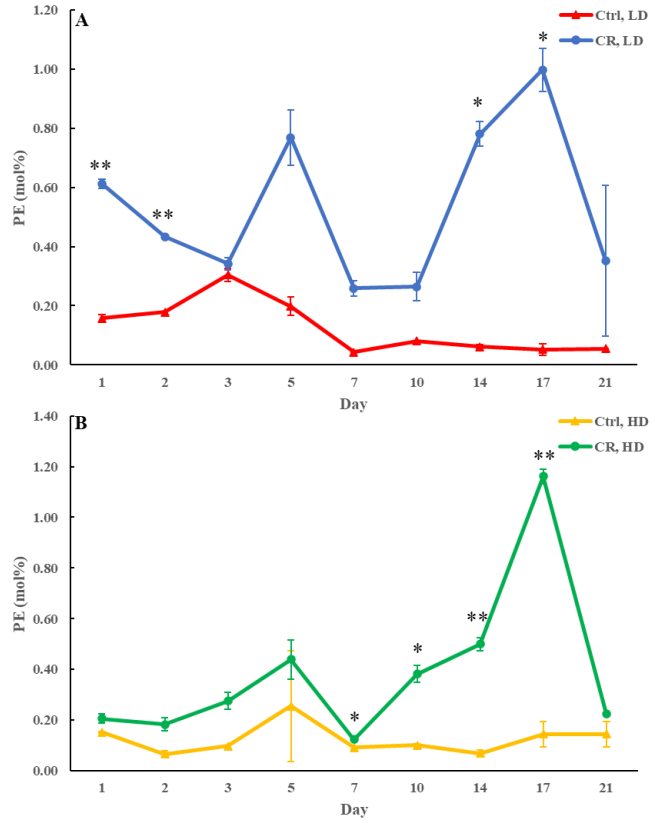

Figure 3.20. CR significantly rises PE concentration in both HD and LD cells through the chronological lifespan. Samples of WT yeast cultured in YP medium initially containing 0.2% glucose (CR conditions) or 2% glucose (control non-CR conditions) were recovered on different days of culturing and subjected to centrifugation in Percoll density gradient to purify HD and LD cell sub-populations. PE concentrations were measured by LC-MS/MS. Data are presented as means ± SD (n = 2; *P < 0.05; **P < 0.01).

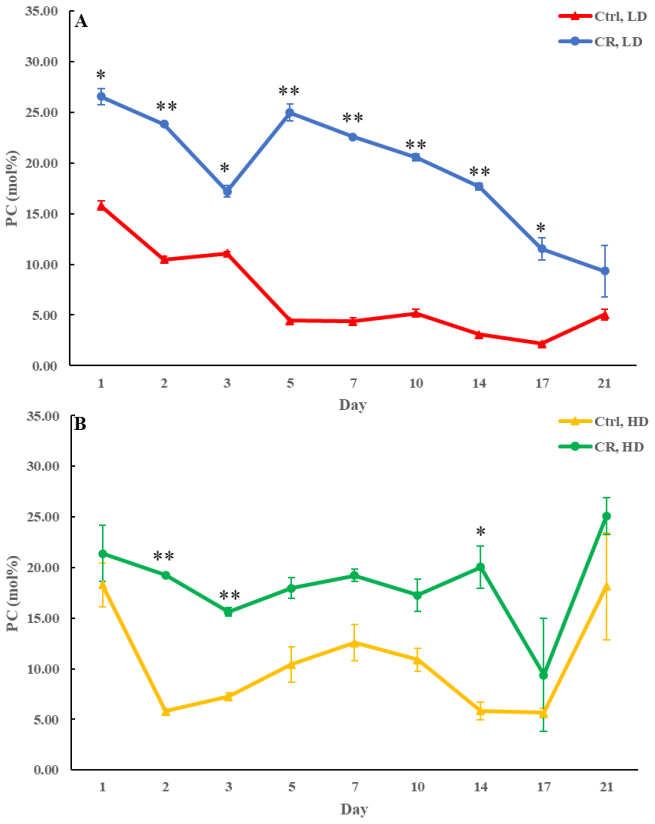

Figure 3.21. CR increases PC concentration in both HD and LD cells through the chronological lifespan. Samples of WT yeast cultured in YP medium initially containing 0.2% glucose (CR conditions) or 2% glucose (control non-CR conditions) were recovered on different days of culturing and subjected to centrifugation in Percoll density gradient to purify HD and LD cell sub-populations. PC concentrations were measured by LC-MS/MS. Data are presented as means ± SD (n = 2; *P < 0.05; **P < 0.01).

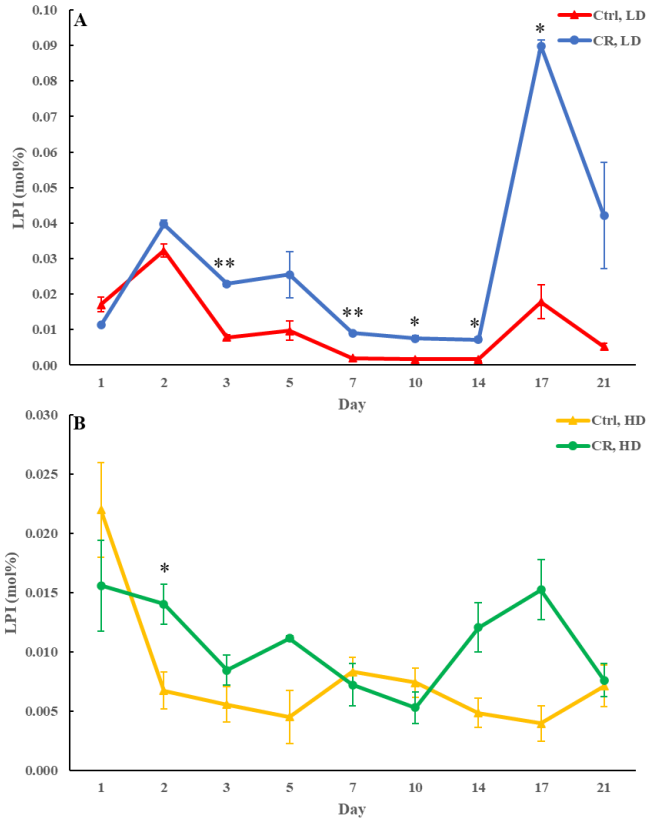

Figure 3.22. CR increases LPI concentration in LD cells throughout the chronological lifespan. Samples of WT yeast cultured in YP medium initially containing 0.2% glucose (CR conditions) or 2% glucose (control non-CR conditions) were recovered on different days of culturing and subjected to centrifugation in Percoll density gradient to purify HD and LD cell sub-populations. LPI concentrations were measured by LC-MS/MS. Data are presented as means ± SD (n = 2; *P < 0.05; **P < 0.01).

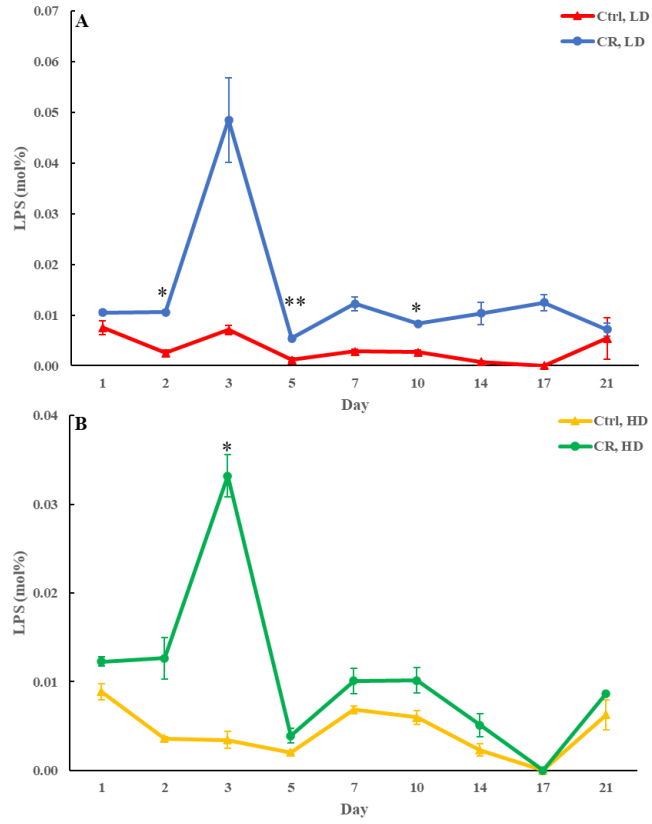

Figure 3.23. CR increases LPS concentration in LD and to a lesser degree in HD cells through the chronological lifespan. Samples of WT yeast cultured in YP medium initially containing 0.2% glucose (CR conditions) or 2% glucose (control non-CR conditions) were recovered on different days of culturing and subjected to centrifugation in Percoll density gradient to purify HD and LD cell sub-populations. LPS concentrations were measured by LC-MS/MS. Data are presented as means ± SD (n = 2; *P < 0.05; **P < 0.01).

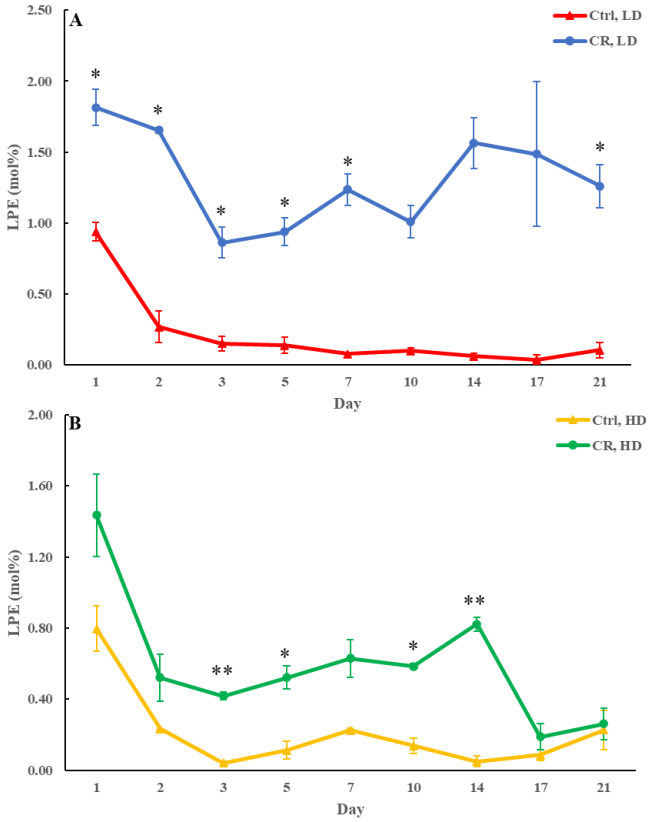

Figure 3.24. CR significantly increases LPE concentration in HD and especially in LD cells throughout the chronological lifespan. Samples of WT yeast cultured in YP medium initially containing 0.2% glucose (CR conditions) or 2% glucose (control non-CR conditions) were recovered on different days of culturing and subjected to centrifugation in Percoll density gradient to purify HD and LD cell sub-populations. LPE concentrations were measured by LC-MS/MS. Data are presented as means ± SD (n = 2; *P < 0.05; **P < 0.01).

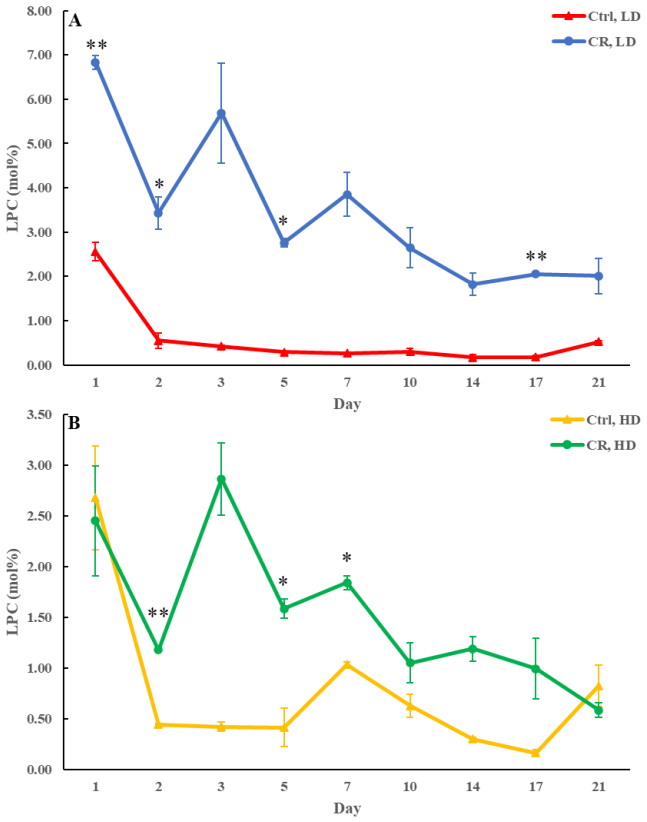

Figure 3.25. CR significantly rises LPC concentration in both HD and LD cells through the chronological lifespan. Samples of WT yeast cultured in YP medium initially containing 0.2% glucose (CR conditions) or 2% glucose (control non-CR conditions) were recovered on different days of culturing and subjected to centrifugation in Percoll density gradient to purify HD and LD cell sub-populations. LPC concentrations were measured by LC-MS/MS. Data are presented as means ± SD (n = 2; *P < 0.05; **P < 0.01).

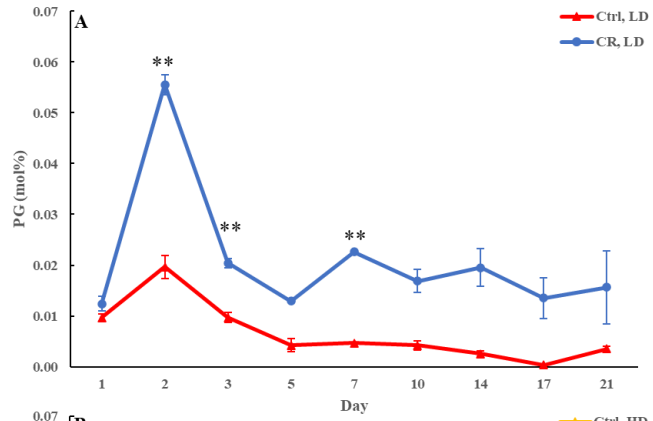

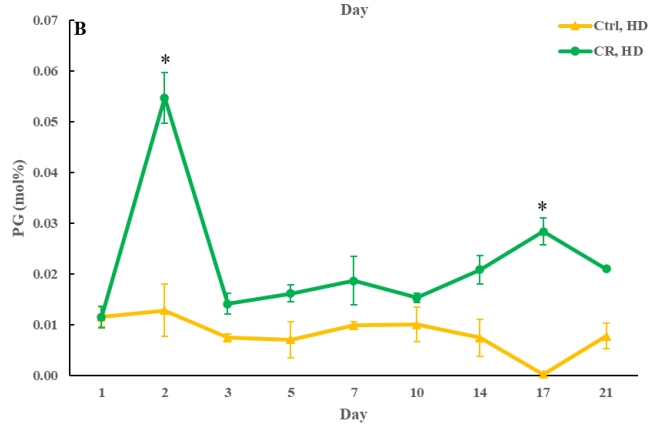

Figure 3.26. CR increases LPS concentration in LD and to a lesser degree in HD cells through the chronological lifespan. Samples of WT yeast cultured in YP medium initially containing 0.2% glucose (CR conditions) or 2% glucose (control non-CR conditions) were recovered on different days of culturing and subjected to centrifugation in Percoll density gradient to purify HD and LD cell sub-populations. LPS concentrations were measured by LC-MS/MS. Data are presented as means ± SD (n = 2; *P < 0.05; **P < 0.01).

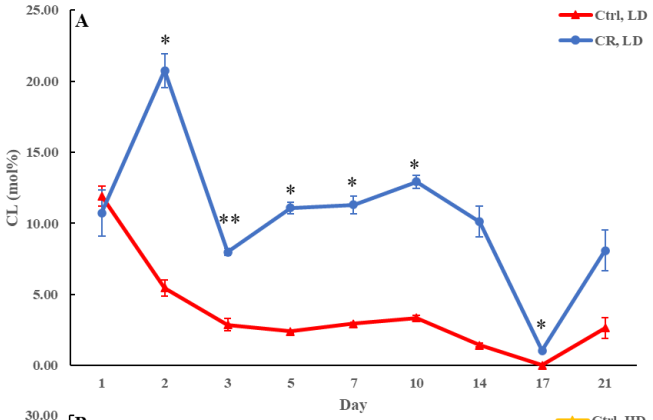

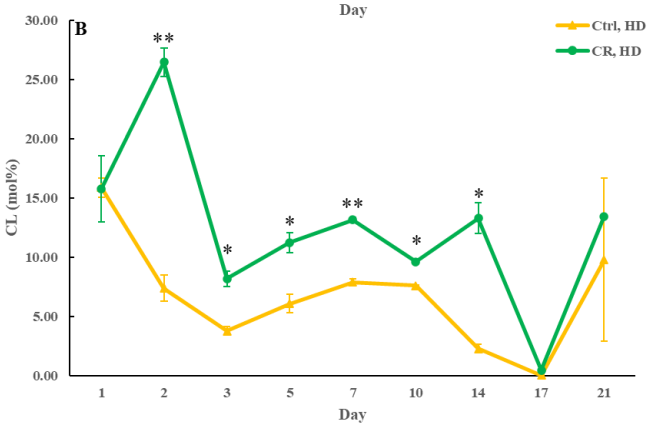

Figure 3.27. CR significantly increases CL concentration in HD and especially in LD cells throughout the chronological lifespan. Samples of WT yeast cultured in YP medium initially containing 0.2% glucose (CR conditions) or 2% glucose (control non-CR conditions) were recovered on different days of culturing and subjected to centrifugation in Percoll density gradient to purify HD and LD cell sub-populations. CL concentrations were measured by LC-MS/MS. Data are presented as means ± SD (n = 2; *P < 0.05; **P < 0.01).

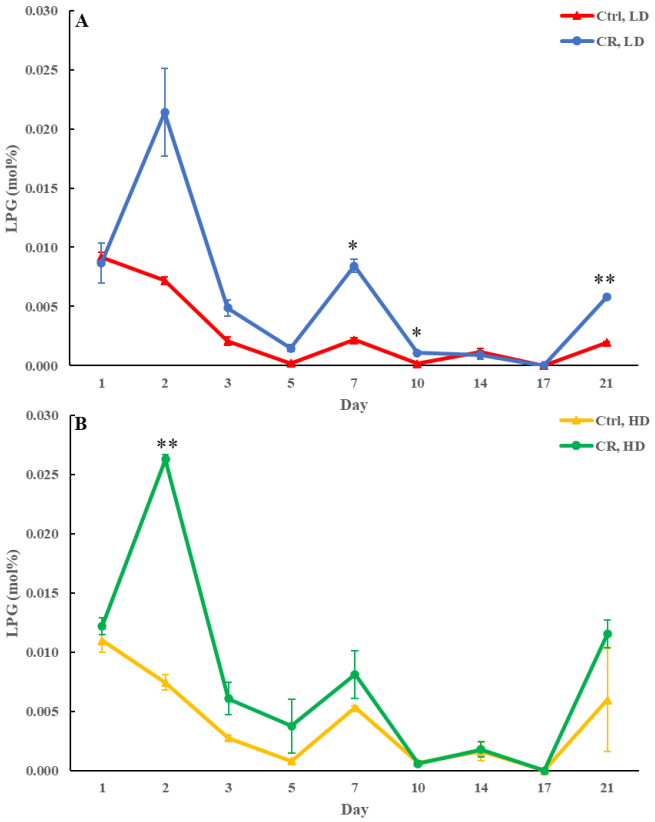

Figure 3.28. CR increases LPG concentration in HD and LD cells through most of the chronological lifespan. Samples of WT yeast cultured in YP medium initially containing 0.2% glucose (CR conditions) or 2% glucose (control non-CR conditions) were recovered on different days of culturing and subjected to centrifugation in Percoll density gradient to purify HD and LD cell sub-populations. LPG concentrations were measured by LC-MS/MS. Data are presented as means ± SD (n = 2; *P < 0.05; **P < 0.01).

Chapter 4: Discussion

4.1 CR causes a distinct remodeling of the entire lipidome in HD and LD cells through most of the chronological lifespan

I used Percoll density centrifugation to purify HD and LD cells from differently aged yeast cultures incubated in a nutrient-rich medium initially containing 0.2% glucose (CR conditions) or 2% glucose (non-CR conditions) as a sole carbon source. An HD cell sub-population contains both Q and NQ cells. In the HD sub-population, Q cells undergo a relatively slow conversion into NQ cells during chronological aging (Leonov et al., 2017). An LD cell sub-population is also a mixture of Q and NQ cells. Q cells in the LD sub-population are converted into NQ cells faster during chronological aging than in HD cells' sub-population (Leonov et al., 2017). I used the LC-MS/MS-based quantitative lipidomics to assess the aging-associated changes in HD and LD cells' lipidomes. Previous studies showed that CR, a robust aging-delaying intervention in budding yeast and many other organisms, decreases TAG concentration and increases CL concentration in HD and LD cells. Here, I provided the first evidence that CR statistically significantly alters the concentrations of 18 different lipid classes through most of the chronological lifespan of HD and LD cells. To assess the aging-associated changes in each of these lipid classes, I calculated their concentrations in mol% of all lipids. My data indicate that CR elicits a characteristic remodeling of HD and LD cell lipidomes. This CR-specific remodeling of the entire cellular lipidome is outlined below and schematically depicted in Figure 4.1.

CR simulates TAG lipolysis in LD, likely by activating the neutral lipid hydrolases Tgl1, Tgl3, Tgl4, Tgl5 and Yju3 (Figure 4.1). The CR-driven stimulation of TAG lipolysis causes a significant rise in the intracellular concentrations of FFA in the cytosol (Figure 4.1). The flow of FFA under CR conditions is directed into the synthesis of CER and all phospholipid classes in the ER. These phospholipid classes include LPA, PA, PI, PS, PE and PC (Figure 4.1). The concentrations of CER, LPA, PA, PI, PS, PE and PC within HD and LD cells cultured under CR conditions exceed those in HD and LD cells not limited in calorie supply (Figure 4.1). CR also promotes PA, PS, PC and PI transport from the ER to mitochondria through the mitochondria-ER contact sites (Figure 4.1). The activation of PS transport into mitochondria results in the CR-dependent excessive synthesis of PE from PS in these organelles (Figure 4.1). The activation of PA, PC, and PI transport into mitochondria elicits the CR-dependent excessive PG and CL

synthesis in these organelles (Figure 4.1). The concentrations of PG and CL within HD and LD cells cultured under CR conditions are higher than those in HD and LD cells not limited in calorie supply (Figure 4.1).

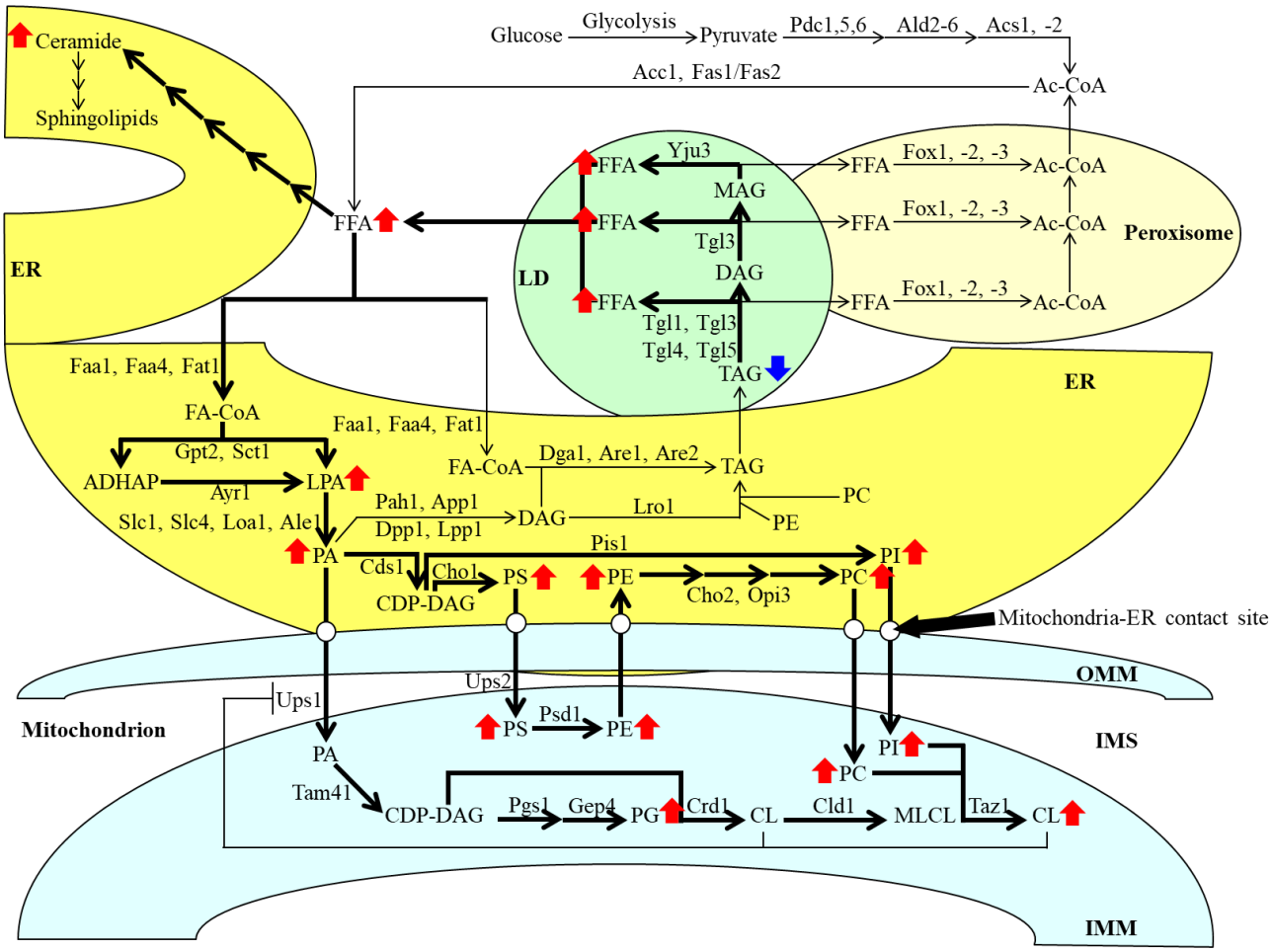

Figure 4.1. A model for a CR-dependent remodeling of lipid metabolism and transport in HD and LD cells. CR stimulates free fatty acids (FFA) formation because this low-calorie diet promotes the lipolysis of the neutral lipids triacylglycerols (TAG). CR also activates the incorporation of FFA into various phospholipid classes in the endoplasmic reticulum (ER) and mitochondria. Arrows next to the names of lipid classes indicate those of them whose concentrations are increased (red arrows) or decreased (blue arrows) in yeast cells cultured under CR conditions. The thickness of black arrows is proportional to the efficiency with which TAG is hydrolyzed, FFA is incorporated into phospholipids and phospholipids are transported from the ER to mitochondria via the mitochondria-ER contact sites. Abbreviations: CL, cardiolipin; CDP,

cytidine diphosphate; DAG, diacylglycerol; IMM, inner mitochondrial membrane; MLCL, monolysocardiolipin; OMM, outer mitochondrial membrane; PC, phosphatidylcholine; PE, phosphatidylethanolamine; PG, phosphatidylglycerol; PI, phosphatidylinositol; PS, phosphatidylserine. Other abbreviations are provided in the legends to Figure 1.5.

I hypothesize that the remodeling of HD and LD cells lipidomes under CR conditions may contribute to the CR-dependent aging delay and longevity extension of these cells. I suggest the following two mechanisms for such contribution. Most phospholipids whose concentrations rise under CR conditions are the ones that are synthesized and reside in the ER (Figure 4.1). The ER lipidome changes affect lipid and protein homeostasis within this organelle. These changes are known to activate the so-called unfolded protein response in the ER (UPR^{ER}) of yeast and other organisms (Fu et al., 2011; Halbleib et al., 2017; Almanza et al., 2019). After being activated, the UPR^{ER} system allows the restoration of lipid and protein homeostasis in the ER. This regulatory system accelerates lipid synthesis, slows protein translation and stimulates a refolding of improperly folded proteins in the ER (Almanza et al., 2019; Karagöz et al., 2019). The UPR^{ER} system is an essential contributor to aging delay and longevity extension in yeast and other organisms (Cui et al., 2015; Chadwick et al., 2019; Karagöz et al., 2019). Therefore, I hypothesize that one mechanism for delaying the chronological aging of yeast synthesizing excessive amounts of phospholipids in the ER under CR conditions may involve the activation of the UPR^{ER} system. The other mechanism for slowing the chronological aging of yeast synthesizing excessive amounts of PE, PG and CL in mitochondria under CR conditions may consist in the resulting improvement of certain aspects of mitochondrial functionality. These aspects include such pro-longevity processes as activated mitochondrial respiration, elevated mitochondrial membrane potential and altered mitochondrial ROS production observed in HD and LD sub-populations of Q and NQ cells (Leonov et al., 2017). Future studies for testing my hypotheses about the two mechanisms through which the observed remodeling of HD and LD cells lipidomes under CR conditions may contribute to the CR-dependent aging delay are needed. These future studies may involve experiments on assessing how mutations affecting the known protein components of the UPR^{ER} system, redundant enzymes catalyzing phospholipid formation in the ER (Figure 4.1) or enzymes catalyzing CL synthesis in the IMM of mitochondria influence the extent of the CR-dependent chronological aging delay in yeast.

I noticed that a relative increase in the concentrations of PI, PS, PE, LPI and LPE within the short-lived LD sub-populations of Q and NQ cells is higher than that within the long-lived HD sub-populations of Q and NQ cells. This observation suggests the existence of an optimal threshold of these phospholipid concentrations at which the maximal aging-delaying effect can be achieved. I hypothesize that the concentrations of PI, PS, PE, LPI and LPE in the long-lived HD sub-populations of Q and NQ cells are within the predicted optimal threshold. In contrast, the higher concentrations (i.e., above the optimal threshold) of PI, PS, PE, LPI and LPE in the short-lived LD sub-populations of Q and NQ cells may shorten their longevity because these concentrations are toxic for the cell. One way of testing my hypothesis in the future is to assess if the mutations affecting redundant enzymes that catalyze phospholipid synthesis in the ER (Figure 4.1) could slow the chronological aging of LD cells.

4.2 The effect of CR on the lipidomes of HD and LD cells differs from the impact of two other geroprotectors, the *tor1Δ* mutation and LCA

To attain my second objective, I compared the effects of CR (a dietary geroprotective intervention), the *tor1Δ* mutation (a genetic geroprotective intervention) and LCA (a pharmacological geroprotective intervention) on the lipidomes of HD and LD cells recovered on different stages of the chronological aging process. My comparative analysis revealed that CR creates a lipidomic pattern of chronologically aging HD and LD cells that differs from the lipidomic pattern of these cells established by the *tor1Δ* mutation and LCA. Indeed, only CR (but not the *tor1Δ* mutation or LCA) significantly decreased TAG concentration in HD and LD cells through most of the chronological lifespan. Furthermore, only CR (but not the *tor1Δ* mutation or LCA) considerably increased FFA concentration in HD and LD cells through most of the chronological lifespan. Moreover, only CR (but not the *tor1Δ* mutation or LCA) increased CER concentration in HD and LD cells through the entire chronological lifespan. Besides, only CR (but not the *tor1Δ* mutation or LCA) significantly raised the concentrations of all ER- and mitochondria-synthesized phospholipids in HD and LD cells through most of the chronological lifespan.

Of note, recent studies in the Titorenko laboratory provided evidence that CR creates a metabolic pattern of chronological aging delay that in budding yeast differs from the metabolic design established by the *tor1Δ* mutation and LCA (Mohammad and Titorenko, submitted). These

metabolites are soluble in aqueous solutions. Thus, it seems that different dietary, genetic and pharmacological geroprotectors differ in their ability to affect the water-insoluble lipidomes and water-soluble metabolomes of chronologically aging budding yeast.

Chapter 5: References

Allen C, Büttner S, Aragon AD, Thomas JA, Meirelles O, Jaetao JE, Benn D, Ruby SW, Veenhuis M, Madeo F, Werner-Washburne M. Isolation of quiescent and nonquiescent cells from yeast stationary-phase cultures. J Cell Biol. 2006; 174:89-100.

Almanza A, Carlesso A, Chintha C, Creedican S, Doultsinos D, Leuzzi B, Luís A, McCarthy N, Montibeller L, More S, Papaioannou A, Püschel F, Sassano ML, Skoko J, Agostinis P, de Belleroche J, Eriksson LA, Fulda S, Gorman AM, Healy S, Kozlov A, Muñoz-Pinedo C, Rehm M, Chevet E, Samali A. Endoplasmic reticulum stress signalling - from basic mechanisms to clinical applications. FEBS J. 2019; 286:241-278.

Aragon AD, Rodriguez AL, Meirelles O, Roy S, Davidson GS, Tapia PH, Allen C, Joe R, Benn D, Werner-Washburne M. Characterization of differentiated quiescent and nonquiescent cells in yeast stationary-phase cultures. Mol Biol Cell. 2008; 19:1271-1280.

Arlia-Ciommo A, Leonov A, Piano A, Svistkova V, Titorenko VI. Cell-autonomous mechanisms of chronological aging in the yeast Saccharomyces cerevisiae. Microb Cell. 2014; 1:163-178.

Beach A, Leonov A, Arlia-Ciommo A, Svistkova V, Lutchman V, Titorenko VI. Mechanisms by which different functional states of mitochondria define yeast longevity. Int J Mol Sci. 2015; 16:5528-5554.

Beach A, Richard VR, Bourque S, Boukh-Viner T, Kyryakov P, Gomez-Perez A, Arlia-Ciommo A, Feldman R, Leonov A, Piano A, Svistkova V, Titorenko VI. Lithocholic bile acid accumulated in yeast mitochondria orchestrates a development of an anti-aging cellular pattern by causing age-related changes in cellular proteome. Cell Cycle. 2015; 14:1643-1656.

Cabib E, Arroyo J. How carbohydrates sculpt cells: chemical control of morphogenesis in the yeast cell wall. Nat Rev Microbiol. 2013; 11:648-655.

Carman GM, Han GS. Regulation of phospholipid synthesis in the yeast Saccharomyces cerevisiae. Annu Rev Biochem. 2011; 80:859-883.

Chadwick SR, Lajoie P. Endoplasmic Reticulum Stress Coping Mechanisms and Lifespan Regulation in Health and Diseases. Front Cell Dev Biol. 2019 May 21;7:84.

Cui HJ, Liu XG, McCormick M, Wasko BM, Zhao W, He X, Yuan Y, Fang BX, Sun XR, Kennedy BK, Suh Y, Zhou ZJ, Kaeberlein M, Feng WL. PMT1 deficiency enhances basal UPR activity and extends replicative lifespan of Saccharomyces cerevisiae. Age (Dordr). 2015; 37:9788.

Dakik P, Medkour Y, Mohammad K, Titorenko VI. Mechanisms Through Which Some Mitochondria-Generated Metabolites Act as Second Messengers That Are Essential Contributors to the Aging Process in Eukaryotes Across Phyla. Front Physiol. 2019; 10: 461.

Davidson GS, Joe RM, Roy S, Meirelles O, Allen CP, Wilson MR, Tapia PH, Manzanilla EE, Dodson AE, Chakraborty S, Carter M, Young S, Edwards B, Sklar L, Werner-Washburne M. The proteomics of quiescent and nonquiescent cell differentiation in yeast stationary-phase cultures. Mol Biol Cell. 2011; 22:988-998.

De Virgilio C. The essence of yeast quiescence. FEMS Microbiol Rev. 2012; 36:306-339.
Feldmann H. *Yeast: Molecular and cell biology*; Wiley-Blackwell: Weinheim, **2012**; ISBN 978-3-527-33252-6.

Dickson RC. Thematic review series: sphingolipids. New insights into sphingolipid metabolism and function in budding yeast. J Lipid Res. 2008; 49:909-921.

Dickson RC. Roles for sphingolipids in Saccharomyces cerevisiae. Adv Exp Med Biol. 2010; 688:217-231.

Fraenkel DG. *Yeast intermediary metabolism*; Cold Spring Harbor Laboratory Press: Cold Spring Harbor, NY, USA, 2011; ISBN 978-0-87969-797-6.

François J, Parrou JL. Reserve carbohydrates metabolism in the yeast Saccharomyces cerevisiae. FEMS Microbiol Rev. 2001; 25:125-145.

Fu S, Yang L, Li P, Hofmann O, Dicker L, Hide W, Lin X, Watkins SM, Ivanov AR, Hotamisligil GS. Aberrant lipid metabolism disrupts calcium homeostasis causing liver endoplasmic reticulum stress in obesity. Nature. 2011; 473:528-531.

Giorgio M, Trinei M, Migliaccio E, Pelicci PG. Hydrogen peroxide: a metabolic by-product or a common mediator of ageing signals? Nat Rev Mol Cell Biol. 2007; 8:722-728.

Gladyshev VN. The origin of aging: imperfectness-driven non-random damage defines the aging process and control of lifespan. Trends Genet. 2013; 29:506-512.

Goldberg AA, Bourque SD, Kyryakov P, Gregg C, Boukh-Viner T, Beach A, Burstein MT, Machkalyan G, Richard V, Rampersad S, Cyr D, Milijevic S, Titorenko VI. Effect of calorie restriction on the metabolic history of chronologically aging yeast. Exp Gerontol. 2009; 44:555-571.

Goldberg AA, Richard VR, Kyryakov P, Bourque SD, Beach A, Burstein MT, Glebov A, Koupaki O, Boukh-Viner T, Gregg C, Juneau M, English AM, Thomas DY, Titorenko VI. Chemical genetic screen identifies lithocholic acid as an anti-aging compound that extends yeast chronological life span in a TOR-independent manner, by modulating housekeeping longevity assurance processes. Aging (Albany NY). 2010; 2:393-414.

Halbleib K, Pesek K, Covino R, Hofbauer HF, Wunnicke D, Hänelt I, Hummer G, Ernst R. Activation of the Unfolded Protein Response by Lipid Bilayer Stress. Mol Cell. 2017; 67:673-684.e8.

Henry SA, Kohlwein SD, Carman GM. Metabolism and regulation of glycerolipids in the yeast Saccharomyces cerevisiae. Genetics. 2012; 190:317-349.

Herker E, Jungwirth H, Lehmann KA, Maldener C, Fröhlich KU, Wissing S, Büttner S, Fehr M, Sigrist S, Madeo F. Chronological aging leads to apoptosis in yeast. J Cell Biol. 2004; 164:501-507.

Kaeberlein M, Burtner CR, Kennedy BK. Recent developments in yeast aging. PLoS Genet. 2007; 3: e84.

Karagöz GE, Acosta-Alvear D, Walter P. The Unfolded Protein Response: Detecting and Responding to Fluctuations in the Protein-Folding Capacity of the Endoplasmic Reticulum. Cold Spring Harb Perspect Biol. 2019; 11:a033886.

Klug L, Daum G. Yeast lipid metabolism at a glance. FEMS Yeast Res. 2014; 14:369-388.

Kohlwein SD, Veenhuis M, van der Klei IJ. Lipid droplets and peroxisomes: key players in cellular lipid homeostasis or a matter of fat--store 'em up or burn 'em down. Genetics. 2013; 193:1-50.

Kyryakov P, Beach A, Richard VR, Burstein MT, Leonov A, Levy S, Titorenko VI. Caloric restriction extends yeast chronological lifespan by altering a pattern of age-related changes in trehalose concentration. Front Physiol. 2012; 3: 256.

Leonov A, Arlia-Ciommo A, Bourque SD, Koupaki O, Kyryakov P, Dakik P, McAuley M, Medkour Y, Mohammad K, Di Maulo T, Titorenko VI. Specific changes in mitochondrial lipidome alter mitochondrial proteome and increase the geroprotective efficiency of lithocholic acid in chronologically aging yeast. Oncotarget. 2017; 8:30672-30691.

Leonov A, Feldman R, Piano A, Arlia-Ciommo A, Lutchman V, Ahmadi M, Elsaser S, Fakim H, Heshmati-Moghaddam M, Hussain A, Orfali S, Rajen H, Roofigari-Esfahani N, Rosanelli L, Titorenko VI. Caloric restriction extends yeast chronological lifespan via a mechanism linking cellular aging to cell cycle regulation, maintenance of a quiescent state, entry into a non-quiescent state and survival in the non-quiescent state. Oncotarget. 2017; 8:69328-69350.

Leonov A, Titorenko VI. A network of interorganellar communications underlies cellular aging. IUBMB Life. 2013; 65:665-674.

Longo VD, Shadel GS, Kaeberlein M, Kennedy B. Replicative and chronological aging in Saccharomyces cerevisiae. Cell Metab. 2012; 16:18-31.

Madeo F, Carmona-Gutierrez D, Hofer SJ, Kroemer G. Caloric Restriction Mimetics against Age-Associated Disease: Targets, Mechanisms, and Therapeutic Potential. Cell Metab. 2019; 29:592-610.

Miles S, Li L, Davison J, Breeden LL. Xbp1 directs global repression of budding yeast transcription during the transition to quiescence and is important for the longevity and reversibility of the quiescent state. PLoS Genet. 2013; 9: e1003854.

Mitrofanova D, Dakik P, McAuley M, Medkour Y, Mohammad K, Titorenko VI. Lipid metabolism and transport define longevity of the yeast Saccharomyces cerevisiae. Front Biosci (Landmark Ed). 2018; 23:1166-1194.

Mohammad K, Jiang H, Hossain MI, Titorenko VI. Quantitative Analysis of the Cellular Lipidome of Saccharomyces Cerevisiae Using Liquid Chromatography Coupled with Tandem Mass Spectrometry. J Vis Exp. 2020; 157: 60616.

Ogrodnik M, Salmonowicz H, Gladyshev VN. Integrating cellular senescence with the concept of damage accumulation in aging: Relevance for clearance of senescent cells. Aging Cell. 2019; 18: e12841.

Richard VR, Beach A, Piano A, Leonov A, Feldman R, Burstein MT, Kyryakov P, Gomez-Perez A, Arlia-Ciommo A, Baptista S, Campbell C, Goncharov D, Pannu S, Patrinos D, Sadri B, Svistkova V, Victor A, Titorenko VI. Mechanism of liponecrosis, a distinct mode of programmed cell death. Cell Cycle. 2014; 13):3707-3726.

Sagot I, Laporte D. The cell biology of quiescent yeast - a diversity of individual scenarios. J Cell Sci. 2019; 132: jcs213025.

Sheibani S, Richard VR, Beach A, Leonov A, Feldman R, Mattie S, Khelghatybana L, Piano A, Greenwood M, Vali H, Titorenko VI. Macromitophagy, neutral lipids synthesis, and peroxisomal fatty acid oxidation protect yeast from "liponecrosis", a previously unknown form of programmed cell death. Cell Cycle. 2014; 13:138-147.

Sinclair DA. Toward a unified theory of caloric restriction and longevity regulation. Mech Ageing Dev. 2005; 126:987-1002.

Tamura Y, Kawano S, Endo T. Organelle contact zones as sites for lipid transfer. J Biochem. 2019; 165:115-123.

Werner-Washburne M, Roy S, Davidson GS. Aging and the survival of quiescent and non-quiescent cells in yeast stationary-phase cultures. Subcell Biochem. 2012; 57:123-143.

Chapter 6: Appendix

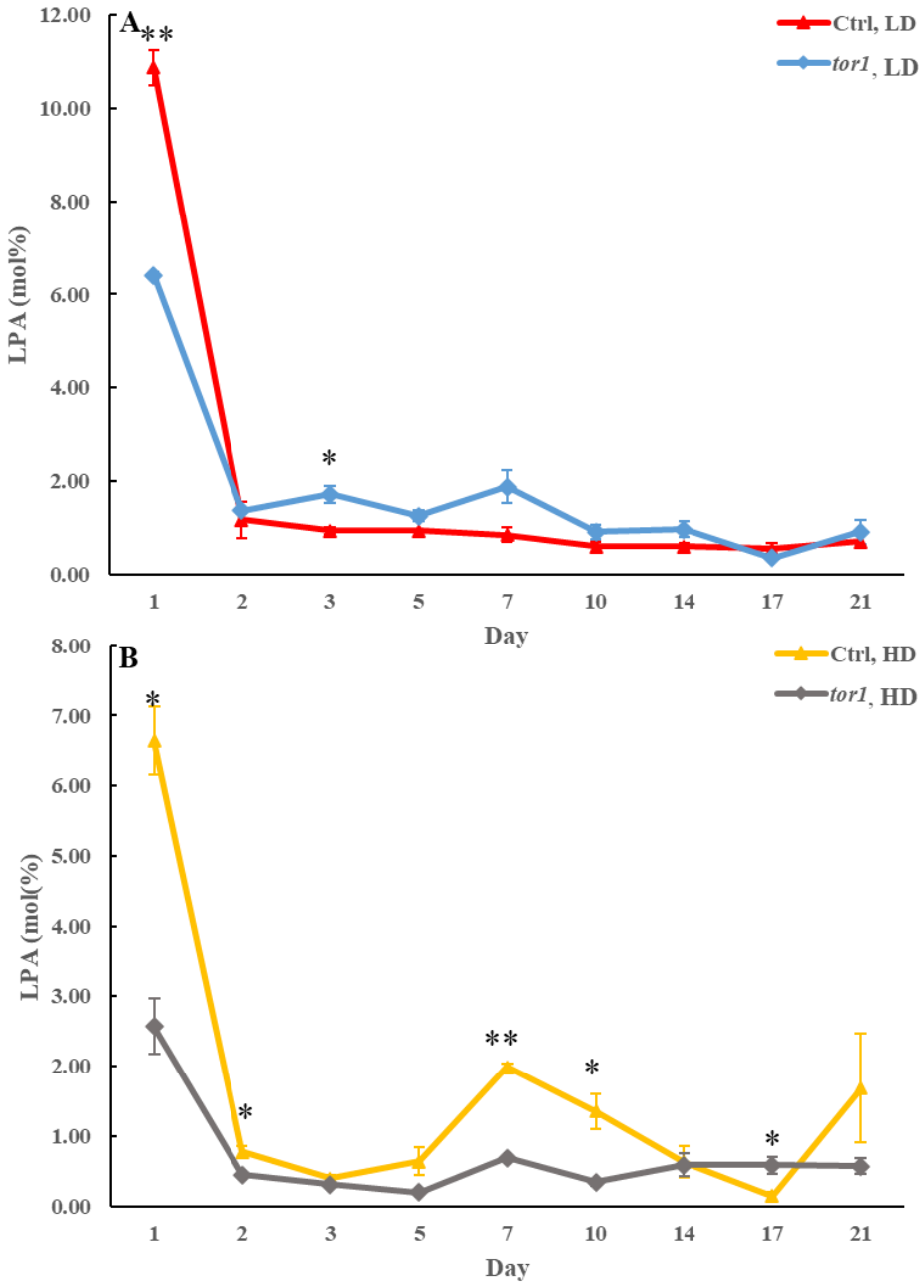

Figure 6.1. The *tor1Δ* mutation does not have a significant long-lasting effect on LPA concentration in HD and LD cells through the chronological lifespan. Samples of WT (control) and *tor1Δ* yeast cultured in YP medium initially containing 2% glucose (non-CR conditions) were recovered on different days of culturing and subjected to centrifugation in Percoll density gradient to purify HD and LD cell sub-populations. LPA concentrations were measured by LC-MS/MS. Data are presented as means ± SD (n = 2; *P < 0.05; **P < 0.01).

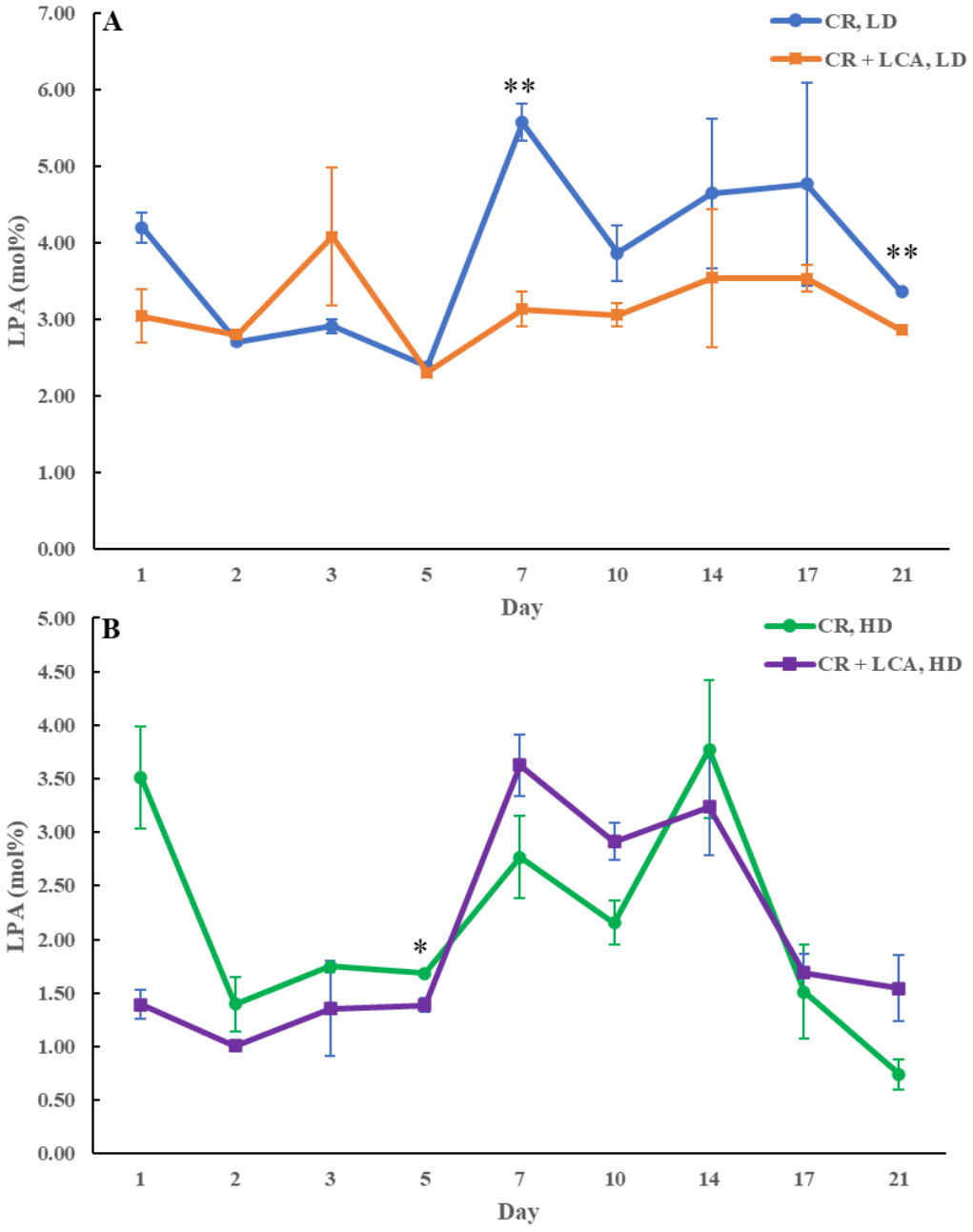

Figure 6.2. LCA does not have a significant long-lasting effect on LPA concentration in HD and LD cells through the chronological lifespan. Samples of WT yeast cultured in YP medium initially containing 0.2% glucose (CR conditions) with 50 μM LCA or without it (control) were recovered on different days of culturing and subjected to centrifugation in Percoll density gradient to purify HD and LD cell sub-populations. LPA concentrations were measured by LC-MS/MS. Data are presented as means ± SD (n = 2; *P < 0.05; **P < 0.01).

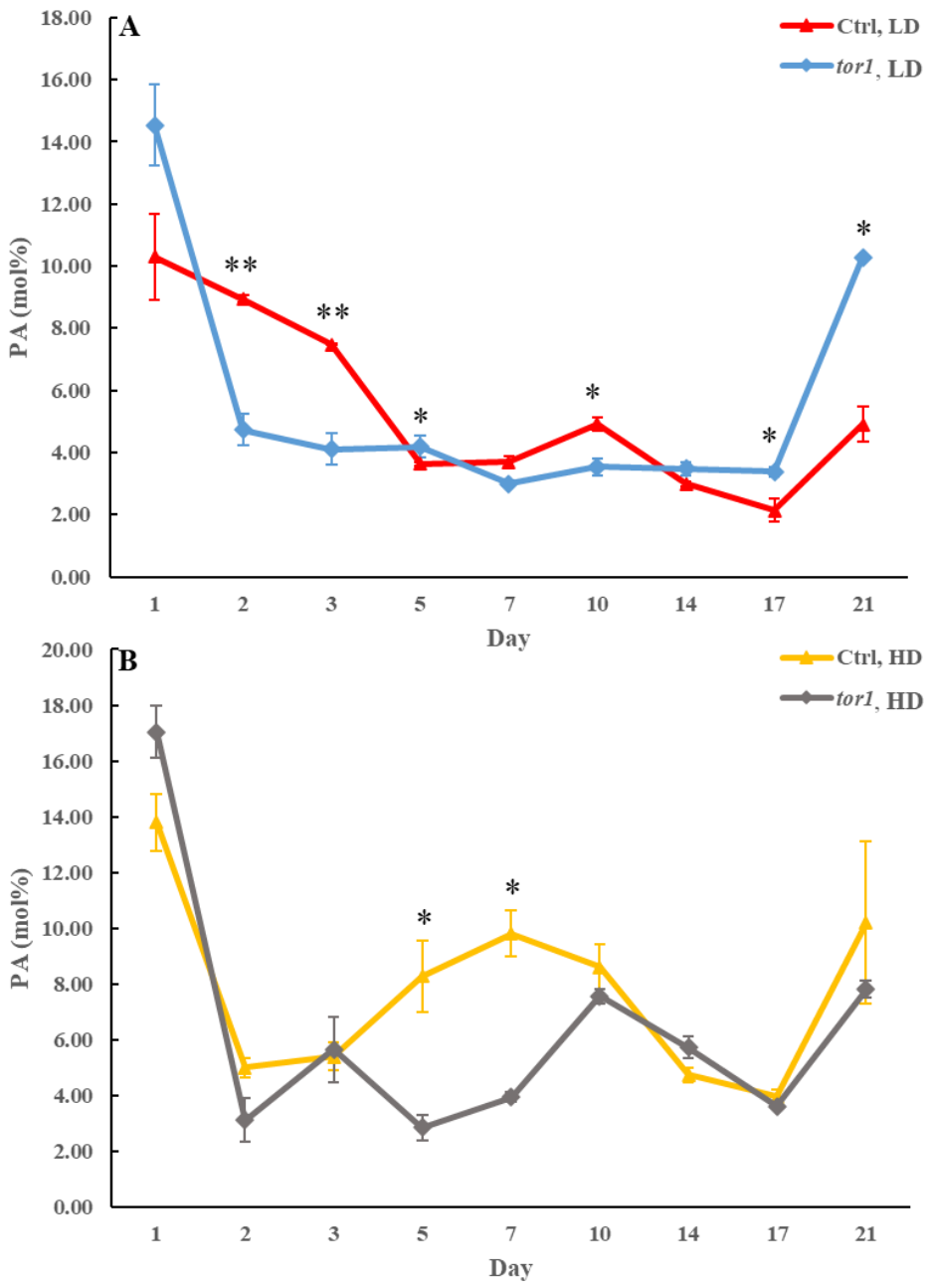

Figure 6.3. The *tor1Δ* mutation does not have a significant long-lasting effect on PA concentration in HD and LD cells through the chronological lifespan. Samples of WT (control) and *tor1Δ* yeast cultured in YP medium initially containing 2% glucose (non-CR conditions) were recovered on different days of culturing and subjected to centrifugation in Percoll density gradient to purify HD and LD cell sub-populations. PA concentrations were measured by LC-MS/MS. Data are presented as means ± SD (n = 2; *P < 0.05; **P < 0.01).

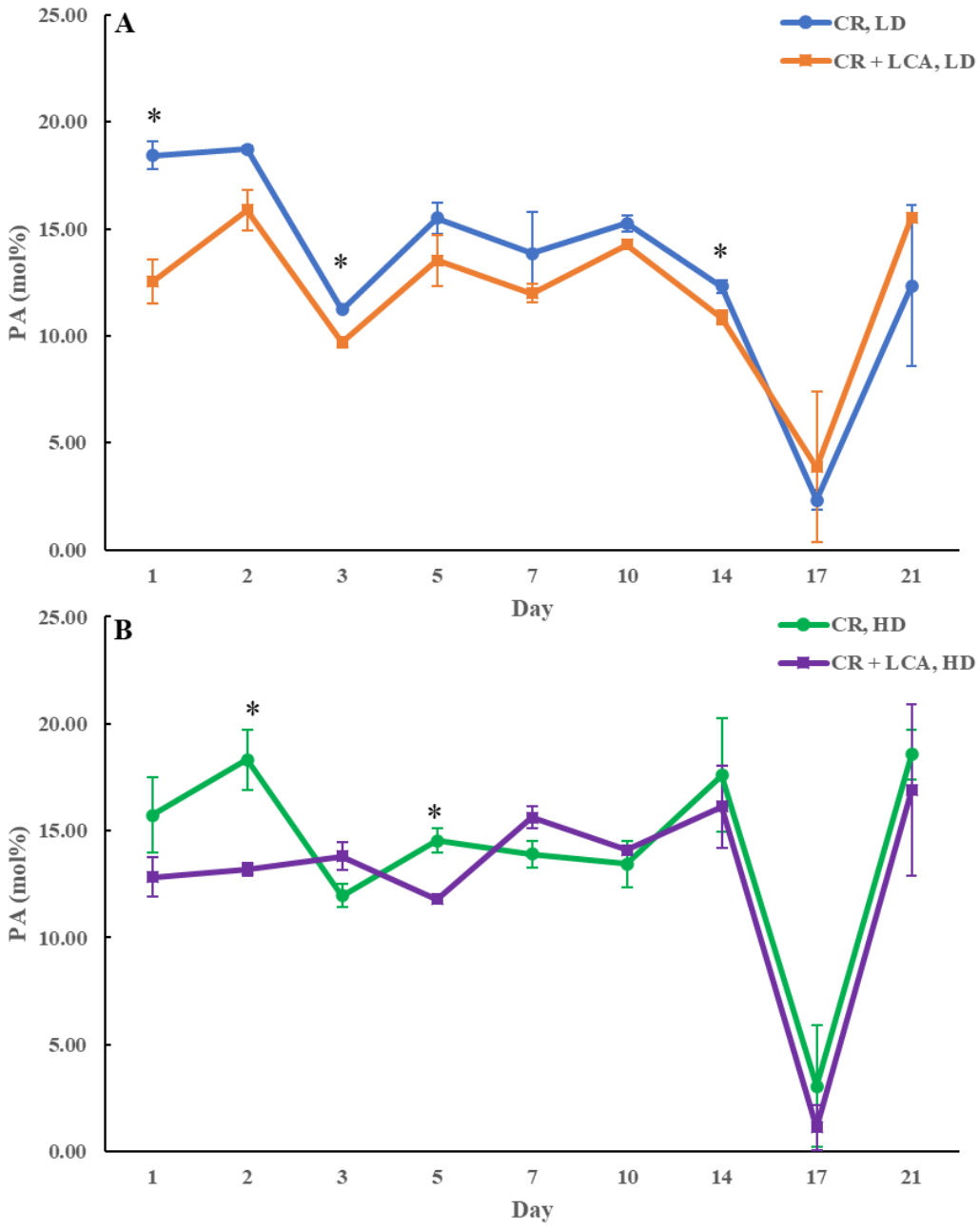

Figure 6.4. LCA does not have a significant long-lasting effect on PA concentration in HD and LD cells through the chronological lifespan. Samples of WT yeast cultured in YP medium initially containing 0.2% glucose (CR conditions) with 50 µM LCA or without it (control) were recovered on different days of culturing and subjected to centrifugation in Percoll density gradient to purify HD and LD cell sub-populations. PA concentrations were measured by LC-MS/MS. Data are presented as means ± SD (n = 2; *P < 0.05).

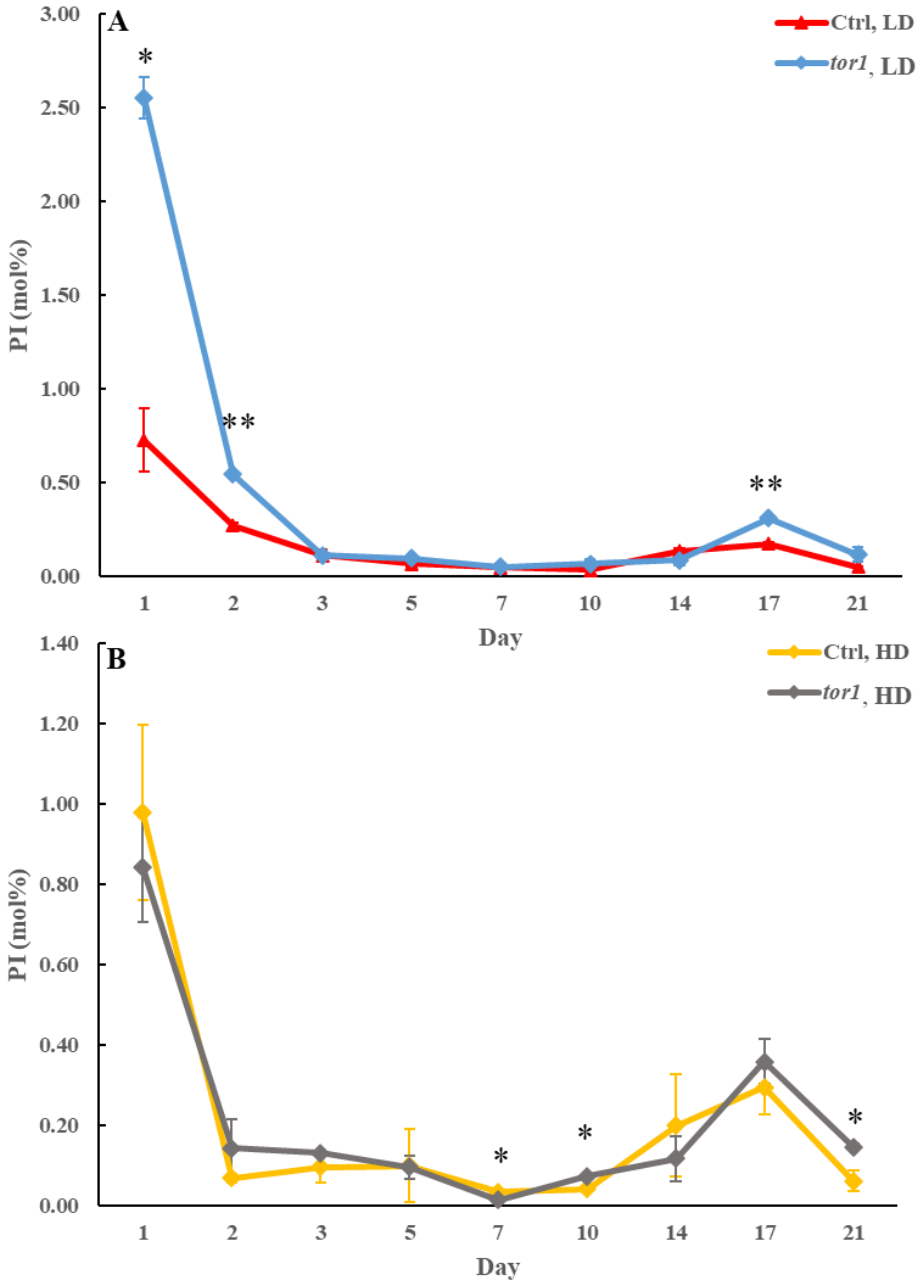

Figure 6.5. The *tor1Δ* mutation does not have a significant long-lasting effect on PI concentration in HD and LD cells through the chronological lifespan. Samples of WT (control) and *tor1Δ* yeast cultured in YP medium initially containing 2% glucose (non-CR conditions) were recovered on different days of culturing and subjected to centrifugation in Percoll density gradient to purify HD and LD cell sub-populations. PI concentrations were measured by LC-MS/MS. Data are presented as means ± SD (n = 2; *P < 0.05; **P < 0.01).

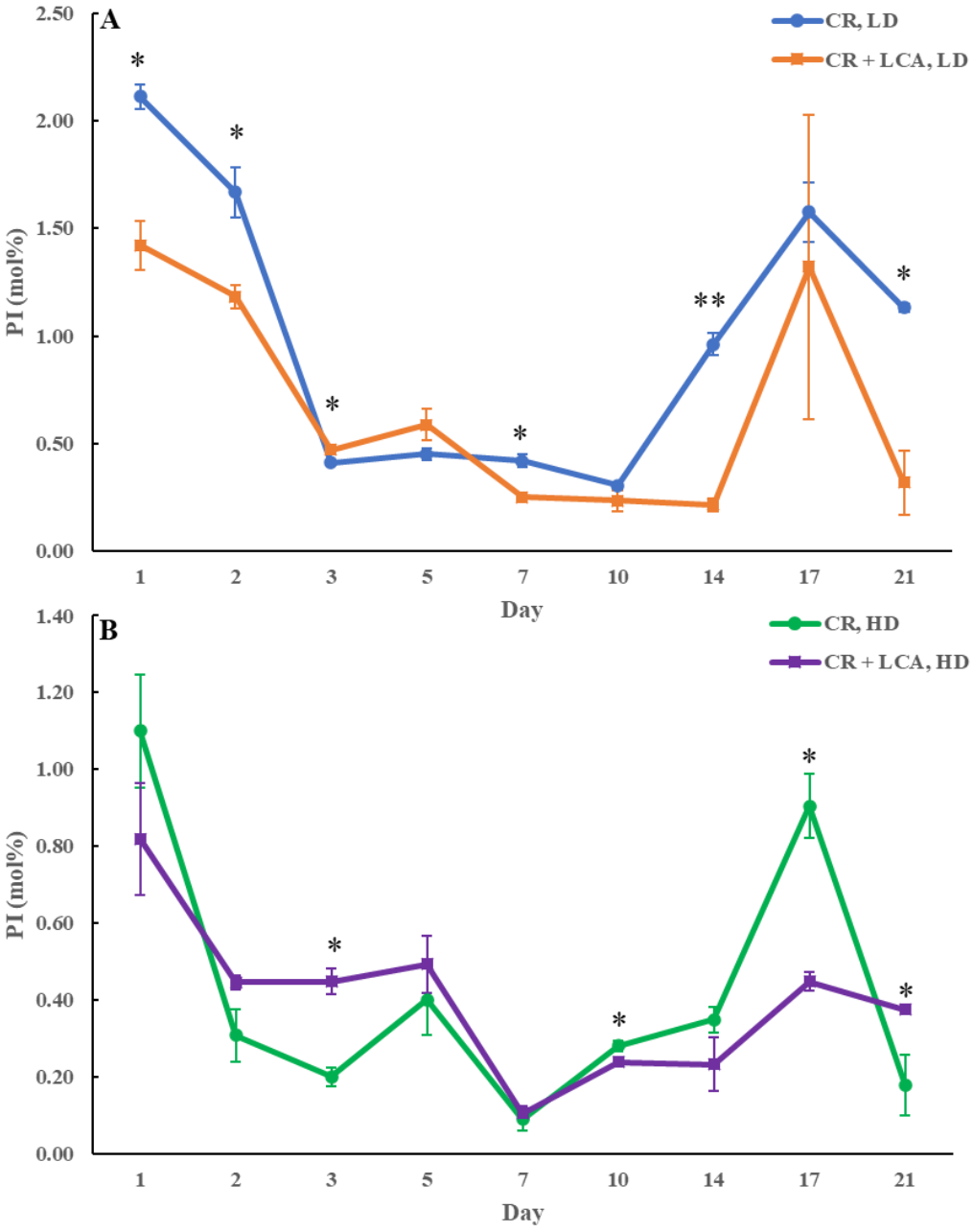

Figure 6.6. LCA does not have a significant long-lasting effect on PI concentration in HD and LD cells through the chronological lifespan. Samples of WT yeast cultured in YP medium initially containing 0.2% glucose (CR conditions) with 50 µM LCA or without it (control) were recovered on different days of culturing and subjected to centrifugation in Percoll density gradient to purify HD and LD cell sub-populations. PI concentrations were measured by LC-MS/MS. Data are presented as means ± SD (n = 2; *P < 0.05).

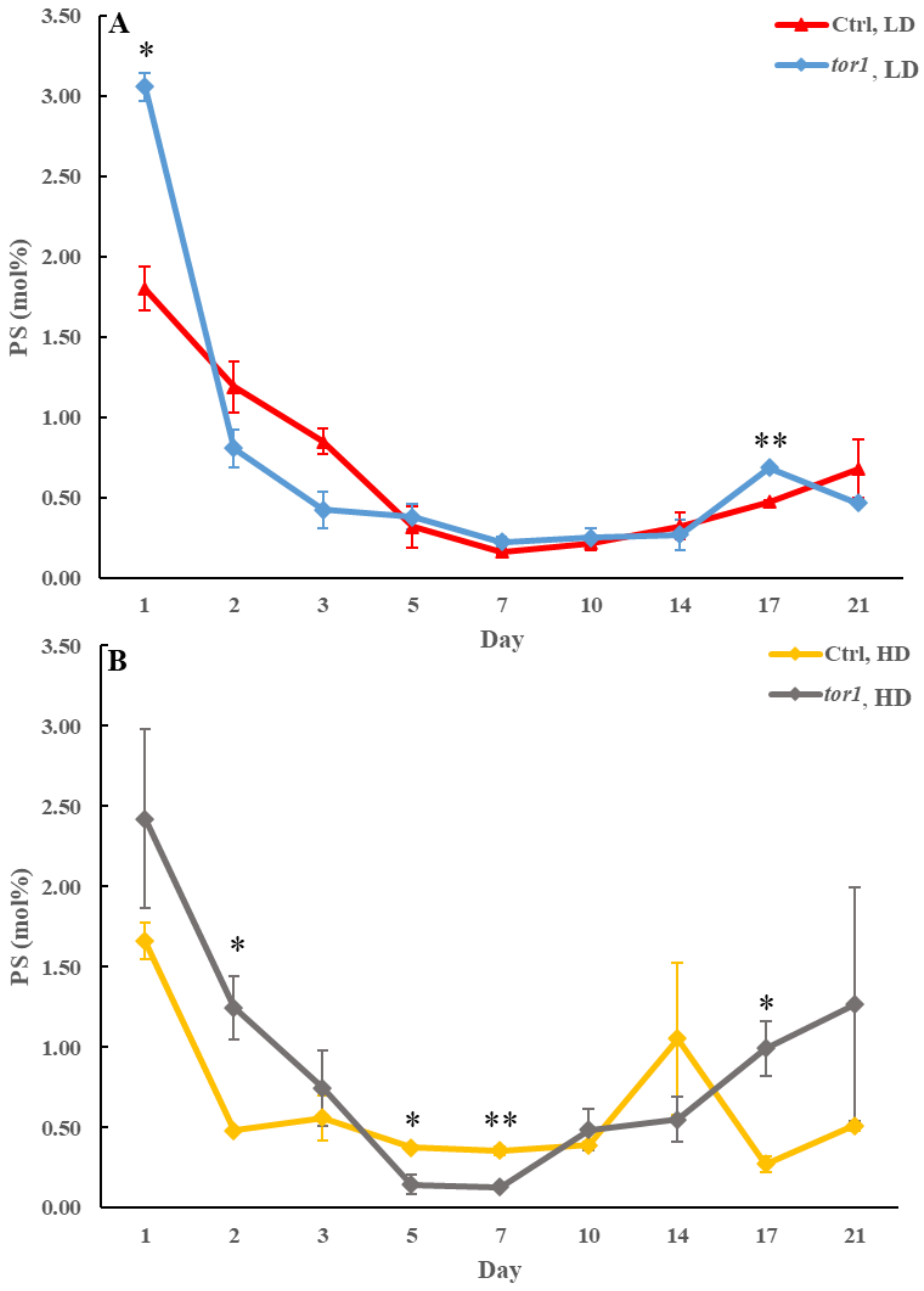

Figure 6.7. The *tor1Δ* mutation does not have a significant long-lasting effect on PS concentration in HD and LD cells through the chronological lifespan. Samples of WT (control) and *tor1Δ* yeast cultured in YP medium initially containing 2% glucose (non-CR conditions) were recovered on different days of culturing and subjected to centrifugation in Percoll density gradient to purify HD and LD cell sub-populations. PS concentrations were measured by LC-MS/MS. Data are presented as means ± SD (n = 2; *P < 0.05; **P < 0.01).

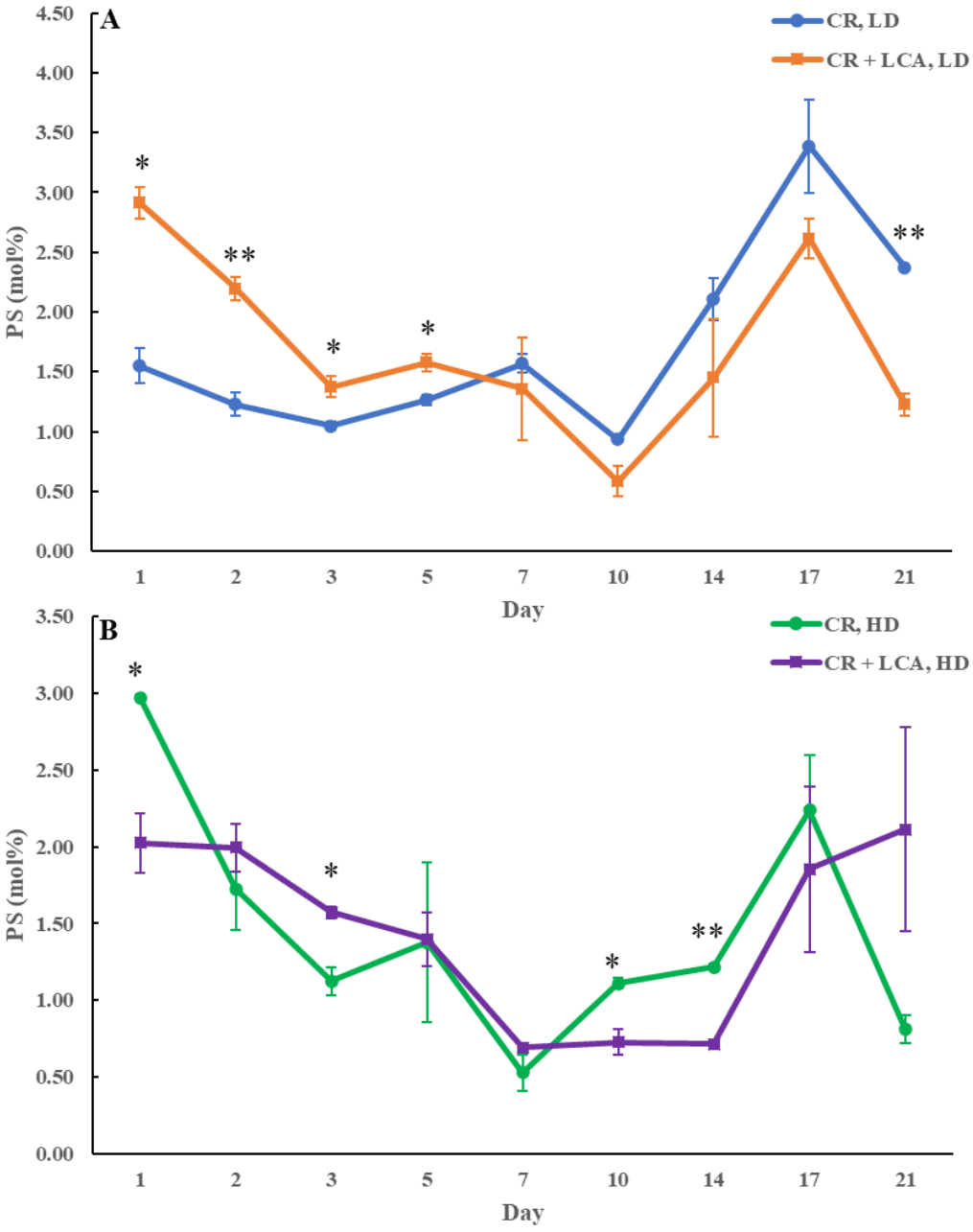

Figure 6.8. LCA does not have a significant long-lasting effect on PS concentration in HD and LD cells through the chronological lifespan. Samples of WT yeast cultured in YP medium initially containing 0.2% glucose (CR conditions) with 50 µM LCA or without it (control) were recovered on different days of culturing and subjected to centrifugation in Percoll density gradient to purify HD and LD cell sub-populations. PS concentrations were measured by LC-MS/MS. Data are presented as means ± SD (n = 2; *P < 0.05).

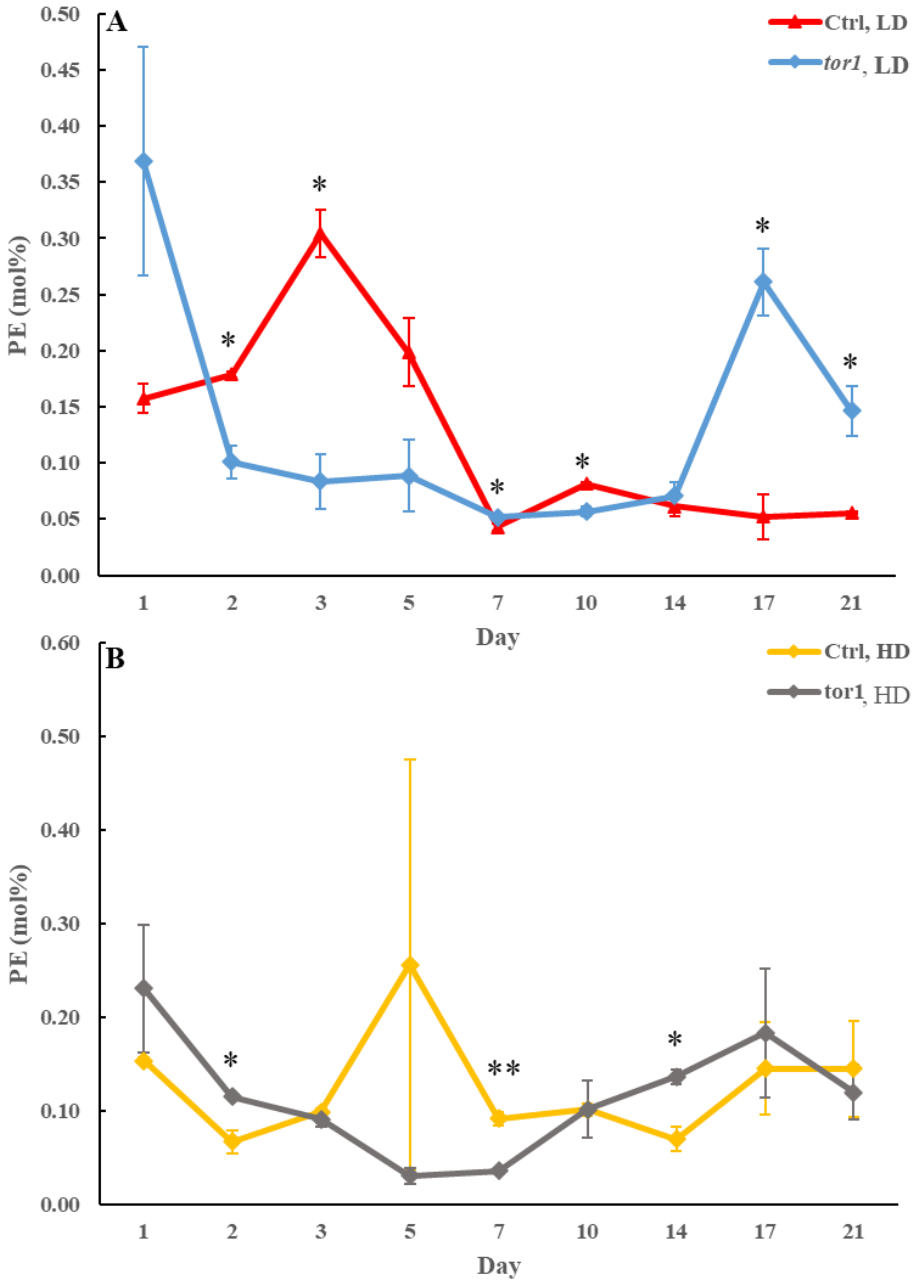

Figure 6.9. The *tor1Δ* mutation does not have a significant long-lasting effect on PE concentration in HD and LD cells through the chronological lifespan. Samples of WT (control) and *tor1Δ* yeast cultured in YP medium initially containing 2% glucose (non-CR conditions) were recovered on different days of culturing and subjected to centrifugation in Percoll density gradient to purify HD and LD cell sub-populations. PE concentrations were measured by LC-MS/MS. Data are presented as means ± SD (n = 2; *P < 0.05; **P < 0.01).

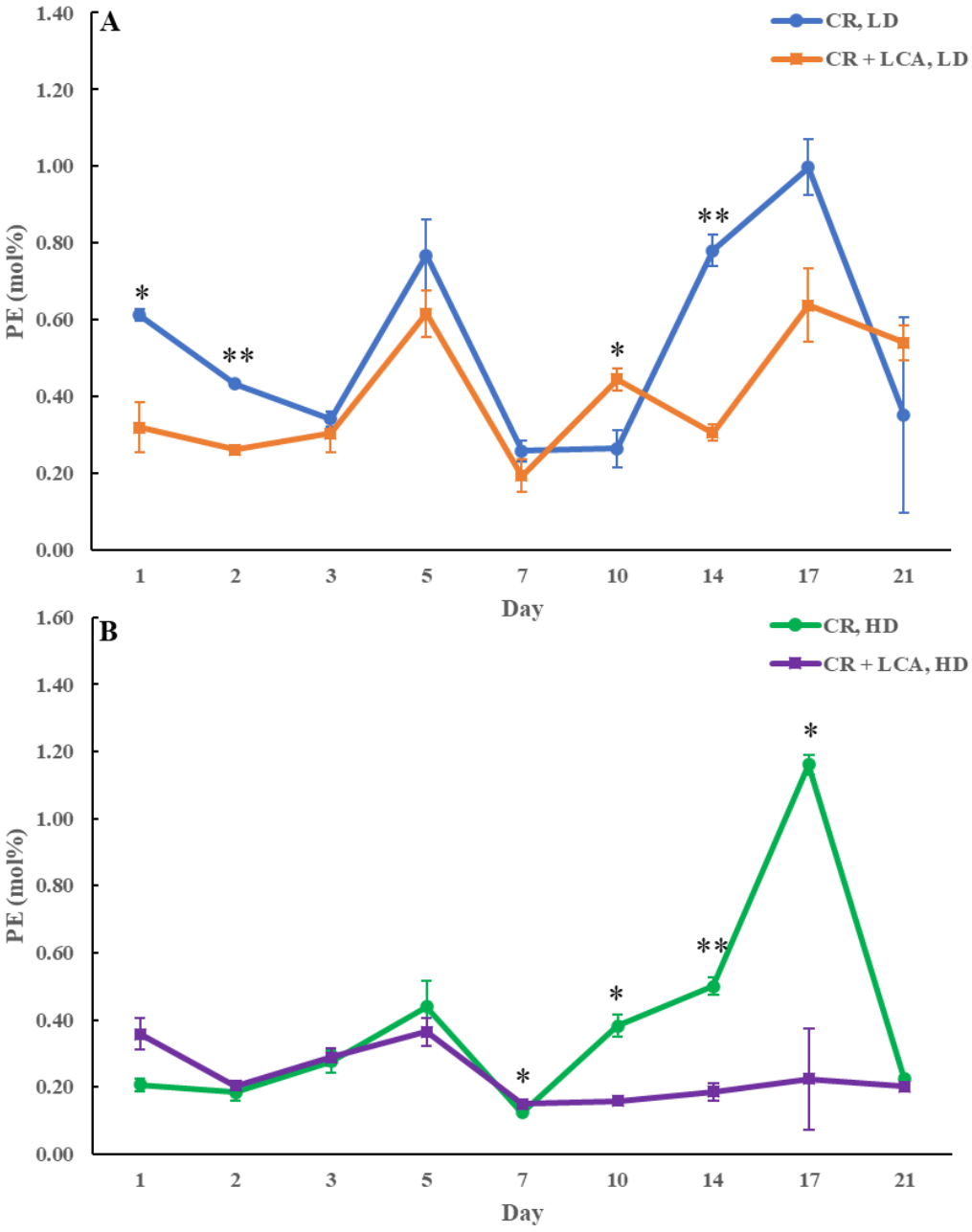

Figure 6.10. LCA does not have a significant long-lasting effect on PE concentration in HD and LD cells through the chronological lifespan. Samples of WT yeast cultured in YP medium initially containing 0.2% glucose (CR conditions) with 50 μM LCA or without it (control) were recovered on different days of culturing and subjected to centrifugation in Percoll density gradient to purify HD and LD cell sub-populations. PE concentrations were measured by LC-MS/MS. Data are presented as means ± SD (n = 2; *P < 0.05; **P < 0.01).

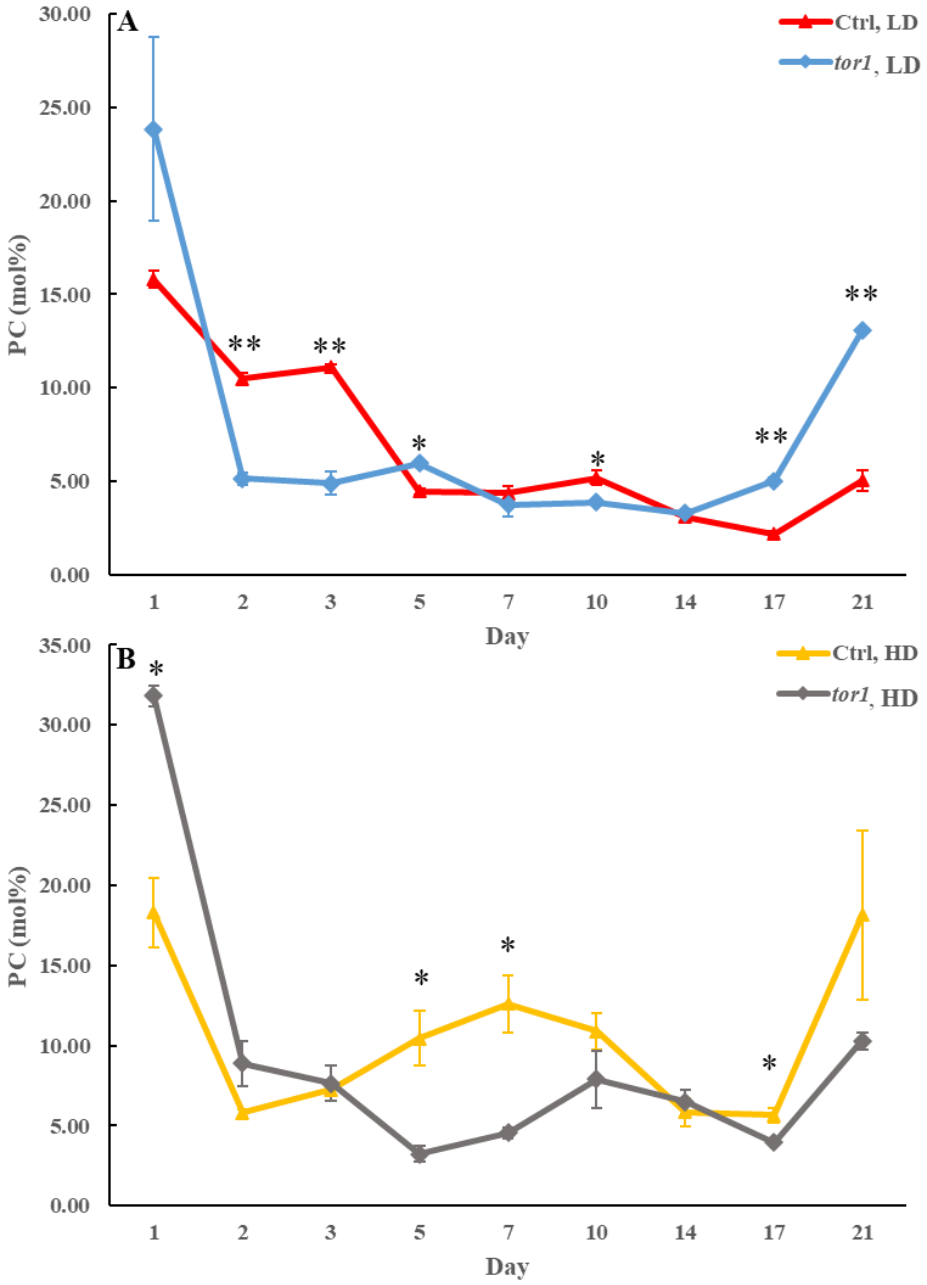

Figure 6.11. The *tor1Δ* mutation does not have a significant long-lasting effect on PC concentration in HD and LD cells through the chronological lifespan. Samples of WT (control) and *tor1Δ* yeast cultured in YP medium initially containing 2% glucose (non-CR conditions) were recovered on different days of culturing and subjected to centrifugation in Percoll density gradient to purify HD and LD cell sub-populations. PC concentrations were measured by LC-MS/MS. Data are presented as means ± SD (n = 2; *P < 0.05; **P < 0.01).

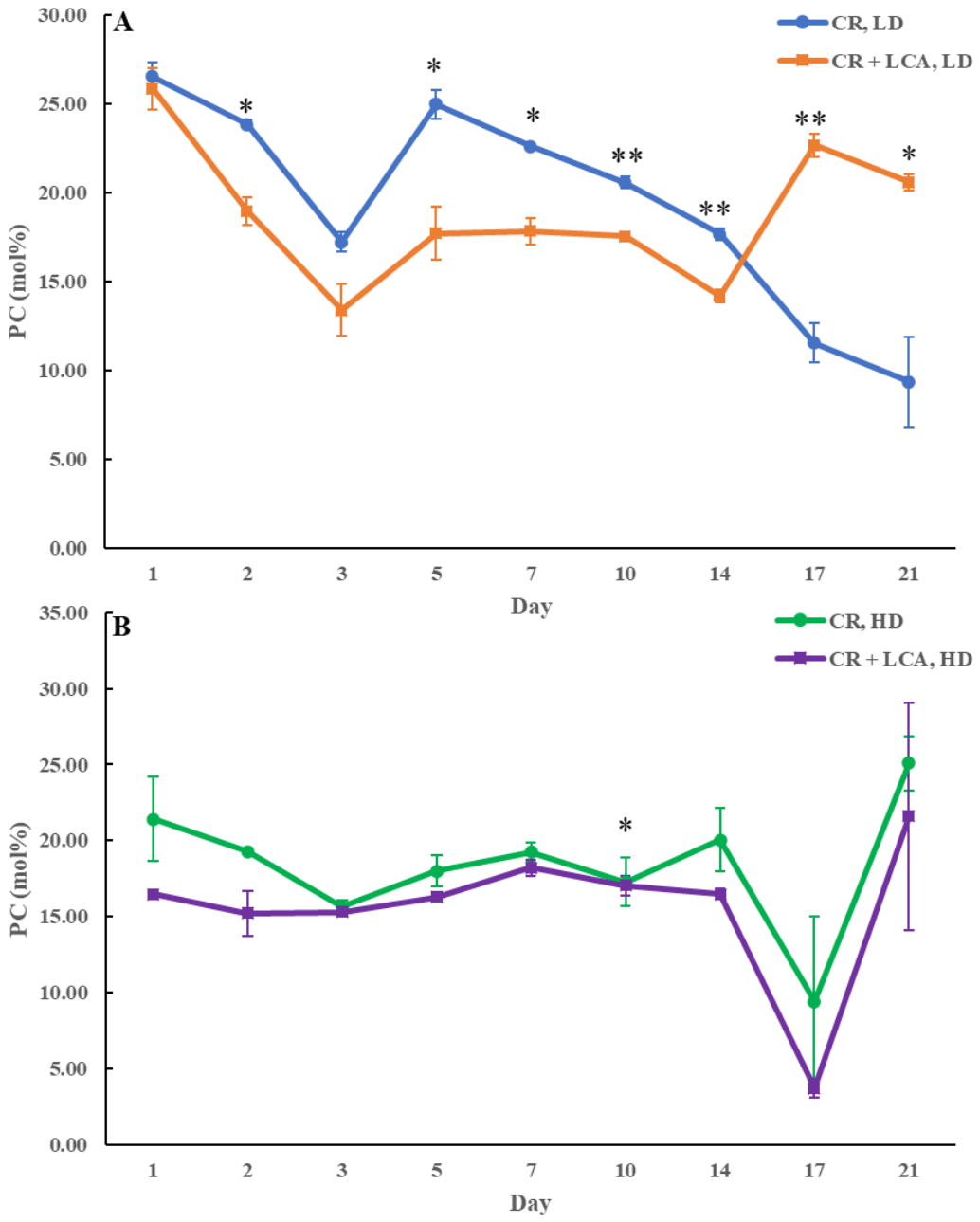

Figure 6.12. LCA does not have a significant long-lasting effect on PC concentration in HD and LD cells through the chronological lifespan. Samples of WT yeast cultured in YP medium initially containing 0.2% glucose (CR conditions) with 50 µM LCA or without it (control) were recovered on different days of culturing and subjected to centrifugation in Percoll density gradient to purify HD and LD cell sub-populations. PC concentrations were measured by LC-MS/MS. Data are presented as means ± SD (n = 2; *P < 0.05; **P < 0.01).

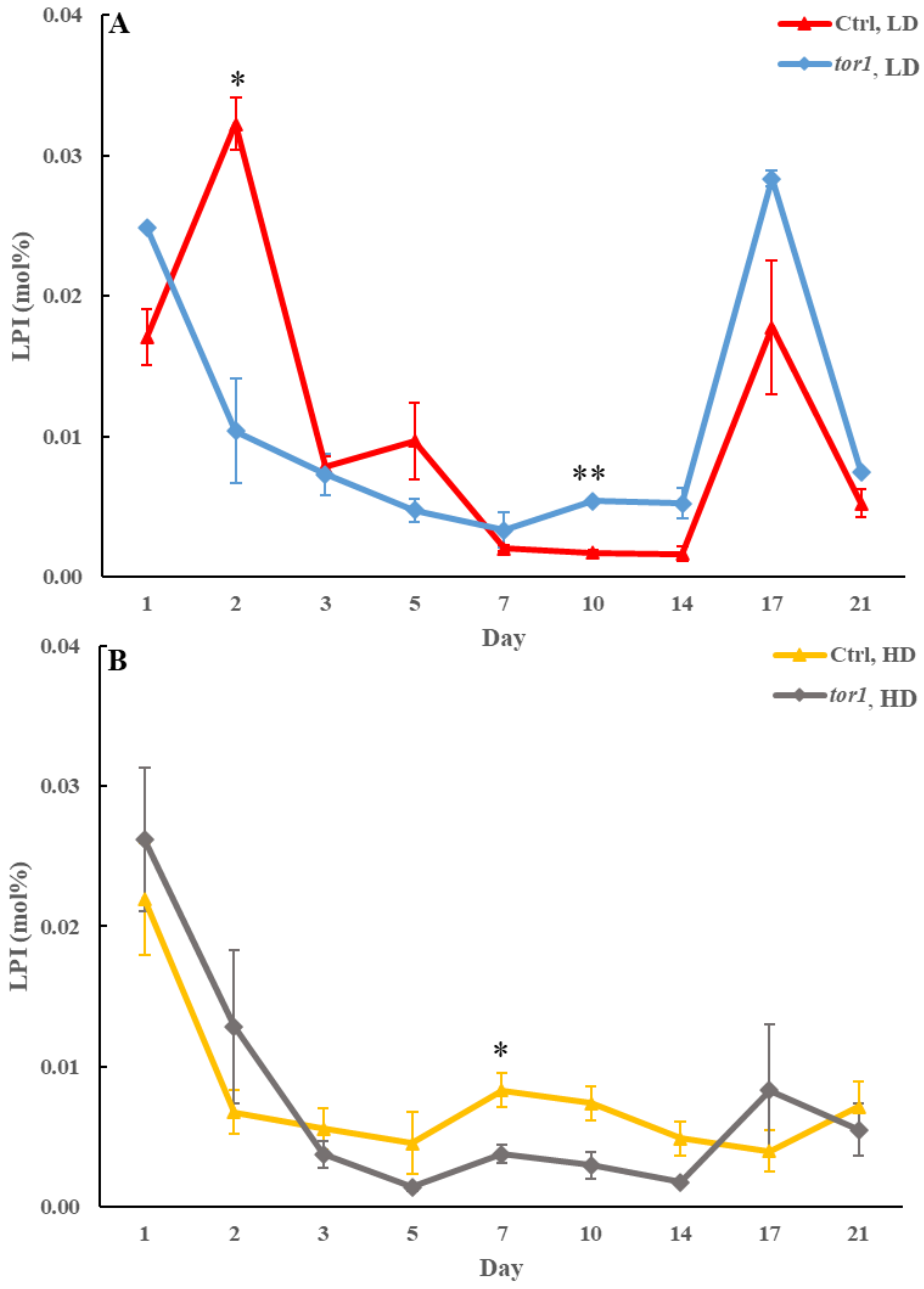

Figure 6.13. The *tor1Δ* mutation does not have a significant long-lasting effect on LPI concentration in HD and LD cells through the chronological lifespan. Samples of WT (control) and *tor1Δ* yeast cultured in YP medium initially containing 2% glucose (non-CR conditions) were recovered on different days of culturing and subjected to centrifugation in Percoll density gradient to purify HD and LD cell sub-populations. LPI concentrations were measured by LC-MS/MS. Data are presented as means ± SD (n = 2; *P < 0.05; **P < 0.01).

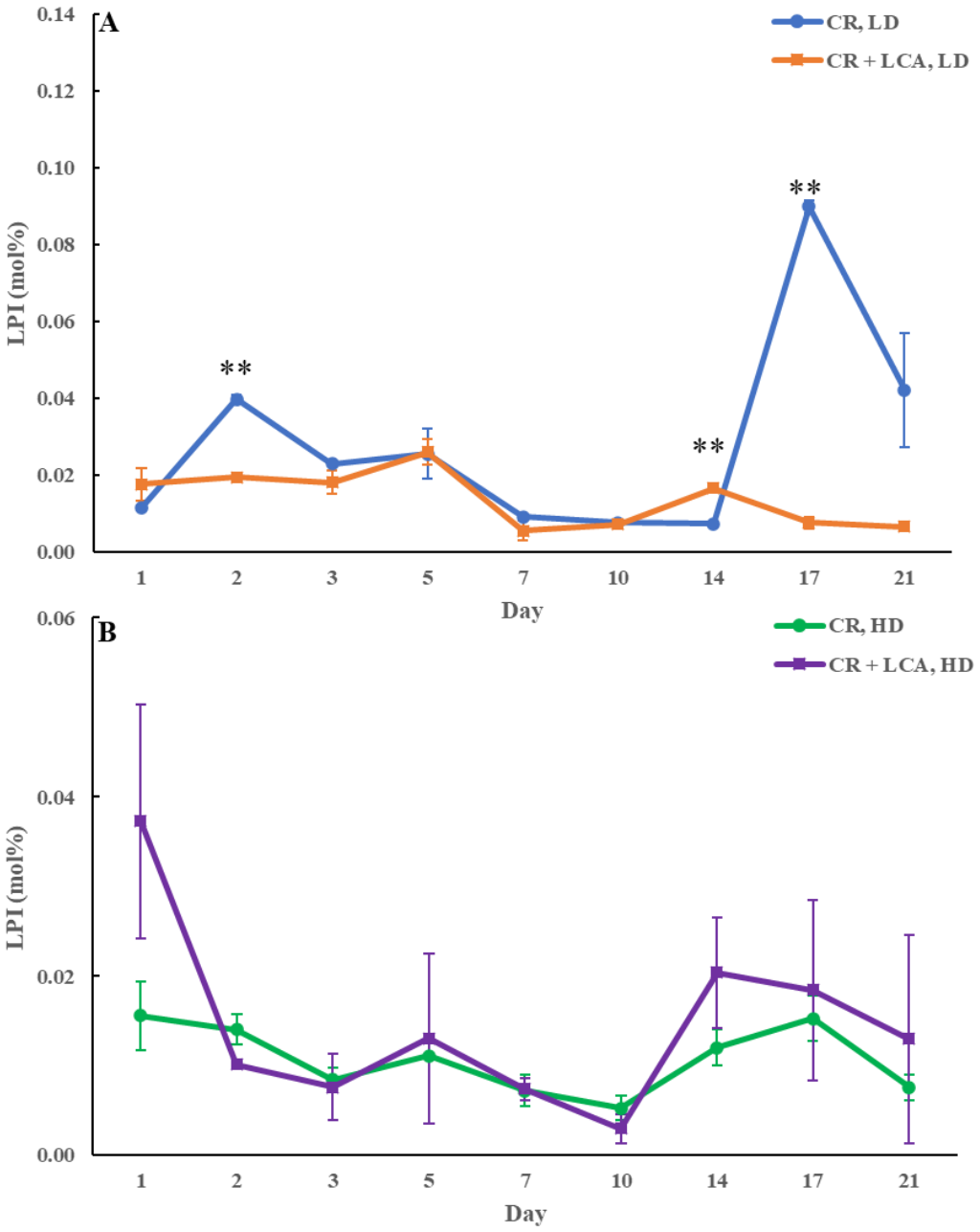

Figure 6.14. LCA does not have a significant long-lasting effect on LPI concentration in HD and LD cells through the chronological lifespan. Samples of WT yeast cultured in YP medium initially containing 0.2% glucose (CR conditions) with 50 μM LCA or without it (control) were recovered on different days of culturing and subjected to centrifugation in Percoll density gradient to purify HD and LD cell sub-populations. LPI concentrations were measured by LC-MS/MS. Data are presented as means ± SD (n = 2; **P < 0.01).

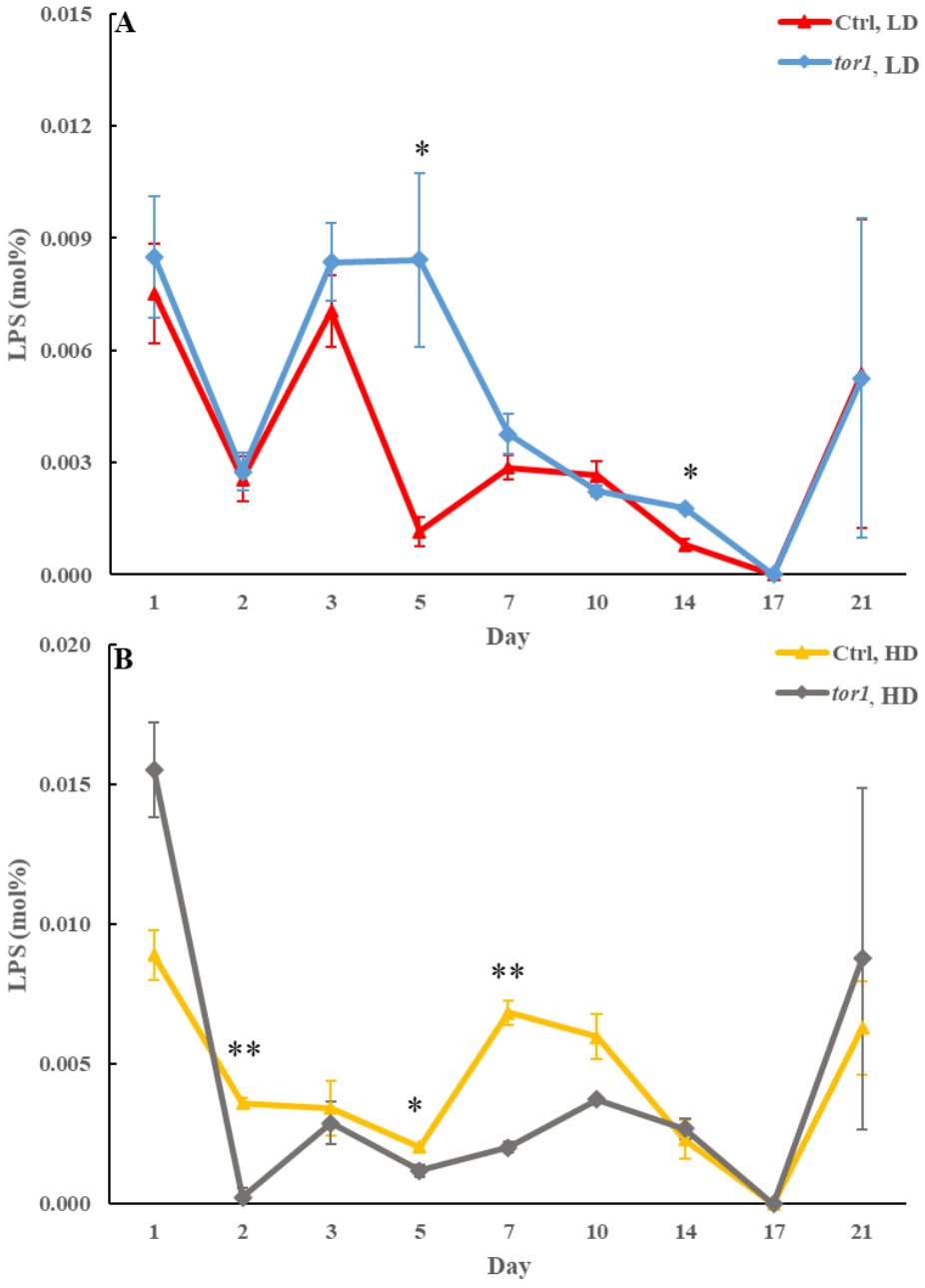

Figure 6.15. The *tor1Δ* mutation does not have a significant long-lasting effect on LPS concentration in HD and LD cells through the chronological lifespan. Samples of WT (control) and *tor1Δ* yeast cultured in YP medium initially containing 2% glucose (non-CR conditions) were recovered on different days of culturing and subjected to centrifugation in Percoll density gradient to purify HD and LD cell sub-populations. LPS concentrations were measured by LC-MS/MS. Data are presented as means ± SD (n = 2; *P < 0.05; **P < 0.01).

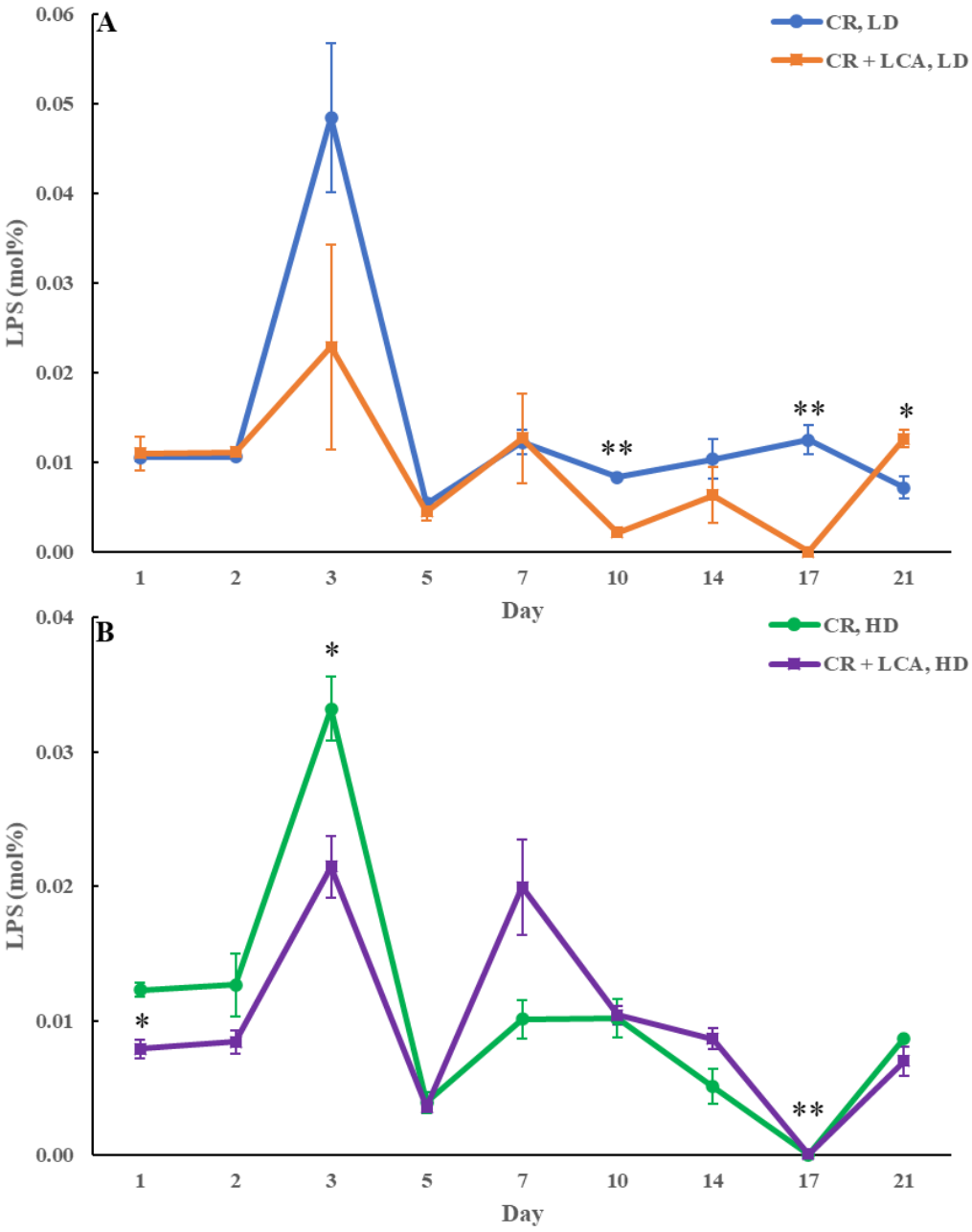

Figure 6.16. LCA does not have a significant long-lasting effect on LPS concentration in HD and LD cells through the chronological lifespan. Samples of WT yeast cultured in YP medium initially containing 0.2% glucose (CR conditions) with 50 μM LCA or without it (control) were recovered on different days of culturing and subjected to centrifugation in Percoll density gradient to purify HD and LD cell sub-populations. LPS concentrations were measured by LC-MS/MS. Data are presented as means ± SD (n = 2; *P < 0.05; **P < 0.01).

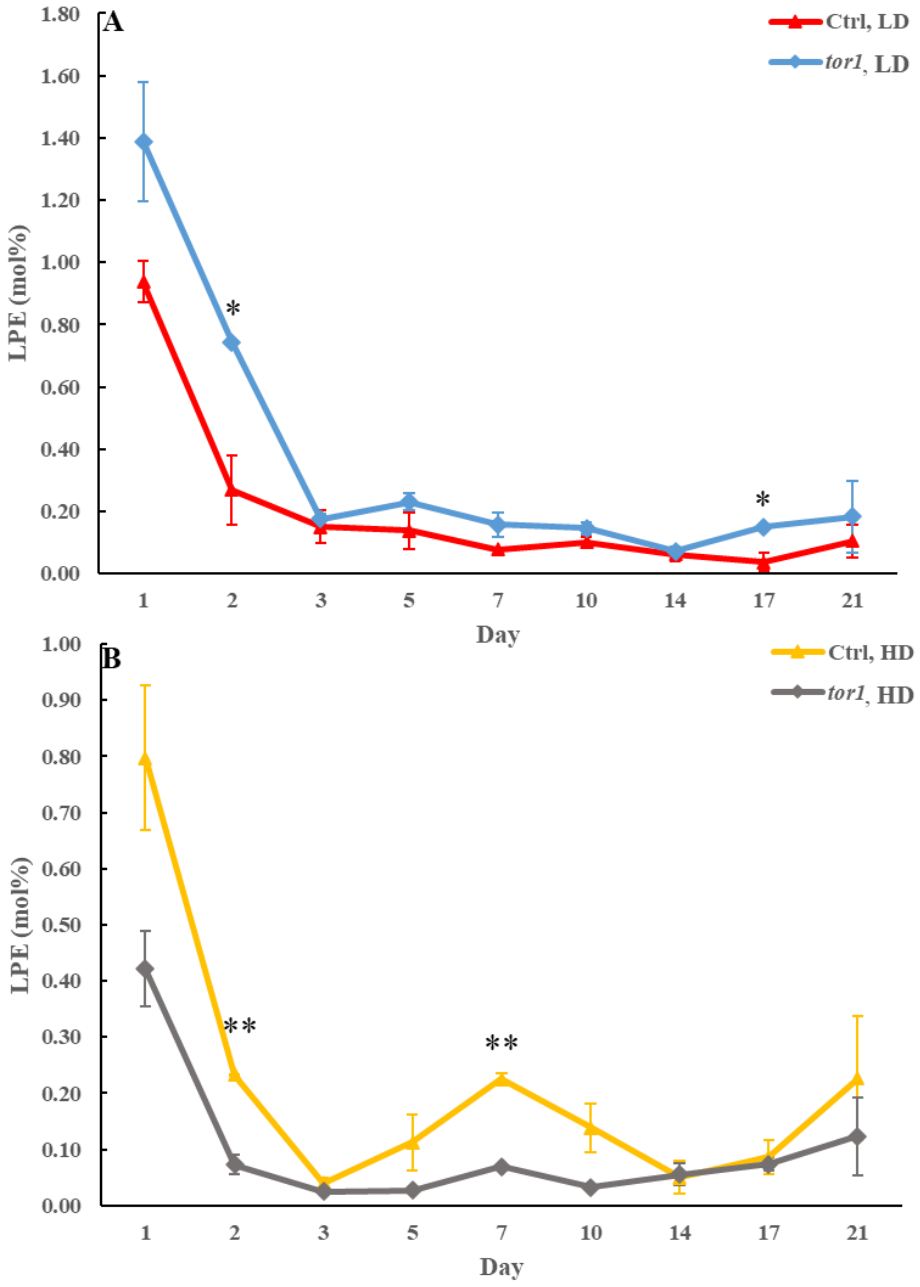

Figure 6.17. The *tor1Δ* mutation does not have a significant long-lasting effect on LPE concentration in HD and LD cells through the chronological lifespan. Samples of WT (control) and *tor1Δ* yeast cultured in YP medium initially containing 2% glucose (non-CR conditions) were recovered on different days of culturing and subjected to centrifugation in Percoll density gradient to purify HD and LD cell sub-populations. LPE concentrations were measured by LC-MS/MS. Data are presented as means ± SD (n = 2; *P < 0.05; **P < 0.01).

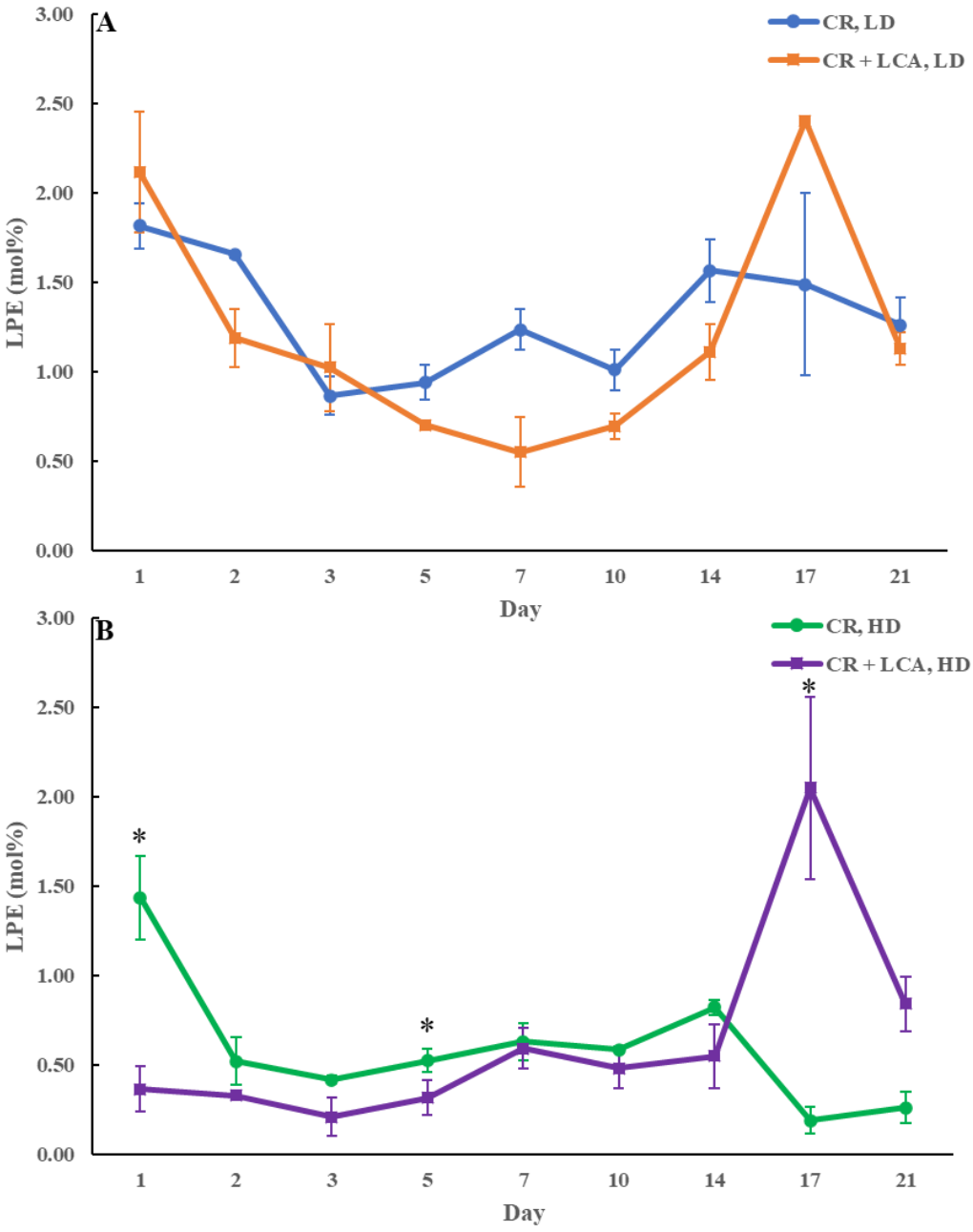

Figure 6.18. LCA does not have a significant long-lasting effect on LPE concentration in HD and LD cells through the chronological lifespan. Samples of WT yeast cultured in YP medium initially containing 0.2% glucose (CR conditions) with 50 µM LCA or without it (control) were recovered on different days of culturing and subjected to centrifugation in Percoll density gradient to purify HD and LD cell sub-populations. LPE concentrations were measured by LC-MS/MS. Data are presented as means ± SD (n = 2; *P < 0.05).

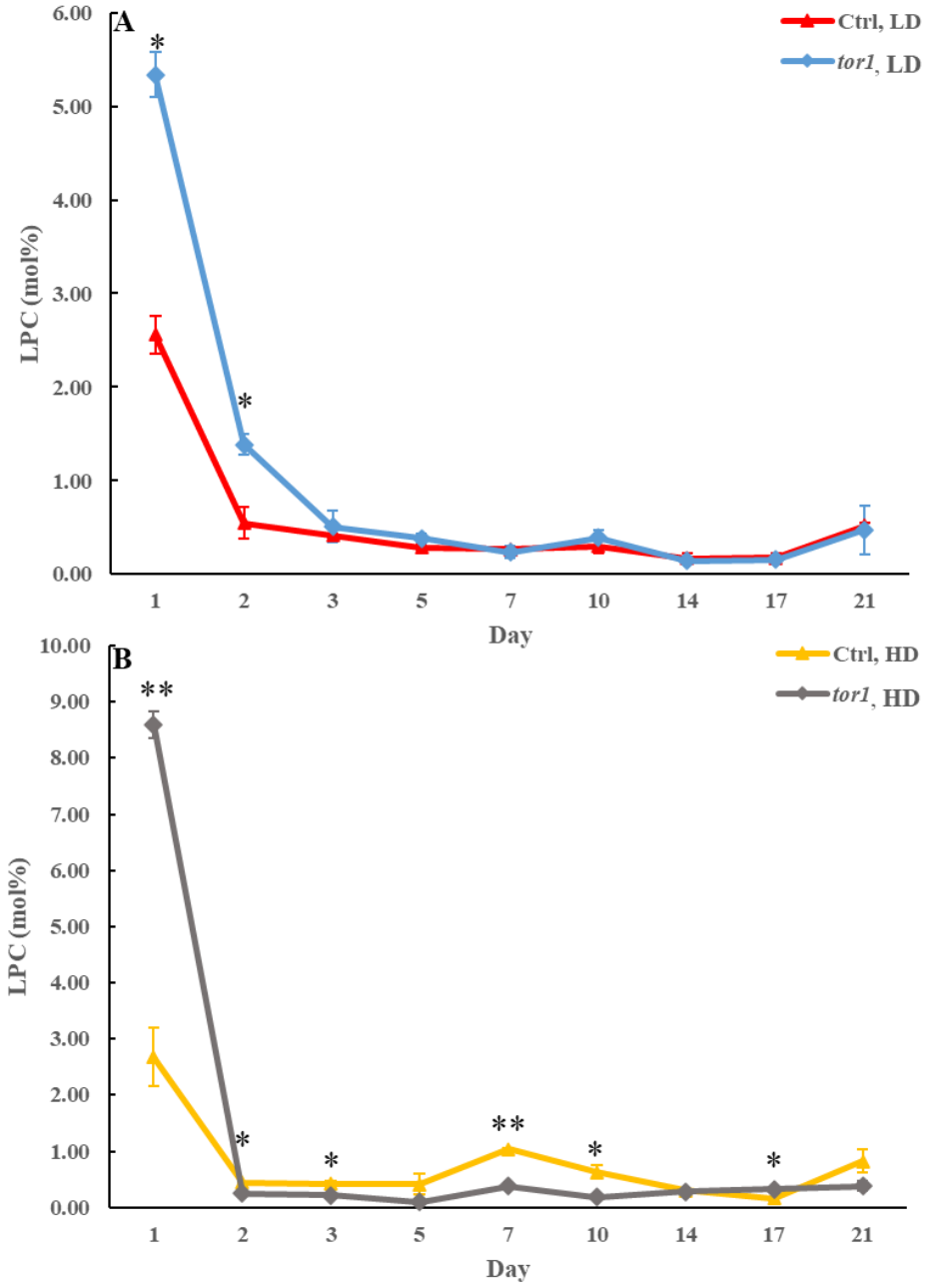

Figure 6.19. The *tor1Δ* mutation does not have a significant long-lasting effect on LPC concentration in HD and LD cells through the chronological lifespan. Samples of WT (control) and *tor1Δ* yeast cultured in YP medium initially containing 2% glucose (non-CR conditions) were recovered on different days of culturing and subjected to centrifugation in Percoll density gradient to purify HD and LD cell sub-populations. LPC concentrations were measured by LC-MS/MS. Data are presented as means ± SD (n = 2; *P < 0.05; **P < 0.01).

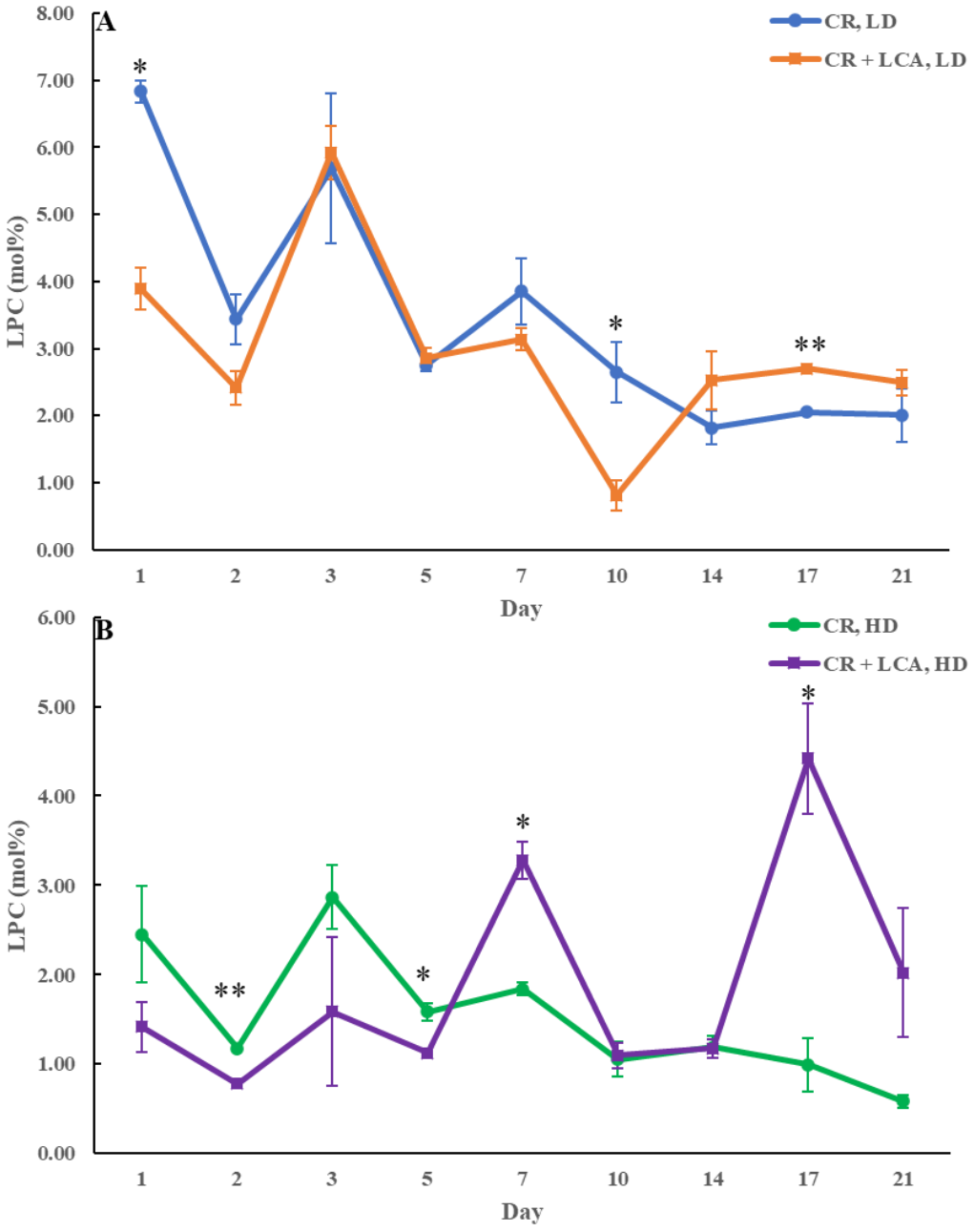

Figure 6.20. LCA does not have a significant long-lasting effect on LPC concentration in HD and LD cells through the chronological lifespan. Samples of WT yeast cultured in YP medium initially containing 0.2% glucose (CR conditions) with 50 µM LCA or without it (control) were recovered on different days of culturing and subjected to centrifugation in Percoll density gradient to purify HD and LD cell sub-populations. LPC concentrations were measured by LC-MS/MS. Data are presented as means ± SD (n = 2; *P < 0.05; **P < 0.01).

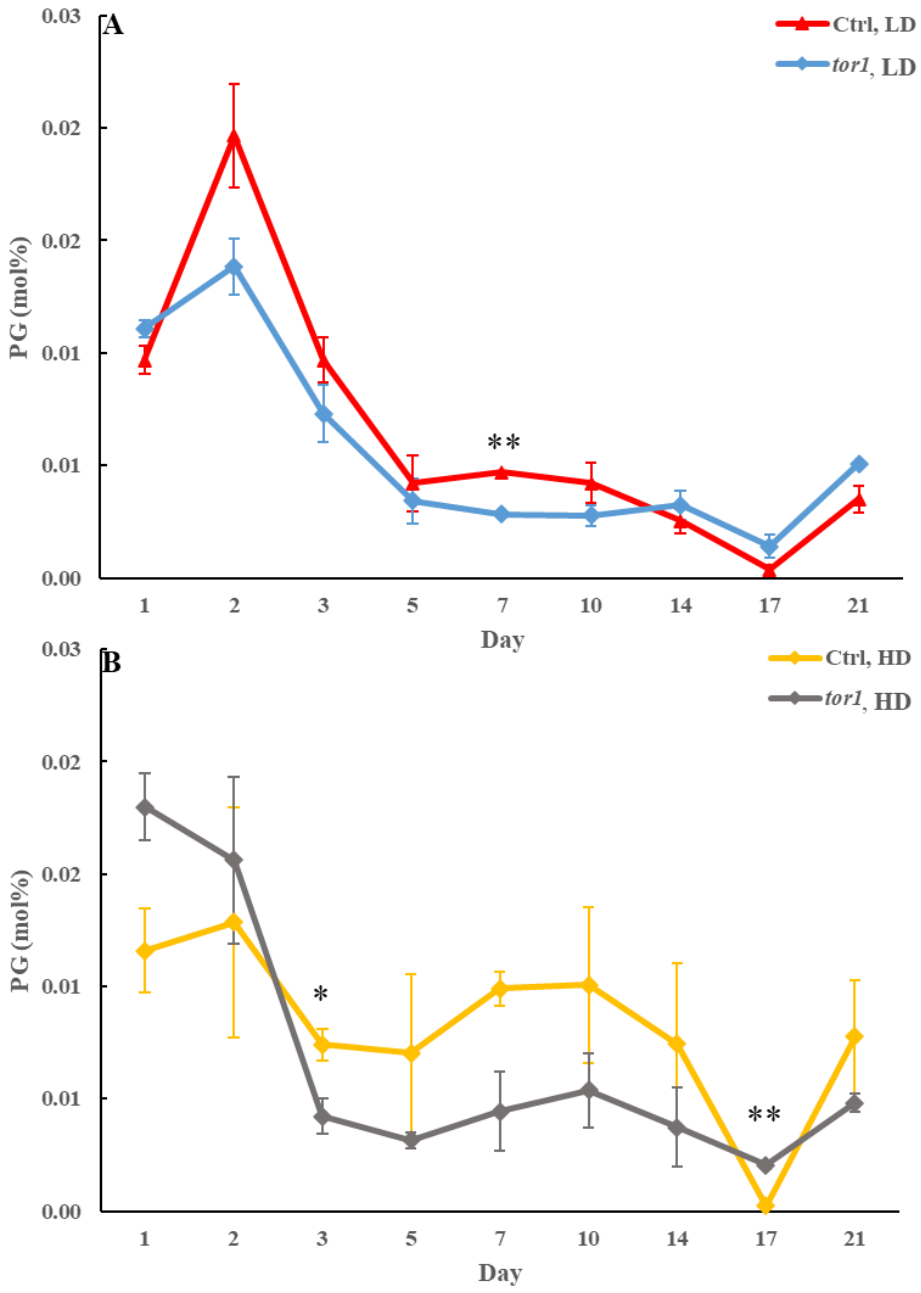

Figure 6.21. The *tor1Δ* mutation does not have a significant long-lasting effect on PG concentration in HD and LD cells through the chronological lifespan. Samples of WT (control) and *tor1Δ* yeast cultured in YP medium initially containing 2% glucose (non-CR conditions) were recovered on different days of culturing and subjected to centrifugation in Percoll density gradient to purify HD and LD cell sub-populations. PG concentrations were measured by LC-MS/MS. Data are presented as means ± SD (n = 2; *P < 0.05; **P < 0.01).

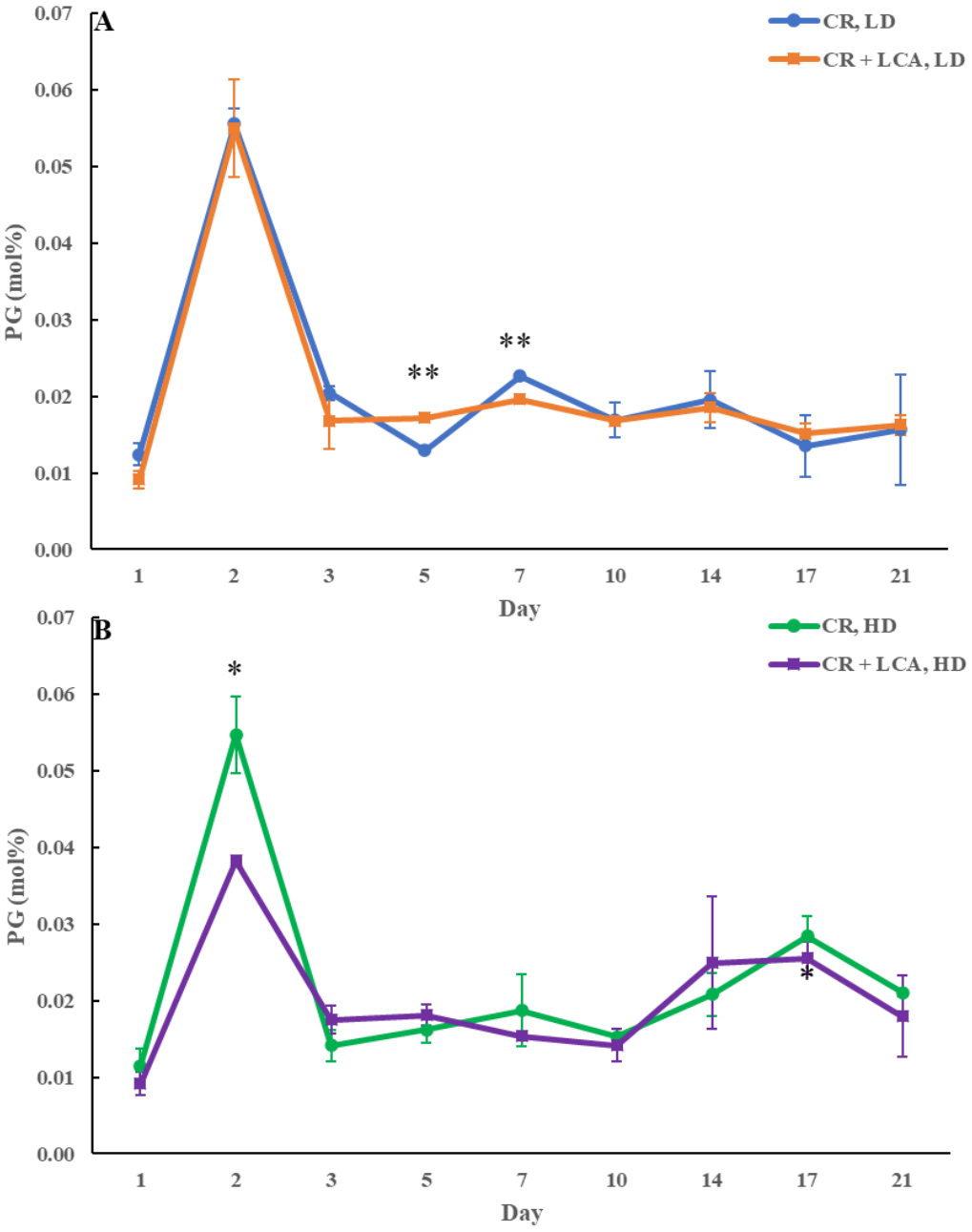

Figure 6.22. LCA does not have a significant long-lasting effect on PG concentration in HD and LD cells through the chronological lifespan. Samples of WT yeast cultured in YP medium initially containing 0.2% glucose (CR conditions) with 50 μM LCA or without it (control) were recovered on different days of culturing and subjected to centrifugation in Percoll density gradient to purify HD and LD cell sub-populations. PG concentrations were measured by LC-MS/MS. Data are presented as means ± SD (n = 2; *P < 0.05; **P < 0.01).

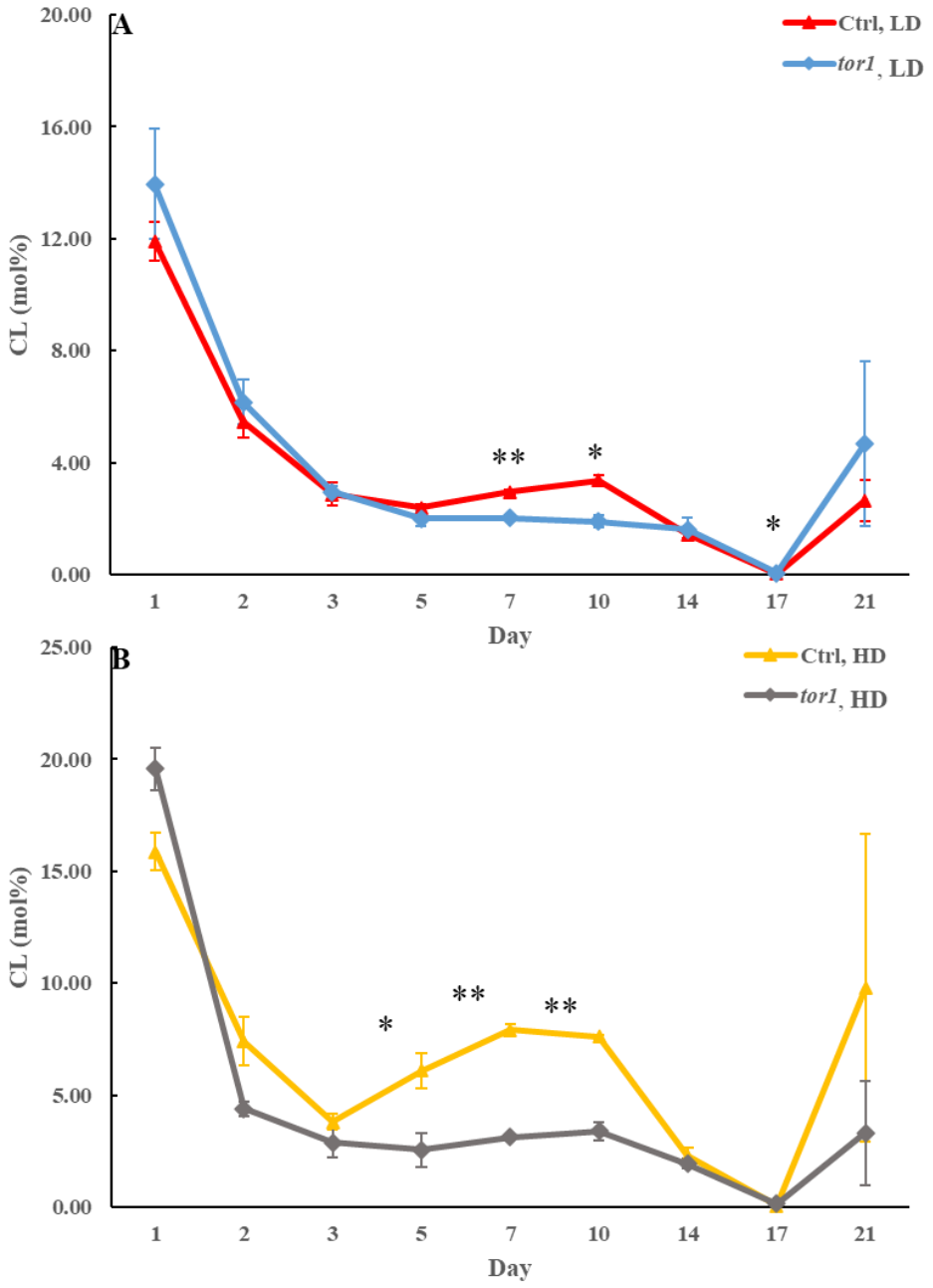

Figure 6.23. The *tor1Δ* mutation does not have a significant long-lasting effect on CL concentration in HD and LD cells through the chronological lifespan. Samples of WT (control) and *tor1Δ* yeast cultured in YP medium initially containing 2% glucose (non-CR conditions) were recovered on different days of culturing and subjected to centrifugation in Percoll density gradient to purify HD and LD cell sub-populations. CL concentrations were measured by LC-MS/MS. Data are presented as means ± SD (n = 2; *P < 0.05; **P < 0.01).

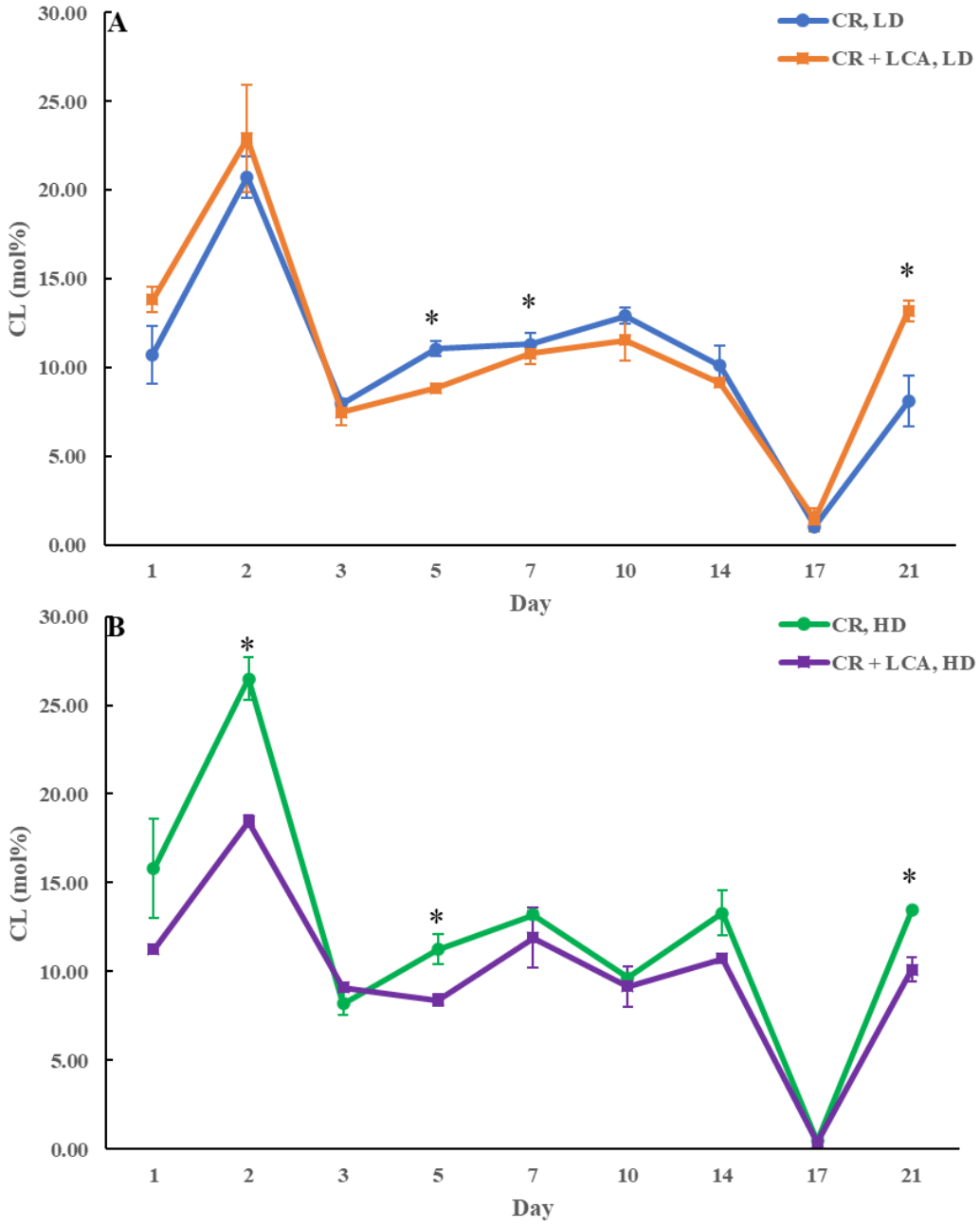

Figure 6.24. LCA does not have a significant long-lasting effect on CL concentration in HD and LD cells through the chronological lifespan. Samples of WT yeast cultured in YP medium initially containing 0.2% glucose (CR conditions) with 50 μM LCA or without it (control) were recovered on different days of culturing and subjected to centrifugation in Percoll density gradient to purify HD and LD cell sub-populations. CL concentrations were measured by LC-MS/MS. Data are presented as means ± SD (n = 2; *P < 0.05).

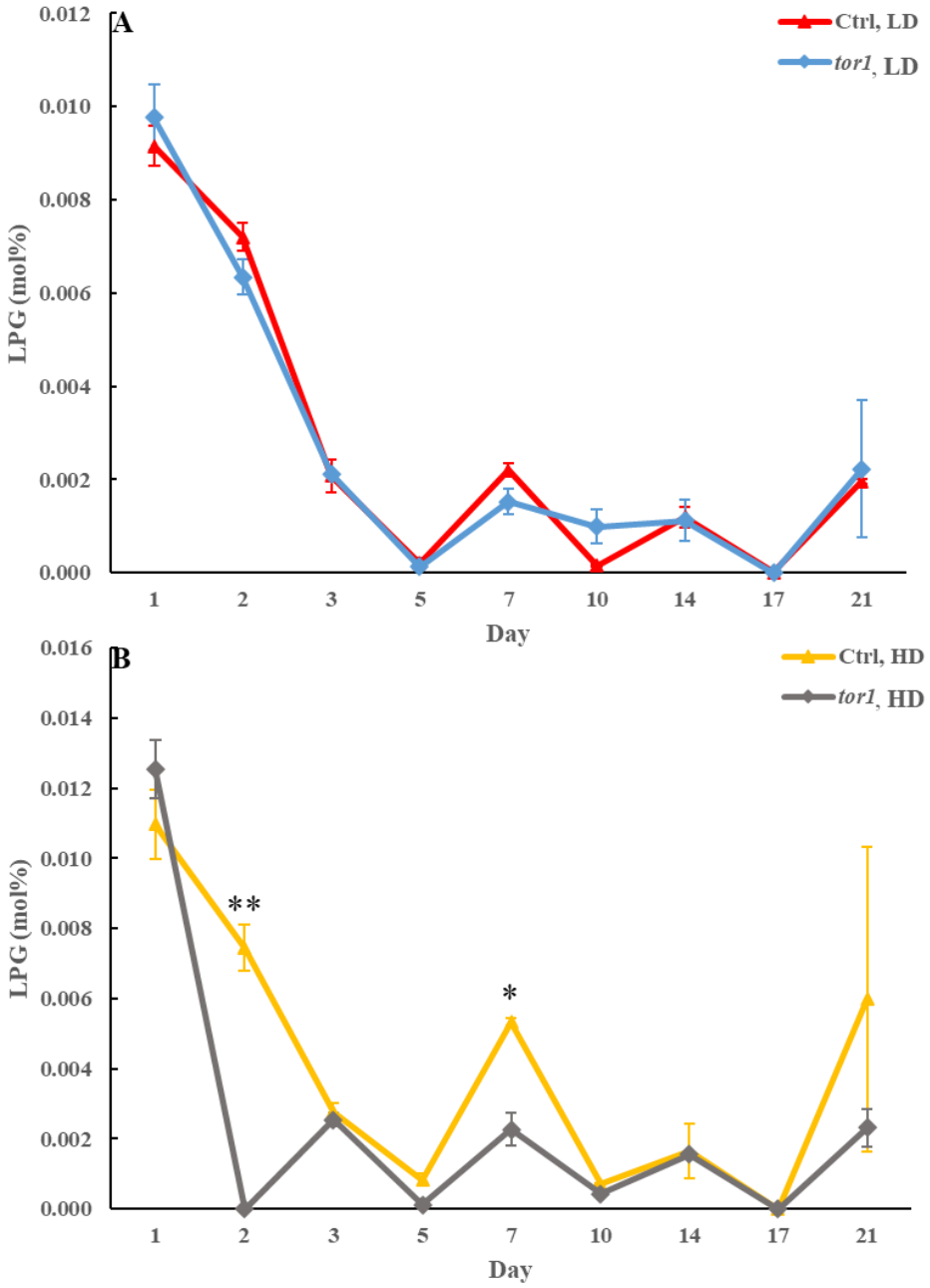

Figure 6.25. The *tor1Δ* mutation does not have a significant long-lasting effect on LPG concentration in HD and LD cells through the chronological lifespan. Samples of WT (control) and *tor1Δ* yeast cultured in YP medium initially containing 2% glucose (non-CR conditions) were recovered on different days of culturing and subjected to centrifugation in Percoll density gradient to purify HD and LD cell sub-populations. LPG concentrations were measured by LC-MS/MS. Data are presented as means ± SD (n = 2; *P < 0.05; **P < 0.01).

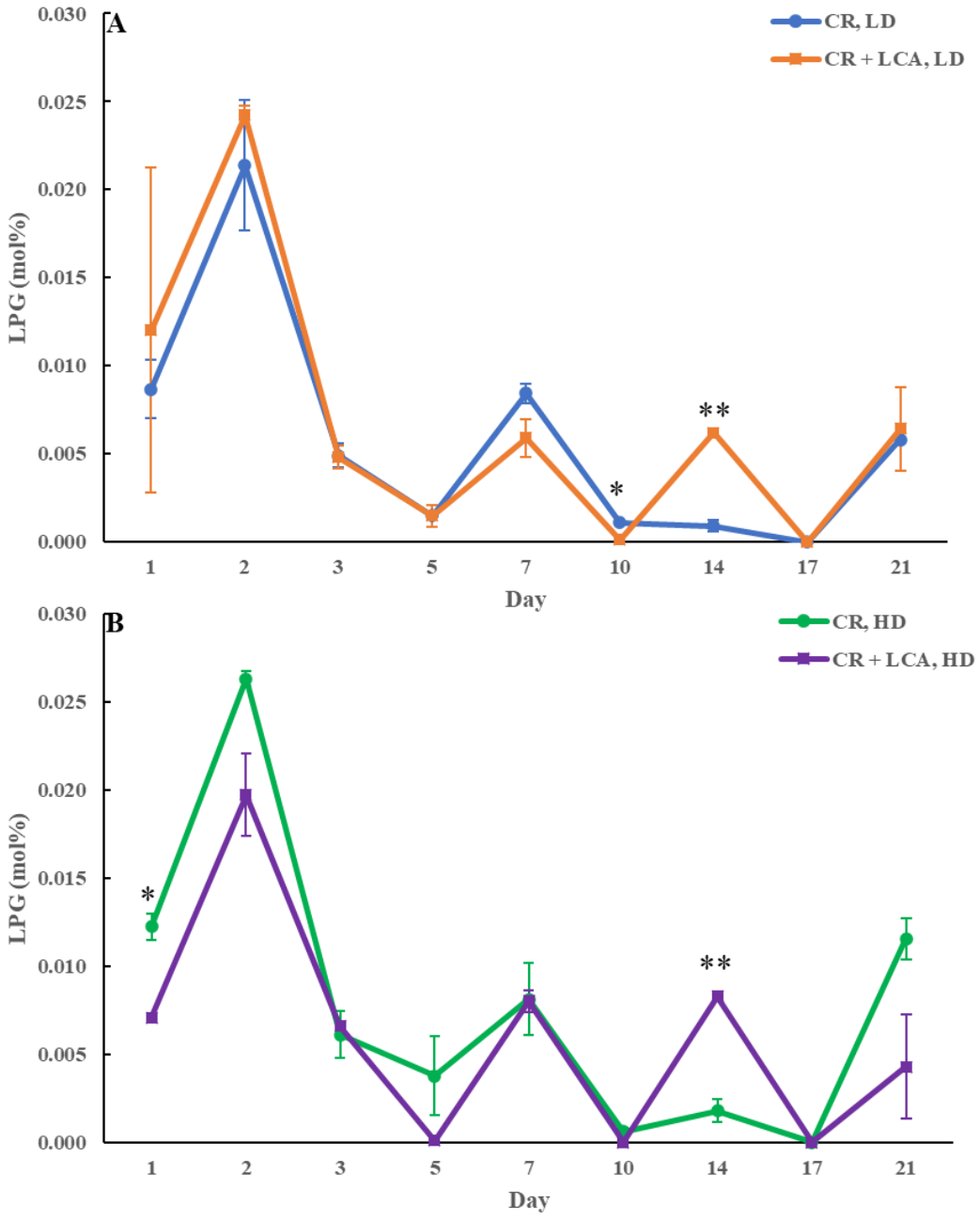

Figure 6.26. LCA does not have a significant long-lasting effect on LPG concentration in HD and LD cells through the chronological lifespan. Samples of WT yeast cultured in YP medium initially containing 0.2% glucose (CR conditions) with 50 µM LCA or without it (control) were recovered on different days of culturing and subjected to centrifugation in Percoll density gradient to purify HD and LD cell sub-populations. LPG concentrations were measured by LC-MS/MS. Data are presented as means ± SD (n = 2; *P < 0.05; **P < 0.01).